Allosteric Integrase Inhibitors Reveal a Role for Integrase During HIV-1 Maturation

Allosteric integrase inhibitors reveal a role for integrase during HIV-1 maturation

A dissertation presented

by

Kellie Ann Jurado

to

The Division of Medical Sciences

in partial fulfillment of the requirements

for the degree of

Doctor of Philosophy

in the subject of

Virology

Harvard University

Cambridge, Massachusetts

September 2015

Dissertation Advisor: Professor Alan N. Engelman Kellie Ann Jurado

Allosteric integrase inhibitors reveal a role for integrase during HIV-1 maturation

Abstract

Integration of the DNA copy of the HIV-1 genome is an essential step for virus replication and is mediated by a homotetrameric complex of the viral protein integrase (IN) in association with the ends of linear viral DNA (vDNA). HIV-1 integrates into actively transcribed genes, a trait mediated by cellular host cofactor LEDGF/p75. LEDGF/p75 engages IN in a pocket formed by dimerization of the IN catalytic core domain, a region that has been validated as a drug target for allosteric IN inhibitors (ALLINIs). Previous in vitro work suggested that ALLINIs function through disruption of two integration-associated functions: IN-vDNA complex formation and the IN-LEDGF/p75 interaction. We now demonstrate that ALLINI potency is accounted for during the late phase of HIV-1 replication where the inhibitors block the formation of the viral core, converting the normally electron-dense conical core to an eccentric phenotype where the electron-density exists as a condensate situated between a translucent core and the viral membrane. We have further elucidated the eccentric condensates to represent non-packaged viral ribonucleoprotein (vRNP) complexes and that either genetic or pharmacological inhibition of IN can impair vRNP encapsidation. Supplying IN in trans as part of a Vpr-IN fusion protein partially restored the formation of conical cores with the internal electron density. Moreover the ability of ALLINIs to induce eccentric condensate formation required both IN and viral RNA. Based on these observations, we propose an active role for IN during HIV-1 maturation that involves initiating core morphogenesis and vRNP encapsidation.

Acknowledgements

“At times our own light goes out and is rekindled by a spark from another person. Each of us has cause to think with deep gratitude of those who have lighted the flame within us.”

-Albert Schweitzer

I have immense gratitude to all (loved ones and strangers alike) who have helped to kindle my glow throughout my graduate career. It is because of you that this body of work has come to fruition and in that same notion I dedicate this to you.

Table of Contents

Table of Figures

List of Abbreviations

ΔIN	IN deletion mutant
AIDS	Acquired immunodeficiency syndrome
AEBSF	4-(2-Aminoethyl) benzenesulfonyl fluoride hydrochloride
ALLINI	Allosteric integrase inhibitor
AZT	Azidothymidine
CA	Capsid
CCD	Catalytic core domain
CPSF6	Cleavage and polyadenylation specificity factor 6
cryo-ET	Cryo-electron tomography
CTD	C-terminal domain
CypA	Cyclophilin A
DTG	Dolutegravir
DMEM	Dulbecco's Modified Eagle Medium
EC_{50}	Effective dose 50%
EFV	Efavirenz
eGFP	Enhanced green fluorescent protein
Env	Envelope
ERT	Early reverse transcription
ESCRT	Endosomal sorting complexes required for transport
EVG	Elvitegravir
FBS	Fetal bovine serum
GL3-B	pGL3-basic

HAART	Highly active antiretroviral therapy
HIV-1	Human immunodeficiency virus type-1
HTRF	Homogenous time resolve fluorescence
IBD	IN-binding domain
IC_{50}	Inhibitory concentration 50%
IN	Integrase
INLAIs	IN-LEDGF/p75 allosteric inhibitors
INSTIs	IN strand transfer inhibitors
LEDGF/p75	Lens epithelium-derived growth factor
LEDGINs	LEDGF-IN inhibitors
LRT	Late reverse transcription
LTRs	Long terminal repeats
MA	Matrix
MINIs	Multimeric IN inhibitors
NC	Nucleocapsid
NCINI	Non-catalytic site IN inhibitors
NIH ARRRP	National Institutes of Health AIDS Research and Reference Reagent Program
NNRTI	Nonnucleoside RT inhibitor
NTD	N-terminal domain
NUP	Nucleoporin
PBMC	Peripheral blood mononuclear cell
PFV	Prototype foamy virus

PIC	Preintegration complex
PIs	Protease inhibitors
PR	Protease
RAL	Raltegravir
RNAi	RNA interference
RNP	Ribonucleoprotein
RT	Reverse transcriptase
RTC	Reverse transcription complex
SEC	Size exclusion chromatography
SN2	Bimolecular nucleophilic substitution
tBPQAs	Tert-butoxy-(4-phenyl-quinolin-3-yl)-acetic acids
TEM	Transmission electron microscopy
TNPO3	Transportin 3
TSD	Target site duplication
vDNA	Viral DNA
VLPs	Virus-like particles
Vpr	Viral protein R
vRNA	Viral RNA
vRNP	Viral ribonucleoprotein
VSV-G	Vesicular stomatitis virus G
WT	Wildtype

Chapter 1

Introduction

HIV-1 epidemic

In 2013, there were an estimated 1.6 million deaths from human immunodeficiency virus type-1 (HIV-1) infections (1). Historically known as human T-cell leukemia/ T-cell lymphotrophic virus III, HIV-1 was found to be the causative agent of acquired immunodeficiency syndrome (AIDS) in 1983 (2-4). At that time, an AIDS or HIV-1 diagnosis was a death sentence. Through targeting cells critical for proper immune function, HIV-1 weakens the infected individual's ability to combat normally encountered, opportunistic pathogens. In fact, increased incidence of the normally rare diseases of Kaposi sarcoma and pneumocystis pneumonia were the first indicators that instigated the hunt leading to the discovery of HIV-1 (5-7).

In a mere three decades, science has elucidated the most intimate details regarding the basic biology behind the HIV-1 viral lifecycle. This foundational work has led to the development and production of combination antiretroviral therapies that have transformed the future outlook for an infected individual. The first small molecule inhibitor of HIV-1 replication was FDA approved for clinical use within the United States in just four years post-identification (8). The combined government and science-fueled achievement introducing azidothymidine (AZT) into the clinic demonstrated that HIV-1 could be effectively inhibited within patients and therefore was a treatable disease (9). Although AZT monotherapy proved to be inadequate for long-term treatment (10, 11), the pace of discovery-to-clinic provided precedent for the development of other small molecule inhibitors against HIV-1. Multiple antiretroviral drugs targeting several key steps of viral replication soon followed suit (8). Distribution and effective modes of prescription within the United States led to the precipitous drop in deaths due to HIV infection in 1995 with a corresponding increase in people living with HIV (Figure 1-1) (12). This

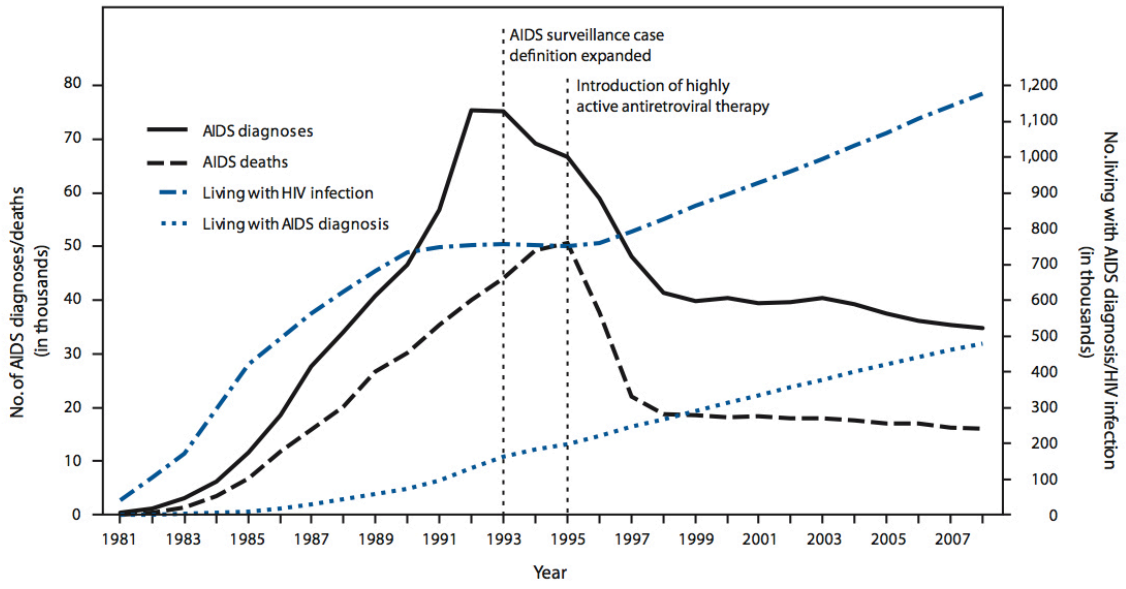

Figure 1-1. CDC estimated number of AIDS deaths and diagnoses and estimated number of individuals living with HIV infection within the United States from 1981-2008

Figure extracted from Center for Disease Control and Prevention, HIV Surveillance --- United States, 1981-2008, MMWR Morb Mortal Wkly Rep 60(21), (2011) 689-693.

was a monumental feat within science, government and medicine and continues to serve as the prime example of effective streamlining of drug development. Yet, despite all of our scientific and clinical progress, HIV-1 remains a global epidemic and the possibility of an effective cure and/or vaccine remains uncertain.

The HIV-1 replication cycle: Virion assembly to proviral DNA

HIV-1 (species) belongs to the subgroup of Retroviridae (family) known as lentiviruses (genus) (13). Lentiviruses package their genomes into virions as single-stranded RNA and reverse transcribe this genetic information into DNA shortly after entry into a susceptible host cell. In order to remain a permanent feature of the host cell, the viral cDNA is integrated into the genome of the cell targeted for infection. The HIV-1 lifecycle occurs in a step-wise process and therefore can be divided into *early* and *late* stages (Figure 1-2). The integration step demarcates the transition from the *early* stage to the *late* stage of the retroviral lifecycle. Viral DNA integration accordingly switches a susceptible host cell that was the target of the infecting-virus (target cell) into a cell that is capable of producing new infectious viral progeny (producer cell).

Transcription of the integrated DNA and translation of the transcribed mRNA (which also serves as the viral genome) begin the late steps of HIV-1 replication. Subsequent to the formation of the RNA and protein components of the virus, the final steps of HIV-1 replication can be further divided into three main steps: colocation of viral components on the plasma membrane forming the immature virion (assembly), departure of the immature particle across the plasma membrane (budding), and cleavage of polyproteins to allow for their rearrangements into an infectious virion (maturation). The early stage of the viral lifecycle includes receptor-mediated ingress into a target host cell (entry), conversion of viral genomic RNA into cDNA

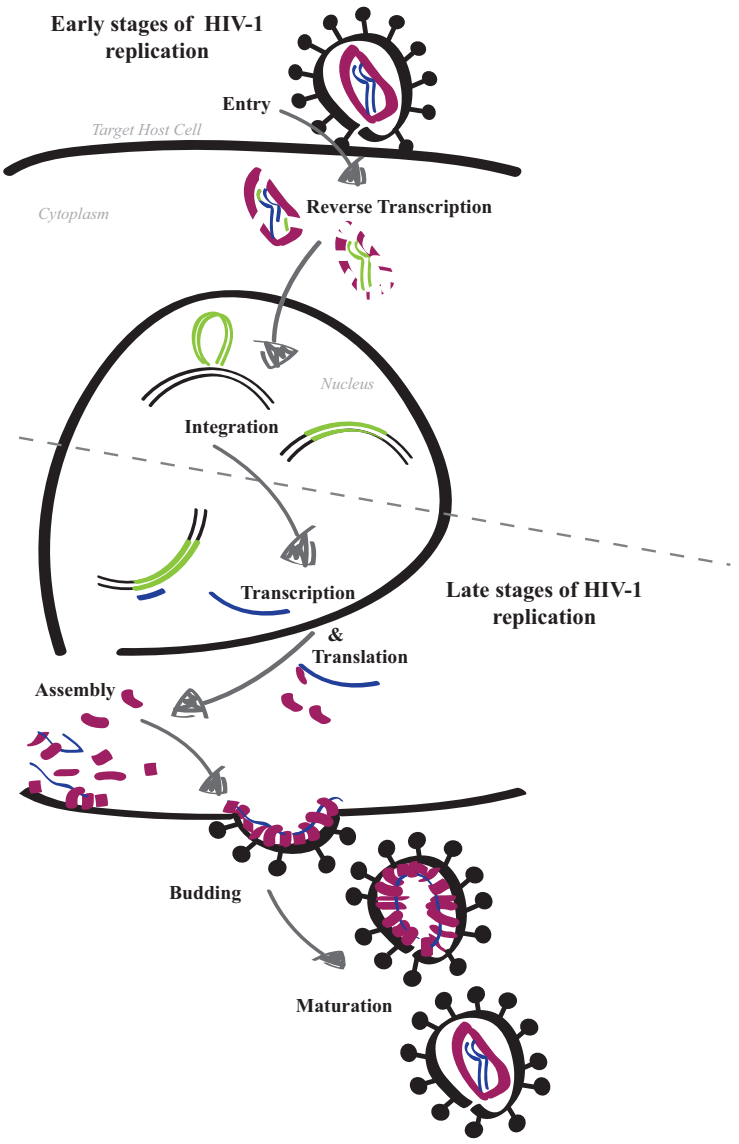

Figure 1-2. HIV-1 lifecycle: Schematic of the early and late stages of virus replication

The early stage of the HIV-1 lifecycle includes viral entry, reverse transcription (conversion of genomic RNA into DNA) and integration (insertion of the viral genomic DNA) into the infected-host cell genome. The late stage begins by production of viral components through transcription and translation. Viral components assemble on the plasma membrane to form an immature virion. The non-infectious immature particle buds, and cleavage of the polyproteins allow for rearrangement/maturation into an infectious virion.

(reverse transcription) and insertion of the viral genomic cDNA into the infected-host cell genome (integration).

The viral components

The basic constituents of an immature HIV-1 particle are the viral envelope (Env) (120 kDa), two copies of viral RNA (vRNA) (9.1 kb) and two precursor polyproteins, Gag (55 kDa) and Gag-Pol (160 kDa) (14-18). By utilizing polyproteins, HIV-1 minimizes the number of components that need to be directed to the site of assembly. The Gag precursor consists of structural proteins: matrix (MA), capsid (CA) and nucleocapsid (NC) as well as the C-terminal p6 protein that is critical for virus particle budding (see below). The Pol component of the Gag-Pol is the precursor to the three viral enzymes: protease (PR), integrase (IN) and reverse transcriptase (RT). The Gag-Pol polyprotein is translated as a result of -1 ribosomal frameshift, wherein the overlapping ~250 nucleotides of the *gag* and *pol* genes are brought into the same translational frame resulting in a fusion Gag-Pol protein (19, 20). The frameshift occurs at a frequency of ~5% of Gag production allowing for coordinated production of structural-to-enzymatic components (19).

Late stage: Assembly, budding, and maturation

Only the Gag polyprotein is needed for the assembly and budding of immature particles to occur (21), indicating that all signals necessary for these steps can be accounted for within this protein (22). In fact, all structural components of Gag play crucial roles for assembly and budding. MA is the main mediator for targeting Gag to the plasma membrane, specifically to the inner leaflet of the lipid membrane (23). Plasma membrane targeting through MA is thought to regulated by interaction with tRNA (24), and achieved in a bipartite manner: 1.) a co-

translational addition of a myristyl group to the N-terminal glycine of MA (in turn Gag and Gag-Pol) increases the affinity for interaction with hydrophobic partners (25, 26); 2.) MA contains a cluster of basic amino acids that aid in MA binding to the acidic phospholipids of the plasma membrane (27). Once membrane associated, Gag continues to multimerize at the site of assembly through lateral addition, eventually forming an electron dense spherical structure protruding from the plasma membrane (28). The C-terminal domain of CA has a dimerization interface that serves to promote lateral association of Gag molecules during assembly (29). The basic residues of NC bind to RNA in a nonspecific manner and ultimately result in a scaffolding effect that corroborates the Gag oligomerization effort indirectly through RNA-mediated Gag-Gag interactions (30, 31). This poises RNA as a structural element within the immature particle; the most testimonial evidence of this role has been elucidated through disruption of immature retroviral particles upon RNase treatment (32). The RNA scaffolding properties of NC are essential for assembly of immature particles in terms of wildtype (WT) NC (33), but can be functionally replaced by a polypeptide that is capable of forming strong interprotein contacts such as the MS2 bacteriophage coat protein, or the cyclic AMP response element binding protein (CREB) zipper (also known as leucine zipper) domain (34). This functional replacement of NC during assembly also negates the structural role of RNA (35), emphasizing the cooperation between the two elements in assisting Gag oligomerization.

HIV-1 genome packaging is quite efficient with nearly all particles containing a diploid genomic vRNA (17). Selective packaging of vRNA is accomplished through specific interaction between the zinc fingers of NC with the four stable stem-loops present at the 5' end of unspliced vRNA; this area is collectively known as the psi (Ψ) region (36-38). vRNA dimerizes and becomes associated with a lower-order Gag multimer within the cytoplasm prior to diffusion to

the site of assembly (39, 40). In the cytoplasm, vRNA undergoes dynamic diffusion, only becoming membrane-associated upon expression of Gag (41). The selective incorporation of vRNA is not essential for assembly and budding, since nonspecific cellular RNA can replace the RNA utilized for the Gag-Gag interactions. Deletion of the Ψ region allows for the formation of virus-like particles (VLPs)-- HIV-1 structural particles that lack genomic vRNA (42).

The rate of HIV-1 particle formation increases with the amount of available Gag, but on average the assembly of an immature particle occurs within 5-6 minutes (43). Budding of assembled immature particles from the plasma membrane is accomplished by appropriating the host's cellular endosomal sorting complexes required for transport (ESCRT) pathway. The p6 region of the Gag protein recruits ESCRT machinery to aid in fission from the plasma membrane through two late-budding or L-domain motifs: 'PTAP' (44-46) and 'YPXL' (47). Consistent with this function, delta-p6 Gag expression results in immature assembled particles that remain attached to the plasma membrane via a thin membranous stalk (48). Through p6 recruitment of ESCRT factors, fission and endocytic recycling occurs, allowing the completed immature particle to be released from the host cell.

Budded, immature particles are structurally characterized by uncleaved radially ordered Gag polyprotein with the MA domain remaining membrane-associated and the C-terminal ends pointing inward (membrane-MA-CA-NC-p6) as schematically illustrated in Figure 1-3 (49, 50). Maturation of the immature particle occurs immediately following and/or concomitant with virus budding (51). PR liberates itself from Gag-Pol via auto-processing (52), an event mediated by transient dimeric encounters of polyprotein (53). Mature, dimeric PR then goes on to catalyze cleavages at 10 sites within the Gag and Gag-Pol polyproteins within a tightly regulated series of reactions. Regulation is achieved with sequential processing controlled by rate of PR cleavage

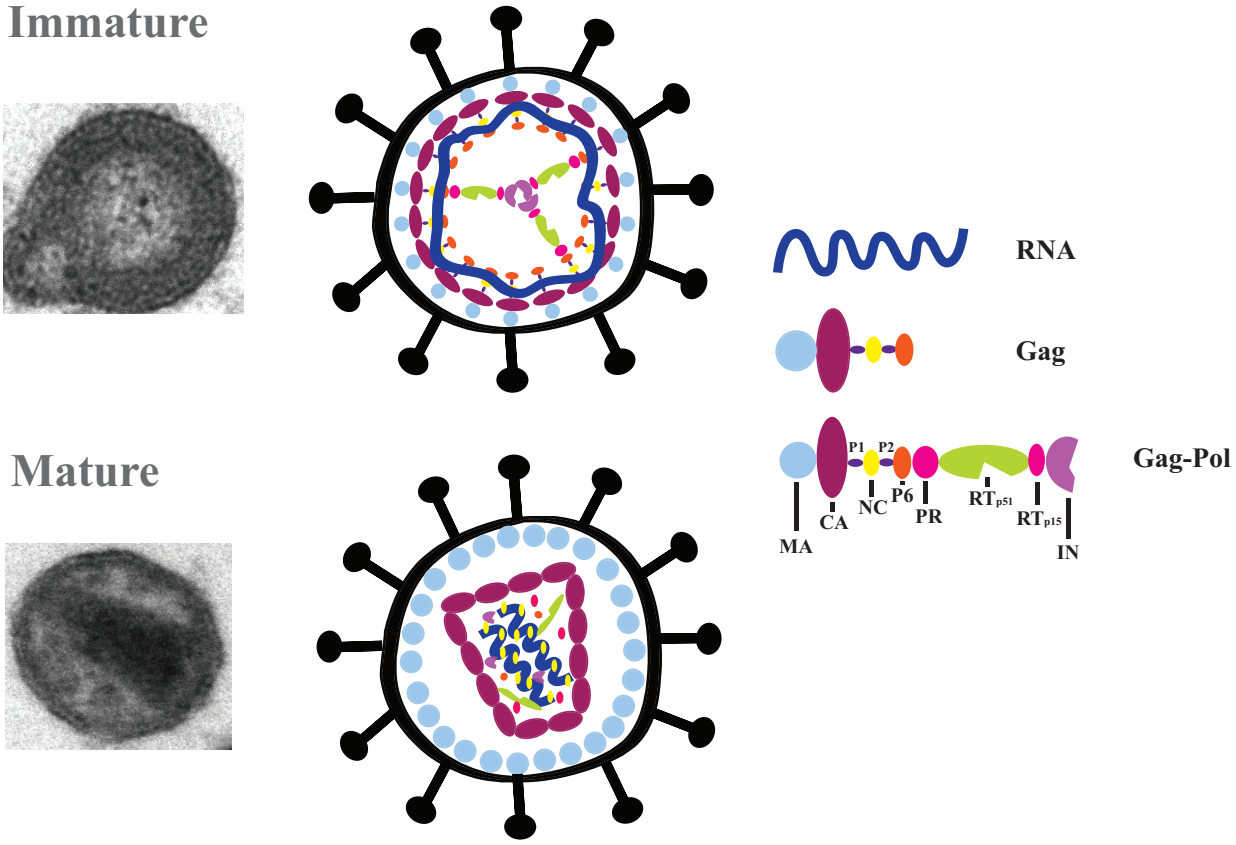

Figure 1-3. Immature and mature HIV-1 particles

HIV-1 buds as an immature, noninfectious particle. Uncleaved Gag polyproteins are radially ordered as diagramed to the right of a representative electron micrograph. The minority of Gag-Pol protein is interspersed within the majority of Gag within the same orientation. PR self-liberates and cleaves polyproteins in a tightly regulated manner, allowing for rearrangement of viral contents and formation of the mature, infectious virion. The protein sequence of the immature virion is maintained (membrane-MA-CA-NC-p6), with MA remaining in contact with the lipid membrane while CA encases the NC-condensed vRNA and viral proteins.

(54, 55). As most sites are dissimilar and variable, PR appears to recognize the overall shape of the cleavage site (56). The context in which the site exists in large part determines its rate of cleavage (57). The processed proteins radically rearrange to form the final infectious HIV-1 virion. Maintaining the radial sequence of the immature particle (membrane-MA-CA-NC-p6), MA remains in contact with the lipid membrane within an unordered fashion (23). Approximately 1200 CA proteins arrange to form a conical encasement around the viral enzymes and NC-wrapped vRNA (or ribonucleoprotein (RNP)) (58). The RNP is typically found to reside within the broad region of the core (59), where CA core assembly may nucleate (60).

Early stage: Entry, Reverse Transcription and Integration

To initiate membrane fusion, HIV-1 virions must first attach to the target host cell. Attachment can be aided through relatively nonspecific charge interactions (61) or by attachment factors (62-64). Interaction of the functional, virion-protruding Env glycoprotein spike with its primary receptor CD4 is an essential step for HIV-1 entry (65-68). Three molecules of non-covalently linked surface gp120 and transmembrane gp41 compose one Env spike (69). Mathematical modeling indicates that each HIV-1 particle may contain as few as 2-3 Env spikes that are both functional and capable of interacting with a host target cell (70). Interaction of the native Env trimer with the primary CD4 receptor induces conformational changes within the spike that activate it (71, 72), allowing interaction with host cell co-receptor CCR5 (73-77) or CXCR4 (78). Co-receptor binding then induces exposure of the hydrophobic transmembrane gp41, allowing fusion of the viral membrane with the plasma membrane of the target cell (79, 80).

Fusion results in the release of viral contents into the host cell cytoplasm, including the conical CA core that encases the RNP and viral enzymes. Since mutations that alter the stability

of the core (increase or decrease) attenuate reverse transcription, it is understood that the core must partially disassociate in order to allow viral DNA (vDNA) synthesis to ensue (81, 82). In fact, uncoating and reverse transcription appear to be intimately linked. Mathematical diagrams guided by soft matter physics indicate that the confinement forces caused by vDNA synthesis would result in core disassembly (83). There is some evidence in support of this model. Uncoating is modestly impaired when the vRNA template is modified so that vDNA synthesis will not form a three-stranded flap structure ('*central DNA flap*'), suggesting that the post-synthesis structure of the vDNA may play a role in initiating disassembly (84). Additionally, stalling of the reverse transcription complex (RTC) results in a delay in uncoating, further linking disassembly with vDNA production (85). It is reasonable that reverse transcription would be synchronized with uncoating in order to avoid diffusion of RT enzymes and/or the vDNA intermediates into the milieu of the host cell cytoplasm, yet still allow for active exchange of other essential constituents for vDNA synthesis (deoxyribonucleotide triphosphates).

RT is capable of utilizing RNA or DNA as a template. Beyond these synthesis capabilities, RT contains an RNase H domain that will degrade RNA only if it exists as an RNA-DNA hybrid. RT utilizes both copies of its positive-sense genome to convert single-stranded vRNA into double-stranded DNA within the RTC (reverse transcription mechanism reviewed in (86)). HIV-1 primes vDNA synthesis with cellular $tRNA^{Lys,\,3}$ (87), which was selectively incorporated into the particle during virus production (88). Although the majority of reverse transcription occurs upon exposure to cytoplasmic deoxyribonucleotide triphosphates within the newly infected target cell, the addition of a few nucleotides to the HIV-1 primer can initiate vDNA synthesis within the matured viral particle (89). The metabolic state of the cell can affect the duration of synthesis (90), but full-length vDNA in typical activated or cycling cells can be

detected within 4 hours of infection, and continues to gradually increase until 8-12 hours post-infection (91, 92).

The preintegration complex (PIC) is composed of full-length vDNA in complex with viral and cellular proteins carried from the RTC. The PIC contains all components necessary for successful import of the nucleoprotein complex into the nucleus and integration of vDNA into the host cell genome. In addition to the IN enzyme, examination of extracted PICs reveal that a number of viral proteins remain engaged: MA, Viral-protein R (Vpr), CA and RT (93-96). Within the PIC, four IN molecules bound to the two ends of newly synthesized full-length vDNA will complete two enzymatic reactions: 3'-processing and strand transfer (97-100). Unlike most retroviruses, where nuclear import can only occur during cellular division when the nuclear envelope is dissolved, HIV-1 can enter cells at any stage of the cell cycle (101, 102). Within non-dividing cells, import through nuclear pores and association with host chromatin is mediated by interactions between CA and numerous cellular factors: nucleoporin (NUP) 358 (103, 104), NUP153 (104, 105), cyclophilin A (CypA) (106), transportin 3 (TNPO3) (107-109), and cleavage and polyadenylation specificity factor 6 (CPSF6) (110, 111). Subsequent to nuclear import, association with host chromatin is influenced by interactions between viral PIC proteins and cellular factors. Lens epithelium-derived growth factor (LEDGF)/p75, a chromatin-bound protein, interacts with IN (112-114), and is a major player in determining specificity of integration site selection (115-117). Other factors also influence the global selection of chromatin-- depletion or disruption of CA interacting proteins NUP358, NUP153 TNPO3 and/or CypA influence integration site distribution (103, 118-120). Moreover, a component of the nuclear pore basket that interacts with hypertranscribed regions of chromatin via nuclear extensions, tpr, has been recently identified to contribute to PIC positioning/integration site

selection (121). Upon association with host cell chromosomal DNA, IN catalyzes strand transfer (100, 122). Host cellular machinery repairs the resultant DNA breaks leading to a stably integrated HIV-1 provirus.

Molecular mechanisms of HIV-1 integration

The IN protein, which contains 288 amino acids (32 kDa), is cleaved from the C-terminus of the Gag-Pol polyprotein during maturation. It is composed of three independent, functional domains: the N-terminal domain (NTD), catalytic core domain (CCD) and the C-terminal domain (CTD). The CCD of IN, which adopts an RNase H fold (123), contains the catalytic triad (D, D-35-E motif) that is indispensible for catalytic activity (124-126). The D, D-35-E amino acid active site is well conserved amongst retroviruses and retrotransposons (125). Initial crystal structures of the HIV-1 IN CCD domain found the two of aspartic acid residues of the catalytic triad (D64 and D116) were responsible for coordinating a single metal ion (127, 128), therefore it was originally unclear as to whether one or two metal ions were important for enzymatic function. Structure-based modeling grounded by the x-ray crystal structure of prototype foamy virus (PFV) IN in complex with its cognate vDNA substrate (129) has since resolved this discrepancy and has implicated the third active site residue E152 with D64 to be involved in metal cofactor coordination of the second metal cofactor (130). IN is a highly dynamic protein that in solution yields a variety of species including monomers, dimers, tetramers and higher-ordered species (131). IN functions as a higher-order multimer (132, 133). Specifically, a pair of IN dimers bring together the vDNA ends to yield an IN tetramer (134). Processing of the 3' ends of vDNA can occur as in the context of an IN dimer in vitro (135, 136), although seems likely to occur under physiological conditions in the context of the tetramer (137, 138).

Enzymatic activities: 3' processing and strand transfer

IN catalyzes two in-line bimolecular nucleophilic substitution (S_N2) reactions in a sequential manner: 3' processing and strand transfer (100). After association with the long terminal repeats (LTRs) at the ends of vDNA, IN catalyzes a dinucleotide cleavage adjacent to a conserved CA sequence (97-99). Utilizing the metallic ion cofactor to activate the oxygen atom of a water molecule and to destabilize the scissile phosphodiester bond, a dinucleotide is eliminated from both ends of the vDNA (100, 139). This enzymatic cleavage creates a 3' hydroxyl group (CA_{OH}-3') that will serve as the nucleophile in the subsequent strand transfer reaction. Utilizing chiral phosphorothioates and a pair of nucleases with strong stereospecificities to phosphorothioates, the strand transfer reaction was identified to occur through a one-step mechanism independent of a covalent intermediate (100), as was initially considered (140). For strand transfer, the metal ion cofactor serves to activate the 3' hydroxyl group at the ends of vDNA and to destabilize the scissile phosphodiester bond of target DNA resulting in a staggered cleavage (Figure 1-4). HIV-1 characteristically cuts in a 5-base pair offset (141, 142). Concomitant with cleavage, the CA_{OH}-3' ends of the vDNA are joined to the 5' phosphates of target DNA leaving a 5-base pair gap at each end. Host cell machinery repairs the DNA breaks and results in 5-base pairs of genomic sequence (target site duplication (TSD)) flanking the integrated proviral DNA. The length of the target site duplication correlates with the amount of flexibility necessary to fit the preferred local target DNA sequence into the active site of IN (143). The x-ray crystal structure of PFV IN in complex with a cognate vDNA substrate has provided significant insight into the molecular mechanism of retroviral integration (129). PFV

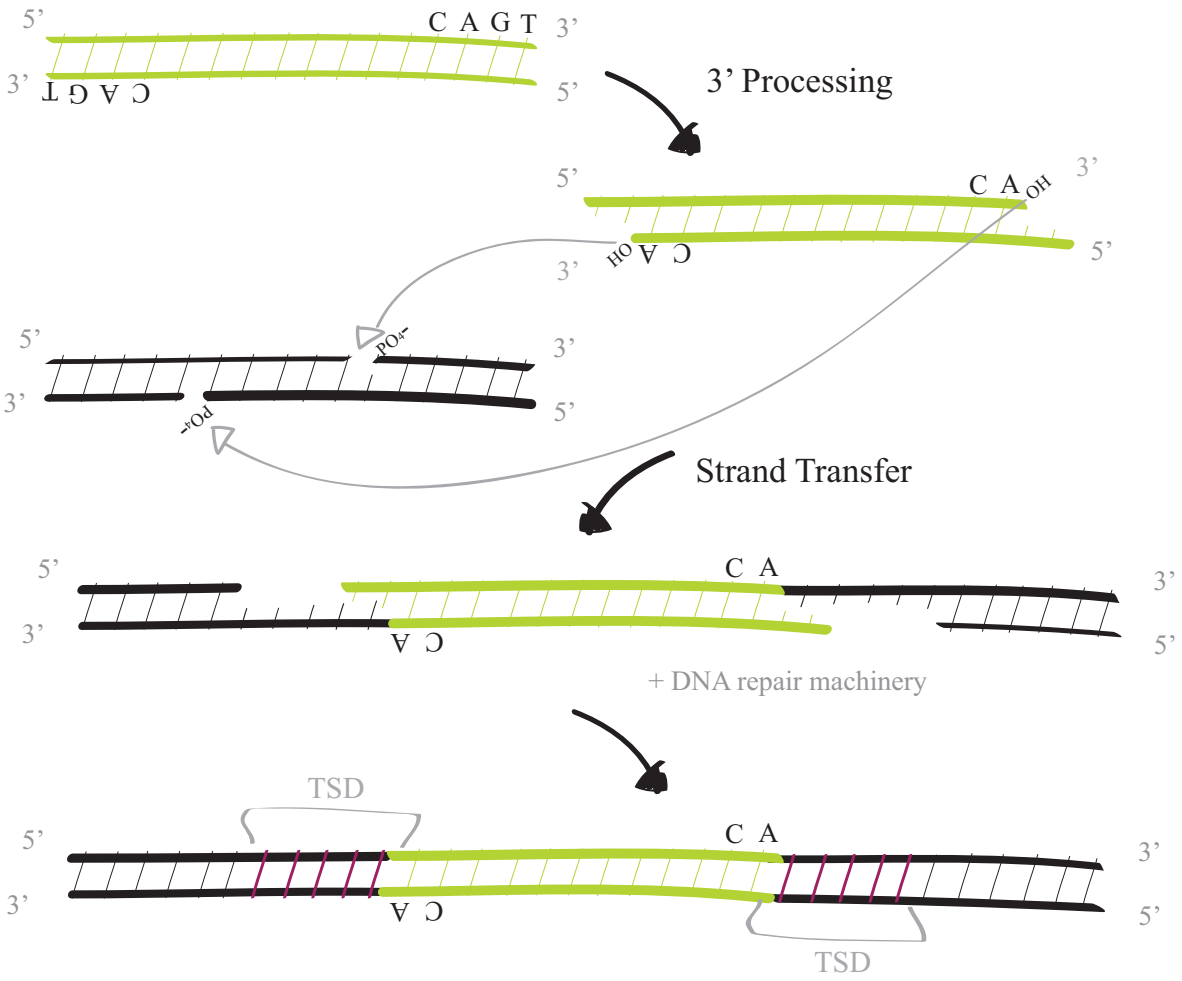

Figure 1-4. HIV-1 Integration

IN catalyzes a dinucleotide cleavage at the 3' ends of newly synthesized viral DNA (3'-processing) leaving an activated hydroxyl group at the end of an invariant CA. After association with target host cell DNA, IN catalyzes strand transfer. Concomitantly with cleavage, the CA_{OH}-3' ends of the vDNA are joined to the 5' phosphates of target DNA with HIV-1 IN leaving a characteristic 5-base pair gap at each end. Host cell machinery repairs the DNA breaks and results in TSD with 5-base pairs of genomic sequence flanking the integrated proviral DNA.

integration reaction intermediates consistent with the described mechanisms of 3'-processing and strand transfer have been elegantly determined in crystallo (137, 144).

Class I and class II IN mutations

Altering the IN protein sequence of HIV-1 can result in a variety of phenotypic outcomes, beyond simply blocking the integration of vDNA (145-149). Replication blocks in reverse transcription, particle assembly and/or particle release have been documented to occur with various IN mutant viruses. Despite being unable to replicate within the context of the virus, IN recombinant protein with these same amino acid substitutions will often still support integration catalytic activity in vitro (150). Therefore, IN mutant viruses are categorized by their associated replication block: class I IN mutant viruses are solely defective for integration, whereas class II IN mutant viruses harbor replication blocks at other steps of the viral lifecycle (reviewed in (150)).

Changing any of the residues that constitute the catalytic triad D, D-35-E motif to alanine yields the class I IN mutant phenotype and these viruses are specifically blocked at the integration step; the E152K active site mutant virus, by contrast, exhibits class II defects (147, 148). In addition to linear integrated provirus, retrovirus infection leads to two forms of circularized vDNA within the nucleus of an infected cell: 1-LTR circles and 2-LTR circles (151). The latter species may be representative of either autointegration or the ligation of the two vDNA ends (152). 1-LTR (147) and 2-LTR (146-148) circles are representative of dead-end products of reverse transcription and therefore will accumulate within the nucleus upon infection with a class I IN mutant virus. Pharmacological inhibition of integration through IN strand transfer inhibitors (INSTIs) likewise results in an increase in 1-LTR and 2-LTR circles (153).

A block in reverse transcription is the most common pleiotropic defect associated with class II IN mutant viruses (145-149). Although interactions between RT and IN have been noted (154-156), the significance of this interaction in the context of an HIV-1 infection has yet to be established. Defective release of viruses that contain class II IN mutations is another reported phenotype, although this defect appears to be somewhat dependent upon the cell line utilized (157). For example, an IN deletion mutant (ΔIN) virus displayed a 15-fold defect when made in HeLa cells, whereas when produced from human 293T or simian COS-7 cells only a 5-fold decrease in production was observed (158).

Another phenotype commonly coupled with class II IN mutant viruses is altered virion morphology (146). Specifically, the electron density that is normally situated within the conical core of a mature HIV-1 virion is present as an eccentric condensate adjacent to a translucent core and the viral membrane. Due to the lack of any other obvious candidates, the electron density within HIV-1 virions has long since been interpreted to represent the RNP. Empirical evidence to confirm this assumption has yet to be reported. Given this widely held assumption, the presence of the electron-density outside of the core suggests misplacement of the viral RNP. IN has been previously implicated in proper genome dimerization within the virions (159, 160), and has been shown to bind in vitro-selected RNAs with different affinities (161). In addition to class II IN mutant viruses, the eccentric virion core morphology has been seen under suboptimal doses of PR inhibitors (162, 163) and with improper Gag polyprotein processing (164).

Class II IN mutant viruses provided the first indication that IN may be involved in other steps of the replication lifecycle. The exact role(s) IN has beyond its catalytic activity remains incompletely defined.

Non-random integration site distribution: HIV-1 integration host factor LEDGF/p75

IN has been reported to interact with several host cell proteins, yet few have been established to have major influences on enzyme activity within the context of infection (reviewed in (165)). One such protein, LEDGF/p75, has been confirmed to play a critical role in determining integration site distribution. The preference of HIV-1 to integrate into the bodies of active genes has been well documented both in vitro (166-168) and within patients (169, 170). The conclusion that LEDGF/p75 played an essential role in determining integration site selection took several years to establish.

LEDGF/p75 is a chromatin-bound (171), transcriptional co-activator (172) that was first identified to interact with IN through coimmunoprecipitation (112, 113) and a yeast two-hybrid screen (114). Inclusion of purified LEDGF/p75 protein within in vitro HIV-1 integration assays stimulated IN activity (112, 173). Upon ectopic expression in animal cells, IN was found to accumulate within the nucleus (112, 174), and LEDGF/p75 knockdown through RNA interference (RNAi) caused IN to relocate to the cytoplasm (114, 175). Additionally, infection of cells depleted for LEDGF/p75 resulted in altered integration preferences among the genome (115). Taken together, these results suggested that LEDGF/p75 might serve to target IN to host chromatin. Despite this apparent chromatin-tethering role, the importance of LEDGF/p75 within the context of an infection remained a debated topic since infectivity was either not affected or only impaired 2 to 4-fold upon seemingly efficient RNAi knockdown (176-178).

Through use of a more intensified lentiviral vector-based RNAi system, Llano et al. (179) showed that the amount of residual LEDGF/p75 protein within the system correlated with the reductions observed in virus infectivity. Ultimately, complete removal of LEDGF/p75 from mouse (116, 117) and human (180, 181) cells through genetic knockout confirmed the critical

role of the cofactor, since these cells were 5 to 12-fold less susceptible to HIV-1 infection than were matched control cells. These findings indicate that even a minute amount of LEDGF/p75 is able to support integration, speaking volumes for the high specificity of this cofactor interaction during integration.

The IN-LEDGF/p75 interaction is mediated by an evolutionarily conserved IN-binding domain (IBD) within the C-terminal region of the 530-residue LEDGF/p75 protein; specifically spanning amino acids 347-429 (173). NMR revealed the IBD to form a compact right-handed bundle of five helices with the IN contact residues mapping to the interhelical loops on one side of the globular structure (182). Mutagenesis of the interhelical loops identified three hotspot contact residues (Ile-365, Asp-366 and Phe-406) that were crucial for interaction with IN (182). A subsequent X-ray co-crystal structure of the IN CCD dimer in complex with the IBD permitted a more in-depth illustration of the protein-protein interface of the interaction (Figure 1-5) (183). The hotspot residues of the IBD anchor ~1280 Å of protein surface into a hydrophobic pocket formed by the dimerization of two IN CCD chains (A and B) (183). LEDGF/p75 hotspot residue Asp-366 forms two hydrogen bonds with the backbone amides of IN residues Glu-170 and His-171 in the A-chain of IN. Structure-based mutagenesis revealed that substitution of Asn for Asp at LEDGF/p75 residue 366 abolished the interaction of the mutant LEDGF/p75^{D366N} with IN (182) and was furthermore incapable of back-complementing infection defects of LEDGF/p75 depletions (116, 179). Single amino acid substitutions within IN reduced the apparent affinity of the protein-protein interaction, but did not largely impact the integration step within the context of infection (184, 185) as compared to a single substitution (D366N) within the LEDGF/p75 protein, indicating that the amino acid side chains crucial for the interaction are chiefly donated by the host factor.

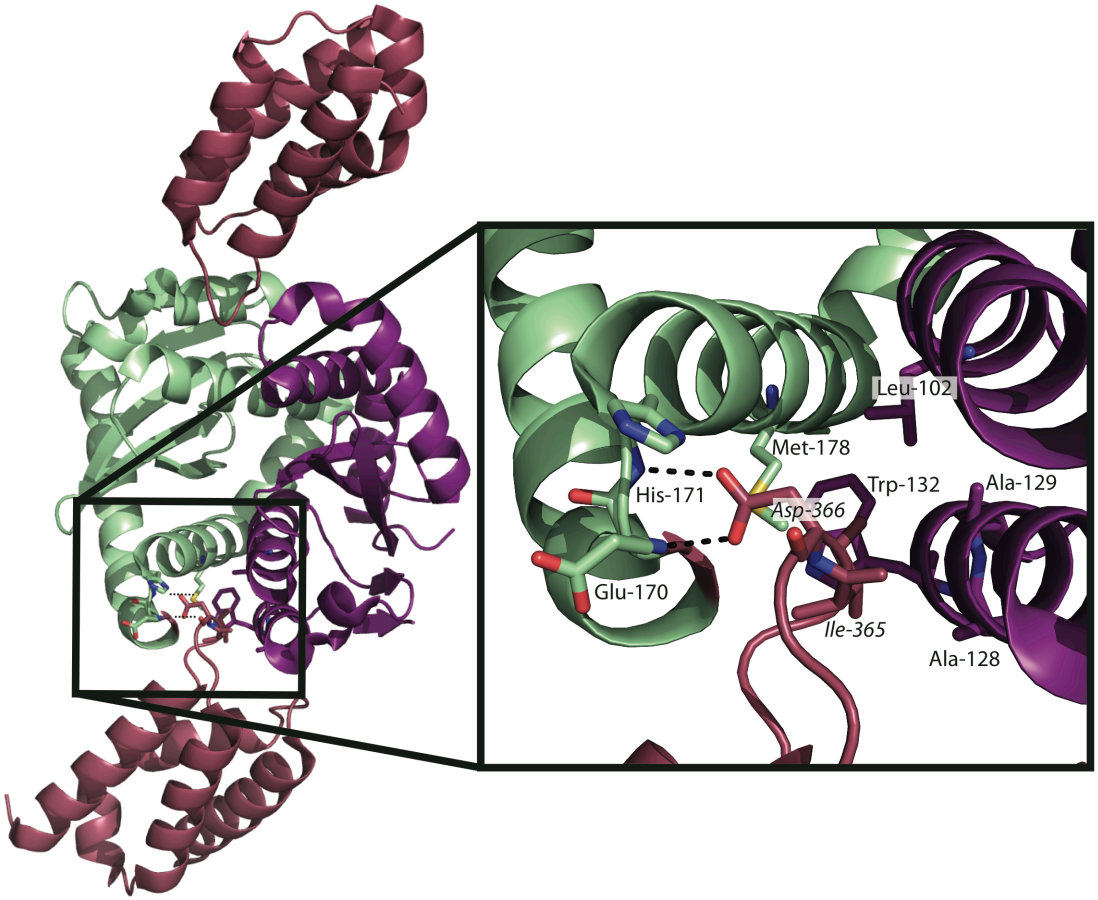

Figure 1-5. The IN-LEDGF/p75 interaction interface

A cartoon representation of the integrase-binding domain (IBD) (raspberry) bound at the CCD-CCD interface of two IN molecules (green/A-chain and purple/B-chain) from protein database code 2B4J. Hydrogen bonds between the Asp-366 residue of the IBD and the backbone amides of His-171 and Glu-170 are represented by dashed lines. The boxed area within the left is expanded to the right to illustrate the details of the IBD–CCD interaction. LEDGF/p75 contact residues Ile-365 and Asp-366 are labeled in italics; IN amino acid residues that participate in IBD binding pocket formation are also indicated.

Figure adapted from Jurado & Engelman, Multmodal mechanism of allosteric integrase inhibitors, Expert Rev Mol Med. 15, (2013) e14.

Over-expression of an IBD-enhanced green fluorescent protein (eGFP) fusion protein resulted in a potent block to HIV-1 infection, demonstrating that the IBD was capable of trandominant inhibition through outcompeting endogenous LEDGF/p75 (179, 186). When HIV-1 was serial passaged in these cells overexpressing an IBD fragment fusion construct, two resistance mutations within IN were selected: A128T in the B chain and E170G in the A chain (187). Both residues mapped to the IN-LEDGF/p75 interface, providing ex vivo data consistent with the IBD-CCD crystallographic structure. These findings importantly demonstrated that manipulating the LEDGF/p75-IN interaction could interfere with HIV-1 replication, thereby highlighting the interaction as a potential drug target.

Suppression of HIV-1 replication

Due to the pre-existence or emergence of drug-resistant mutant viruses, combinations of antiretrovirals were identified to be a more advantageous form of treatment since monotherapy only resulted in success for limited durations within drug-naïve patients (188, 189). HIV-1 RT is inherently error-prone (190, 191). It is estimated that one mutation will be introduced for every 10^3-10^4 nucleotides polymerized (192-194). The HIV-1 genome is ~10^4 nucleotides in length, thereby 1-10 mutations may be generated in each viral genome with every replication cycle. With an estimated production rate of ~10^{10} HIV-1 particles per day (195), there is enormous potential for generating genetic diversity that could result in reduced susceptibility to an antiretroviral compound. Mathematical modeling suggests that any anti-HIV-1 combination therapy would require at least three drugs in order to provide prolonged viral load suppression (189, 196-198).

Current therapeutic approach: Highly active antiretroviral therapy

Highly active antiretroviral therapy (HAART) is a combination of small molecule inhibitors that primarily target the essential enzymes of HIV-1 replication (199). HAART was widely introduced into the clinic after the inclusion of a PR inhibitor with two nucleoside analogues resulted in profound and sustained suppression of viral loads within HIV-1-infected patients (200, 201). Incorporation of the 2-target, 3-drug combination therapy into clinical practice directly resulted in declines in morbidity and mortality amongst HIV-1 infected individuals with advanced immune depletion (202). Success of the current therapeutic approach in large part is due to the decrease in probability of selecting for a virus clone with multiple drug-resistant mutations and the fact that viral fitness is often compromised upon the acquisition of a drug-resistance mutation (203).

There are over thirty FDA-approved antiretroviral drugs amongst six different classes: 1.) nucleoside RT inhibitors, 2.) non-nucleoside RT inhibitor, 3.) PR inhibitors, 4.) IN inhibitors, 5.) fusion inhibitors, and 6.) entry inhibitors. As suggested by the names, the molecular target and mechanism of inhibition of each compound determines the class of the antiretroviral. The broad spectrum of classes provides a heavy hitting armory for treatment of HIV-1 infections. But beyond excellent drugs for prescription, effective therapy requires adherence, drug tolerability, and the lack of interactions with other medications. If any of these requirements are compromised, the evolution of drug resistance can more readily occur. For all antiretroviral classes, drug-resistant viruses have been documented in patients (203).

Integrase strand transfer inhibitors

All clinically available IN inhibitors specifically target the strand transfer reaction of integration, and thereby are classified as INSTIs. Three INSTIs have been FDA approved and are

currently prescribed to patients: raltegravir (RAL), elvitegravir (EVG), and dolutegravir (DTG). INSTIs bind within the active site of IN and act through displacing the terminal deoxyadenylate residue from the IN-vDNA complex (129). INSTIs contain both a metal-binding pharmacophore to sequester the active-site metal co-factors and a hydrophobic group to aid in interaction with vDNA and IN (129, 204). Specificity for inhibition of the strand transfer reaction is achieved through INSTIs preferentially interacting with the IN-vDNA complex (205), aided by extensive contacts with the vDNA ends (129).

INSTI-resistant viruses most often arise through a primary alteration of the amino acids influencing coordination of the essential metal co-factors binding within the active site (N155 and Q148) (129, 206). Replication capacity is reduced within these mutant viruses and therefore specific secondary mutations often accompany the primary mutations (reviewed in (203)). Regardless of the primary and secondary resistant mutations, cross-resistance amongst INSTIs is observed (207, 208). RAL and EVG select for similar resistance mutations (209). DTG, a second-generation INSTI, has a higher barrier to resistance than RAL and EVG (210). The distinct resistance profile of DTG has been proposed to be due to the significantly slower dissociation kinetics of DTG (71 hours) from the IN-vDNA complex as compared to RAL (8.8 hours) and EVG (2.7 hours) (211). Several RAL and EVG-resistant mutations show low-level DTG-resistance, but DTG can still be effectively used to treat patients who have failed RAL/EVG therapies (212). DTG as a component of combination therapy has interestingly not yet led to DTG-resistance within treatment naïve patients (213). Yet, since all three INSTIs bind within the same region of IN and have some level of cross-resistance, future development of IN inhibitors should focus on binding IN at alternative regions to avoid overlapping resistance profiles.

Targeting of IN-IN interfaces for successful allosteric inhibition of HIV-1 integrase activity

There are several challenges when attempting to inhibit protein-protein interactions with small molecule inhibitors. Since the contact surface of a typical protein-protein interface (~1,500-3000 Å) far exceeds the interface formed between a protein and a small molecule (~300-1000 Å), the essential interaction interface must be contiguous, with the presence of divots and/or pockets for the small molecules to occupy (214). A full characterization of the interaction interface is essential to assess the potential for drugability, since drug-targetable hotspot regions on essential interacting protein interfaces are rare finds.

Small molecules that target the HIV-1 IN-IN interface

In 2001, an x-ray crystallographic screen aimed at identifying antiretrovirals that bind the CCD of IN yielded small molecules that specifically bound at the interface of two IN CCD monomers (215). One of these compounds, 3,4-dihydroxyphenyltriphenylarsonium bromide, inhibited the 3' processing and strand transfer activities of IN at micromolar concentrations in vitro (215). Derivatives of tetra-acetylated-chicoric acids, a group of molecules discovered in 1999 to inhibit IN enzymatic catalysis in vitro (216), were additionally found to target IN at the dimer interface (217). Further characterization of the tetra-acetylated-chicoric acid derivatives showed that these small molecules in addition to inhibiting IN enzymatic activities in vitro also modulated the dynamic exchange between IN subunits within solution (131, 218). Another small molecule, 1-pyrrolidineacetamide, was discovered due to its ability to inhibit IN oligomerization on a vDNA substrate in vitro (219). Molecular modeling supported by site-directed mutagenesis of recombinant protein suggested that 1-pyrrolidineacetamide bound within the IN-IN dimer

interface at a similar region as the tetra-acetylated-chicoric acid derivatives (219). These initial findings were the first indication that allosteric inhibition of IN activity was likely a viable route for antiretroviral development, since there were small molecules binding to IN within a region distinct from the active site that still inhibited IN catalysis (albeit, only one group demonstrated antiviral activity in these early studies). Additionally, these studies laid precedent for the LEDGF/p75 binding pocket potentially serving as a drugable target for small molecule disruption of an essential protein-protein interaction.

Targeting the LEDGF/p75 binding pocket with small molecular inhibitors

A coumarin-containing compound, originally identified within a screen for HIV-1 PR inhibitors, was found, in addition to inhibiting PR, to also block HIV-1 IN activity in vitro (220). Affinity-labeling, confirmed through site-directed mutagenesis of recombinant protein, mapped the binding site of the compound to IN amino acids residues 128-136 (221). In particular recombinant IN with Trp-132 mutated (W132A/W132G/W132R) resisted drug-action (221). Trp-132 is a key residue within the LEDGF/p75 binding pocket (Figure 1-5). The complete mechanism of action and the ability of the coumarin-containing compound to influence LEDGF/p75 binding was not assessed. Nevertheless this study indicated a novel drug-binding site within IN that appeared to overlap with the LEDGF/p75 binding pocket.

A wide-variety of experimental approaches have resulted in the identification of an array of small molecules that inhibit the LEDGF/p75-IN interaction (222-227), but the most promising inhibitors to-date (228) spawned from the identification of a class of quinoline-based acetic acid derivatives (225, 226, 229). Two separate groups utilizing vastly different small molecule screening techniques independently discovered a similar pharmacophore. A high-throughput

screen for inhibition of IN 3'-processing activity yielded a series of tert-butoxy-(4-phenyl-quinolin-3-yl)-acetic acids (tBPQAs; also known as non-catalytic site IN inhibitors (NCINI) (229, 230). The second group utilized structure-based virtual screening to identify a hit compound LEDGIN-3 (225) that ultimately led to the synthesis of low-to-submicromolar inhibitors LEDGIN-6 and CX14442 (collectively known as LEDGF-IN inhibitors (LEDGINs)) (225, 231).

Initial reports suggested different mechanism of action for these two independently discovered small molecules, despite the similar pharmacophores (Figure 1-6). The tBPQA/NCINIs were identified by their ability to inhibit 3'-processing activity (226), whereas LEDGINs were reported not to affect 3'-processing (inhibitory concentration at 50% (IC_{50}) >250μM) (225). A study aimed at comparing the mechanism of action of the two representative inhibitors (LEDGIN-6 and BI-1001) found that both compounds displayed potent antiviral activity and inhibited the interaction between IN-LEDGF/p75 and 3'-processing and strand transfer activities in vitro (232). X-ray crystallography of these small molecules and other derivatives bound to the CCD-CCD interface of an IN dimer indicated that the quinoline-based acetic acid derivatives occupied the LEDGF/p75 binding pocket (225, 232-235). Since these small molecules bind IN at a region distinct from the active site, yet still inhibited IN catalysis, they are defined as bona fide allosteric IN inhibitors or ALLINIs. This report additionally implicated the quinoline-based acetic acid derivatives in obstructing proper dynamic exchange of IN subunits within solution. Specifically, through stabilization of an inactive high-order IN multimer, ALLINIs impeded the formation of IN on the vDNA. Initial in vitro work, thereby, indicated that ALLINIs appear to inhibit HIV-1 replicative capacity by a multimodal mechanism through exploitation of the multifunctionality of IN. ALLINIs represent a novel drug class that could inhibit HIV-1 replication at multiple steps (formation of enzymatically active IN on vDNA,

3'-processing, strand transfer, and LEDGF-IN binding) and thereby warranted a clearer elucidation of mechanism of action within the context of the virus lifecycle.

In this thesis, I describe our investigations to uncover the antiviral mechanism of the recently discovered ALLINIs. In contrast to original considerations, we discovered that the small molecules, rather than primarily working during the early phase of replication, when IN is known to catalyze DNA integration, displayed full potency when drug exposure was limited to the late stage of HIV-1 replication. We defined that within an *ex vivo* system, ALLINIs primarily function through promoting higher-ordered IN multimerization to impede HIV-1 maturation. Exposure to the compounds during virus production results in the formation of an aberrant virion, where the electron density that is normally situated within a conical core is instead adjacent to a translucent core and the viral membrane. Tomo-bubblegram imaging revealed that the eccentric condensate adjacent to the translucent core was composed of the viral NC protein-- definitively implicating ALLINI treatment in the inability to successfully encapsidate the NC-encased vRNA into the core of the virus. We further discovered that the ability for ALLINIs to induce the aberrant morphology was dependent upon the presence of vRNA, suggesting a specific interaction between vRNA and IN. I propose that HIV-1 IN plays a direct role in proper capsid assembly and genome encapsidation.

Lastly, we explored the impact of ALLINI exposure on integration site distribution. Our findings indicate that the continued development of ALLINIs, for use within the clinic, should target the IN multimerization functionality as opposed to inhibit LEDGF/p75-binding in order to ensure continuation of the non-oncogenic HIV-1 integration site distribution profile.

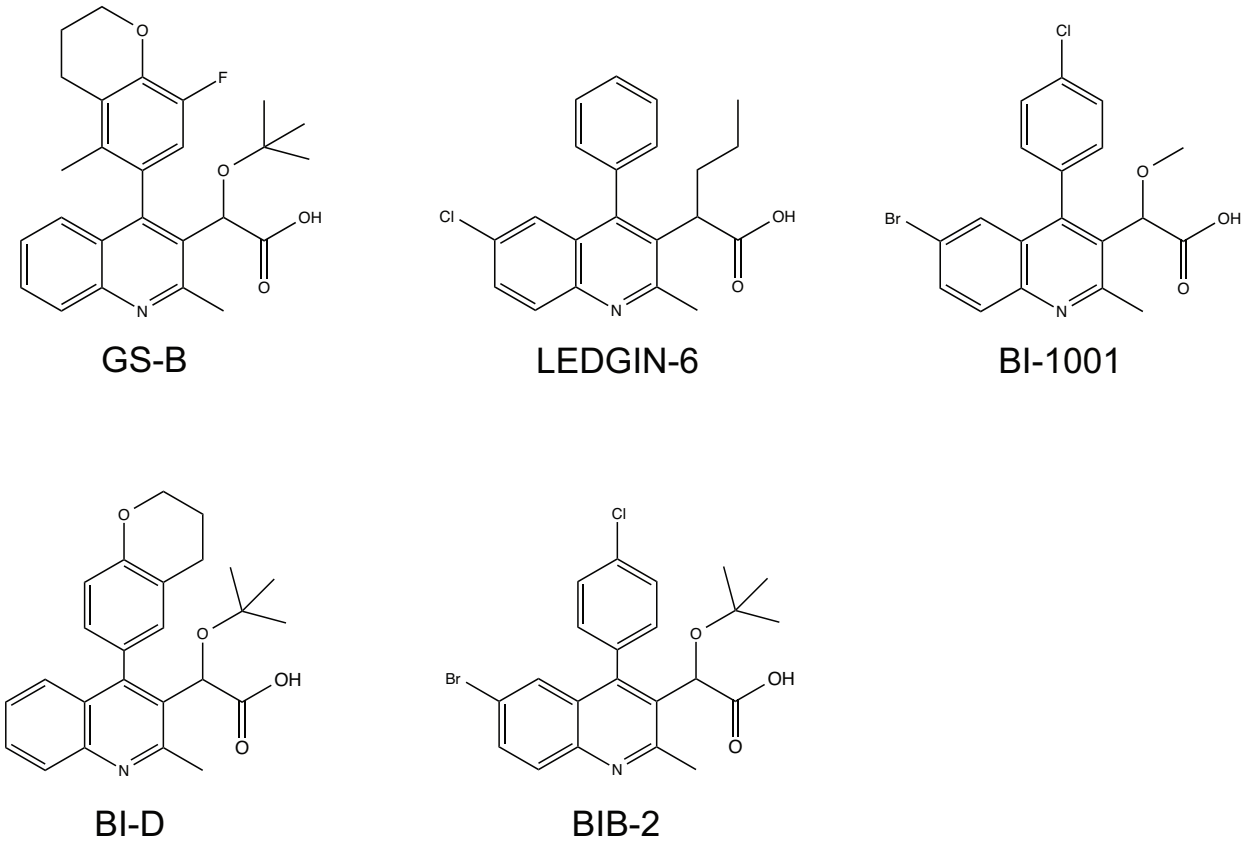

Figure 1-6: Quinoline-based acetic acid derivatives

Chemical structures of representative quinoline-based acetic acid derivatives: GS-B (230), LEDGIN-6 (231), BI-1001 (232), BI-D (236), BIB-2 (237).

Chapter 2

Allosteric integrase inhibitor potency is determined through the inhibition of HIV-1 particle maturation

Allosteric integrase inhibitor potency is determined through the inhibition of HIV-1 particle maturation

Kellie A. Jurado[a], Hao Wang[a], Alison Slaughter[b], Lei Feng[b], Jacques J. Kessl[b], Yasuhiro Koh[a], Weifeng Wang[a], Allison Ballandras-Colas[a], Pratiq A. Patel[c], James R. Fuchs[c], Mamuka Kvaratskehlia[b], and Alan Engelman[a]

[a]Department of Cancer Immunology and AIDS, Dana-Farber Cancer Institute and Department of Medicine, Harvard Medical School, Boston MA 02215; and [b]Center for Retrovirus Research and Comprehensive Cancer Center and [c]Division of Medical Chemistry and Pharmacognosy, College of Pharmacy, The Ohio State University, Columbus, OH 43210.

* This chapter is adapted from the publication:
Jurado KA, Wang H, Slaughter A, Feng L, Kessl JJ, Koh Y, Wang W, Ballandras-Colas A, Patel PA, Fuchs JR, Kvaratskhelia M, and Engelman A. Allosteric integrase inhibitor potency is determined through the inhibition of HIV-1 particle maturation. Proc Natl Acad Sci 2013 May;110(21):8690-5.

Contributions: I preformed experiments associated with Figures 2-1, 2-2, 2-3, 2-4, 2-6, 2-7, 2-8B; and Tables 2-1, 2-2. Alan Engelman and I wrote the manuscript.

Abstract

Integration is essential for HIV-1 replication, and the viral IN protein is an important therapeutic target. ALLINIs that engage the IN dimer interface at the binding site for the host protein LEDGF/p75 are an emerging class of small molecule antagonists. Consistent with the inhibition of a multivalent drug target, ALLINIs display steep antiviral dose–response curves ex vivo. ALLINIs multimerize IN protein and concordantly block its assembly with vDNA in vitro, indicating that the disruption of two integration-associated functions, IN catalysis and the IN-LEDGF/p75 interaction, determines the multimode mechanism of ALLINI action. We now demonstrate that ALLINI potency is unexpectedly accounted for during the late phase of HIV-1 replication. The compounds promote virion IN multimerization and, reminiscent of class II IN mutations, block the formation of the electron-dense viral core and inhibit reverse transcription and integration in subsequently infected target cells. Mature virions are recalcitrant to ALLINI treatment, and compound potency during virus production is independent of the level of LEDGF/p75 expression. We conclude that cooperative multimerization of IN by ALLINIs together with the inability of LEDGF/p75 to effectively engage the virus during its egress from cells underscores the multimodal mechanism of ALLINI action. Our results highlight the versatile nature of allosteric inhibitors to primarily inhibit viral replication at a step that is distinct from the catalytic requirement for the target enzyme. The vulnerability of IN to small molecules during the late phase of HIV-1 replication unveils a pharmacological Achilles' heel for exploitation in clinical ALLINI development.

Introduction

HAART, which treats patients with combinations of antiviral drugs to suppress HIV-1 replication, is the standard of care in the AIDS clinic (199). HAART is most often formulated from compounds that inhibit the activities of the viral RT and PR enzymes. The activity of the viral IN enzyme is also crucial to HIV-1 replication, and RAL, which was licensed by the US Food and Drug Administration in 2007, is the first-in-class INSTI (238). Although the INSTI EVG has since been licensed, IN mutations that confer resistance to RAL in large part convey EVG cross-resistance, thereby limiting clinical INSTI treatment options (239). DVG, an INSTI that remains active in the face of most RAL resistance mutations, may help to circumvent the limitation of cross-resistance to the current clinical IN inhibitors (239). INSTIs inhibit vDNA strand transfer activity by binding to the intasome nucleoprotein complex at the enzyme active site and displacing the terminal deoxyadenylate residue of retroviral DNA that would otherwise be used by IN to cut chromosomal DNA (129). Inhibitors that engage HIV-1 IN at sites separate from the active site, which should retain potency in the face of INSTI resistance mutations, are therefore an important class of investigational antiretroviral drug (240).

HIV-1 preferentially integrates along the bodies of active genes (166), a trait that is largely attributable to an interaction between IN and the host protein LEDGF/ p75 (reviewed in refs. (241, 242)). LEDGF/p75 functions as a bimodal tether during integration: elements within its N-terminal region confer constitutive binding to chromatin, whereas a downstream IBD binds lentiviral IN proteins (173, 243). HIV-1 IN is composed of three domains, the N-terminal domain, the CCD, and the C-terminal domain, and LEDGF/p75 engages IN at a cleft formed through the dimerization of the CCD (183). IN is a highly dynamic protein that functions as a tetramer, and its assembly in the presence of viral DNA is critical to enzyme function (131, 244).

Small molecules that compete for LEDGF/p75 binding enhance IN multimerization in the absence of vDNA and accordingly allosterically inhibit IN activity (230-232). Although various terms, including LEDGINs for LEDGF/p75-IN inhibitors, have been coined for these investigational compounds, we prefer “allosteric IN inhibitor” or ALLINI to highlight the mechanistic basis of compound action (232, 236).

Different classes of antiretroviral drugs display characteristic dose–response curve slopes in antiviral activity assays, which has important implications for the mechanism of drug action. IN is considered a monovalent INSTI target because these compounds display slope parameters of close to 1 (245). Because ALLINIs display significantly steeper slopes, IN by contrast behaves as a multivalent target for this drug class (232). The inhibition of two integration-related functions, IN catalysis and the IN-LEDGF/ p75 interaction, are proposed to underlie the multimodal mechanism of ALLINI action (230-232). Herein we show that ALLINI potency is accounted for during the late stage of HIV-1 replication. The ability for ALLINIs to engage and multimerize IN at a point in the viral life cycle when the virus is apparently unable to interact with the LEDGF/p75 host factor accounts for the unique pharmacology of this class of antiretroviral compounds.

Results

ALLINI potency is accounted for during the late stage of HIV-1 replication.

The ALLINI BI-1001 (Figure 1-6) displayed an effective concentration 50% (EC_{50}) of 5.8 μM in a spreading HIV-1 replication assay (232). IN catalysis is required during the early phase of retroviral replication (199) where the infection of SupT1 cells by an HIV-luciferase (HIV-Luc) reporter virus was potently inhibited by the INSTI RAL (Table 2-1). BI-1001 concentrations of up to 50 μM, by contrast, failed to inhibit HIV-Luc. HIV-Luc producing HEK293T cells were therefore treated with BI-1001, which did not affect the extent of virus accumulation in the cell supernatant. Subsequent challenge of SupT1 cells revealed an EC_{50} of 1.9 ± 0.2 μM despite omitting additional BI-1001 from the target cell cultures (Table 2-1). These results are consistent with a recent report that virus produced in the presence of LEDGIN Cx05045 is noninfectious (231), yet extend it to show that HIV-1 is significantly more vulnerable when it is exposed to an ALLINI in virus producer compared with challenge target cells. Because target cells treated with BI-D (Figure 1-6) are protected from infection by HIV-Luc (236), we next used the more potent compound to dissect the full spectrum of ALLINI action.

BI-D yielded an EC_{50} of 1.17 ± 0.1 μM with an accompanying slope of 1.3 ± 0.2 during the early or acute phase of infection (Figure 2-1, black line, and Table 2-1), indicating that IN in large part behaves as a monovalent target under these conditions (245). The potency of the inhibitor increased ~13-fold, to 0.089 ± 0.023 μM, following titration on HEK293T producer cells. The slope of the dose–response curve, 2.4 ± 0.4, was moreover noticeably greater than 1 (Figure 2-1 solid gray line). Because an EC_{50} of 0.090 ± 0.031 μM with an accompanying slope of 2.8 ± 0.4 was determined in the spreading replication assay (Figure 2-1 dashed gray line), we

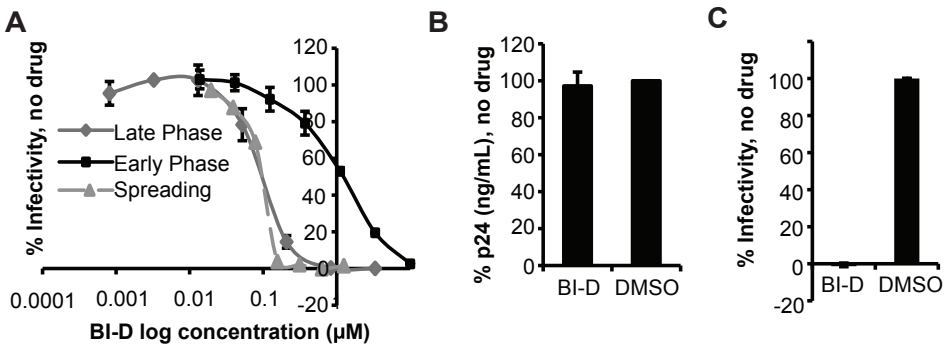

Figure 2-1. BI-D potency is accounted for during the late phase of HIV-1 replication

(A) Dose–response curves under the indicated conditions of drug treatment. Late phase and spreading replication EC_{50} values were not statistically significant (P = 0.94); error bars represent the variation obtained from two to three independent experiments. (B) Release of HIV- 1_{NL4-3} from PBMC cultures following 24 h of BI-D (10 μM) or solvent control treatment at peak of virus replication. (C) Infectivity of ultrafiltered particles from B as assessed in CEMx174 5.25 M7 indicator cells. Results in B and C are averages ± SDs from three independent experiments.

Table 2-1. Antiviral EC_{50} values and slope parameters

	BI-1001		RAL		BI-D	
Treatment condition	EC_{50} (μM)	Slope	EC_{50} (μM)	Slope	EC_{50} (μM)	Slope
Target Cell	>50[a]	NA[b]	0.003 ± 0.001[c]	1.2 ± 0.06[c]	1.17 ± 0.1[c]	1.3 ± 0.2[c]
Producer Cell	1.9 ± 0.2[c]	2.2 ± 0.7[c]	ND[d]	ND[d]	0.089 ± 0.023[c]	2.4 ± 0.4[c]
Replicative Spread	5.8 ± 0.1[e]	3.7 ± 0.2[e]	0.005 ± 0.002[e]	1.1 ± 0.1[e]	0.090 ± 0.031[a]	2.8 ± 0.4[a]

[a]Average ± standard deviation of 2 independent experiments
[b]NA, Not applicable
[c]Average ± standard deviation of 3 independent experiments
[d]ND, Not determined
[e]Data from ref. 232.

conclude BI-D potency is principally accounted for during the late phase of HIV-1 replication. To address physiological relevance, peripheral blood mononuclear cell (PBMC) cultures were treated with 10 μM BI-D, a dose equivalent to ~110 EC_{50} units, during the peak of HIV-1_{NL4-3} replication. Similar levels of HIV-1 were produced from BI-D and DMSO-treated PBMCs (Fig. 1B). Viruses were washed by ultrafiltration to remove excess drug before target cell infection. BI-D treatment rendered HIV-1_{NL4-3} noninfectious (Figure 2-1).

ALLINIs inhibit the formation of the electron-dense HIV-1 core.

Mutational studies provide precedent for the involvement of IN during the late stage of HIV-1 replication. IN mutant viruses are classified I or II based on the nature of associated replication block(s) (150). Class I mutants are specifically blocked for integration, whereas class II mutants are additionally defective for particle assembly/release and/or reverse transcription. The effects of ALLINI treatment were accordingly compared with two class II IN mutant viruses, V165A, which carries a missense mutation in the CCD (246), and ΔIN, which harbors a stop codon at the RT-IN boundary in the pol gene and hence does not express IN (146). Viral protein processing and virion incorporation were analyzed by metabolic labeling followed by immunoprecipitation. Consistent with prior observations (146), IN deletion altered the level of incorporated RT p66/p51 heterodimer (Figure 2-2A, lane 4). Neither BI-D treatment nor the V165A mutation reproducibly affected HIV-1 protein processing or virion incorporation (Figure 2-2, lanes 1–3 and 6–8). The incorporation of HIV-1 genomic RNA into virions was also unaffected by BI-D treatment (Figure 2-2B).

Virion morphology was analyzed by thin-section electron microscopy. Particles purified and concentrated by ion exchange and size exclusion chromatography (247) were categorized as

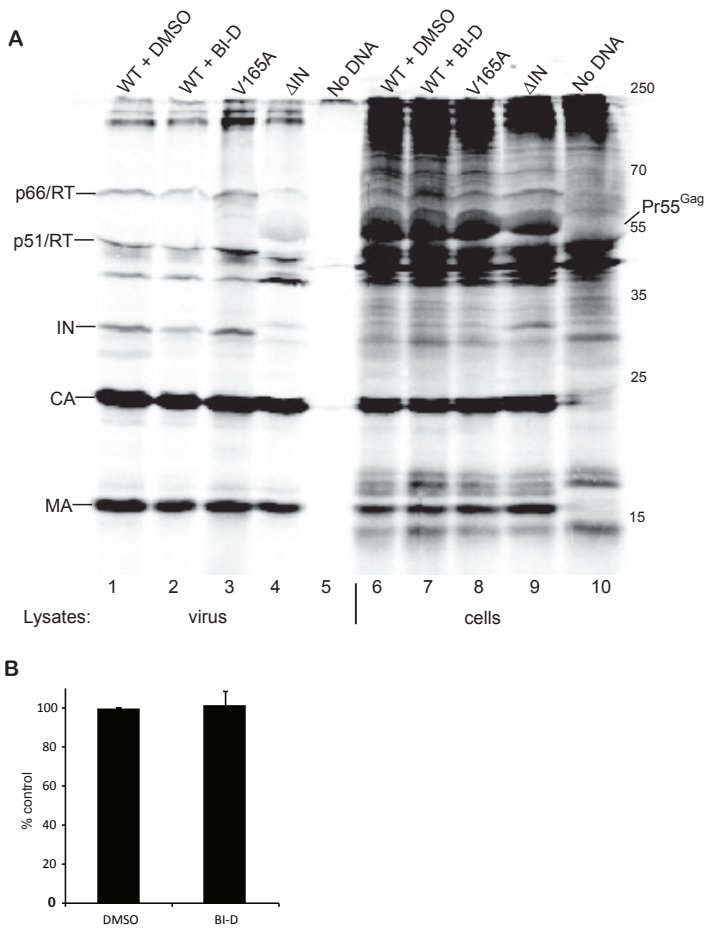

Figure 2-2. BI-D treatment does not affect HIV-1 protein processing or protein or genomic RNA incorporation into virions.

(A) Fluorogram of immunoprecipitated ^{35}S-labeled lysates of cell-free supernatants (lanes 1–5) or corresponding extracts of HEK293T cells (lanes 6–10) transfected with pNL43/XmaI encoding WT IN ± BI-D (lanes 6 and 7), V165A IN (lane 8), ΔIN deletion (lane 9), or no DNA control (lane 10). Migration positions of HIV-1 proteins and mass standards are indicated alongside the gel image. Quantification of IN-to-CA signals indicated no significant differences across lanes 1–3 ($P = 0.23$); results are representative of those obtained in four independent experiments. (B) RNAs isolated from HIV-1_{NL4-3} virions made from transfected HEK293T cells in the presence of DMSO or 10 μM BI-D were assessed for genome content by quantitative PCR. Averages of three independent experiments with associated SD are shown.

(i) mature, containing conical or round cores with associated electron density; (ii) eccentric, with electron dense material situated between translucent cores and the viral membrane; and (iii) immature. Most (93%) HIV-1_{NL4-3} particles were mature, whereas IN deletion yielded gross morphological defects (146): only ~9% of particles were mature, with about 61% and 30% eccentric and immature, respectively (Figure 2-3). The V165A mutation yielded somewhat less intense alterations, with ~18% of particles mature, 70% eccentric, and 12% immature. Similar to the class II mutations, ALLINI treatment significantly enhanced the formation of eccentric HIV-1 cores. BI-D yielded ~8%, 89%, and 3% mature, eccentric, and immature particles, respectively, whereas the values for BI-1001 were ~17%, 76%, and 7% (Figure 2-3).

ALLINI treatment renders HIV-1 defective for reverse transcription and integration.

Quantitative PCR was used to assess the effects of ALLINI treatment on reverse transcription and integration. Primers and probes were designed to detect viral R and U5 (R-U5) sequences indicative of early reverse transcription (ERT) products, the late reverse transcription (LRT) product R-gag, integrated proviruses, and 2-LTR-containing circles that form at low levels in the nucleus through the action of cellular nonhomologous DNA end joining (248, 249). Integration specific blocks yield transient increases in 2-LTR circles due to the increased availability of nuclear viral DNA for cellular DNA metabolism (146, 153).

HIV-Luc supported similar levels of LRT product formation in SupT1 cells treated with DMSO, RAL, or BI-D (Figure 2-4A). BI-D and RAL moreover both inhibited integration (Figure 2-4 B and C); the lack of 2-LTR circle increase in BI-D–treated cultures is likely attributable to relative drug dose (10 μM RAL = 3,333 EC_{50} units, where 10 μM BI-D = 8.5 EC_{50} units; Table 2-1). These results agree with prior reports that ALLINIs behave as

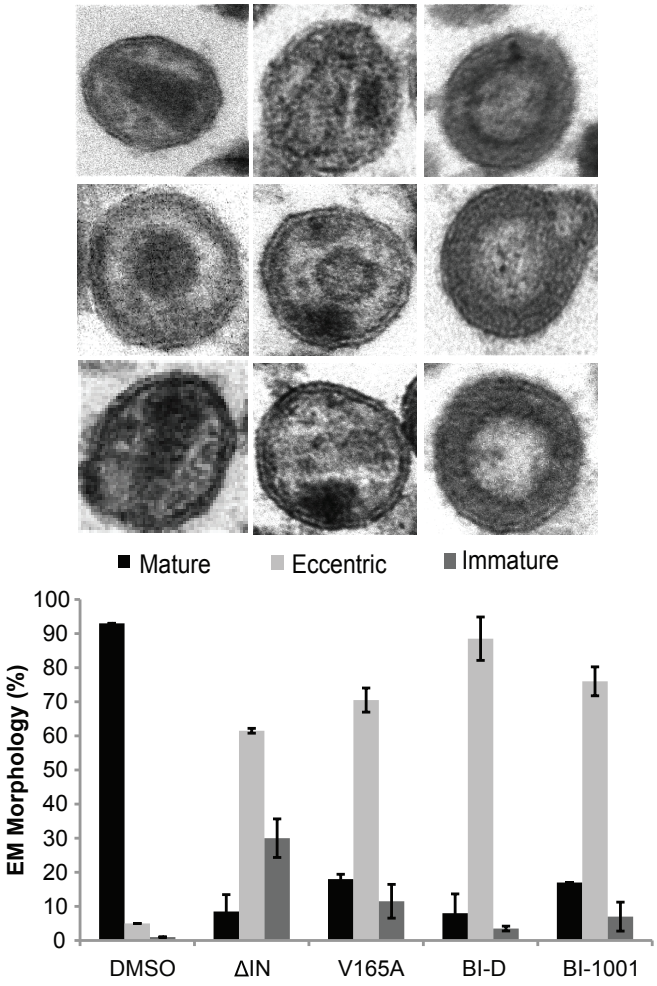

Figure 2-3. ALLINIs inhibit the formation of the electron-dense HIV-1 core.

Upper, representative images of mature, eccentric, and immature particle morphologies. *Lower,* quantitation of core morphology frequencies (average ± SD for n = 2 experiments) for ΔIN, V165A, and wild-type HIV-1_{NL4-3} made in the presence of BI-D (10 μM), BI-1001 (50 μM), or DMSO solvent control. Particles (100 in each experiment) were counted and typed as described in text.

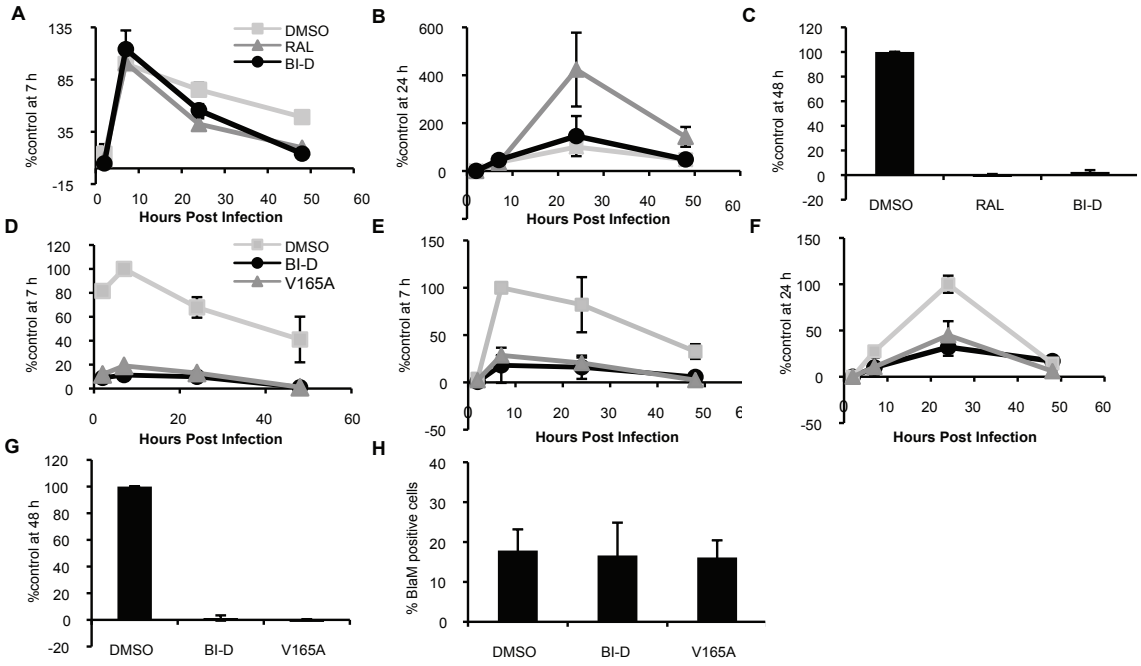

Figure 2-4. BI-D–treated HIV-1 is defective for reverse transcription and integration

(A) DNAs isolated from SupT1 cells infected with HIV-Luc in the presence of DMSO (light gray squares), 10 μM BI-D (black circles), or 10 μM RAL (dark gray triangles) were assessed for LRT product formation by quantitative PCR. (B) Time course of 2-LTR circle formation. (C) Alu-PCR values at 48 h postinfection (DMSO sample set at 100%) for extracts described in A. (D) DNAs isolated from SupT1 cells infected with IN mutant V165A (dark gray triangles), or wild-type HIV-Luc pretreated during virus production with DMSO (light gray squares) or 10 μM BI-D (black circles), were assessed for ERT product formation. (E and F) Levels of LRT and 2-LTR circle product formation, respectively, as a function of time. (G) Alu-PCR values at 48 h postinfection for extracts described in D; values obtained from DMSO-treated HIV-Luc were set at 100%. (H) Percentage of cells positive for betalactamase; similar results were found for HIV-Luc carrying the HIV-1 Env glycoprotein. Results in A and C–G are averages and SDs of two independent infection experiments, with DNA samples queried in duplicate by PCR for each infection; B and H values are averages and SDs from three independent experiments.

integration inhibitors during the acute phase of HIV-1 replication (225, 230). Infection with virions produced in the presence of BI-D revealed strikingly different results. As expected (250), the V165A mutation reduced ERT and LRT product formation by ~70%–80% (Figure 2-4D and E). BI-D–treated virus was also defective for reverse transcription, yielding 11%–18% of the level of ERT and LRT products compared with controls (Figure 2-4 D and E). The DNAs that did form were additionally defective for integration (Figure 2-4 F and G). Both BI-D–treated and V165A mutant virions entered SupT1 cells normally as assessed by the Vpr–beta-lactamase (Vpr-BlaM) fusion protein assay (Figure 2-4H).

IN is the target of ALLINI action during viral egress.

IN is processed from the Gag-Pol polyprotein precursor by the viral PR during HIV-1 maturation (251). To investigate the nature of the drug target, ΔIN virions were transcomplemented with Vpr-IN harboring WT IN or the H171T IN mutant that carries a substitution in the ALLINI binding pocket (Figure 2-5A) and confers ~44-fold resistance to BI-D (226). A similar experimental design previously demonstrated that Gag-Pol, and not IN, was the target of a dominant negative version of the IN-interacting INI1 host factor during HIV-1 egress (252). The ΔIN transcomplemented virions would accordingly resist BI-D action if the precursor Gag-Pol protein were the drug target. BI-D by contrast retained full potency, and the H171T mutation moreover conferred similar drug resistance profiles regardless of its expression in cis from Gag-Pol or in trans from Vpr-IN (Figure 2-6). We therefore conclude that IN is the likely target of BI-D action during the late stage of HIV-1 replication.

Ultrafiltration was used to remove excess compound following incubation with cell-free HIV-Luc to assess virucidal activity. Despite testing concentrations of up to 100 μM, BI-D

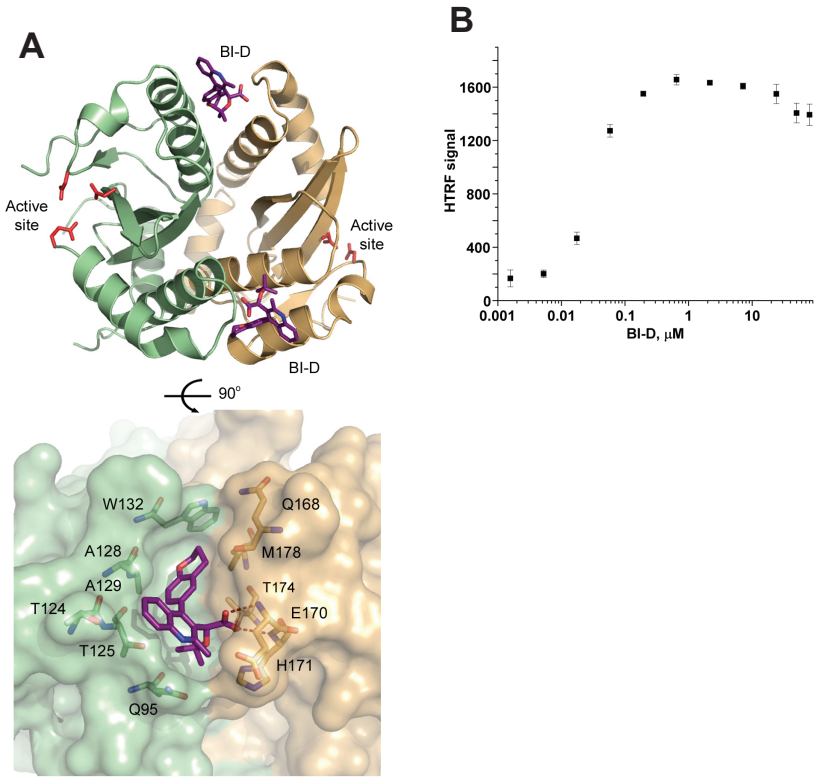

Figure 2-5. BI-D–IN cocrystal structure and influence of BI-D on recombinant IN multimerization

(A, Upper) Ribbon representation of the X-ray crystal structure of the HIV-1 IN CCD with two BI-D molecules (purple sticks) bound at the CCD–CCD interface (pdb code 4ID1). The CCD subunits are colored green and cream, with the carboxylate residues of the enzyme D,D-35-E active site residues in red sticks. (Lower) Rotated close-up view of BI-D within binding pocket. Residues that lie within 4 Å of the drug are highlighted in sticks, with hydrogen bond contacts between the BI-D carboxylate and backbone amides of IN residues Glu170 and His171 in red dashes. (B) Homogenous time resolve fluorescence (HTRF) readout of recombinant IN–IN binding as a function of BI-D concentration. Results are averages ± SD for three independent experiments. The HTRF signal in the absence of drug was 130 ± 16.5.

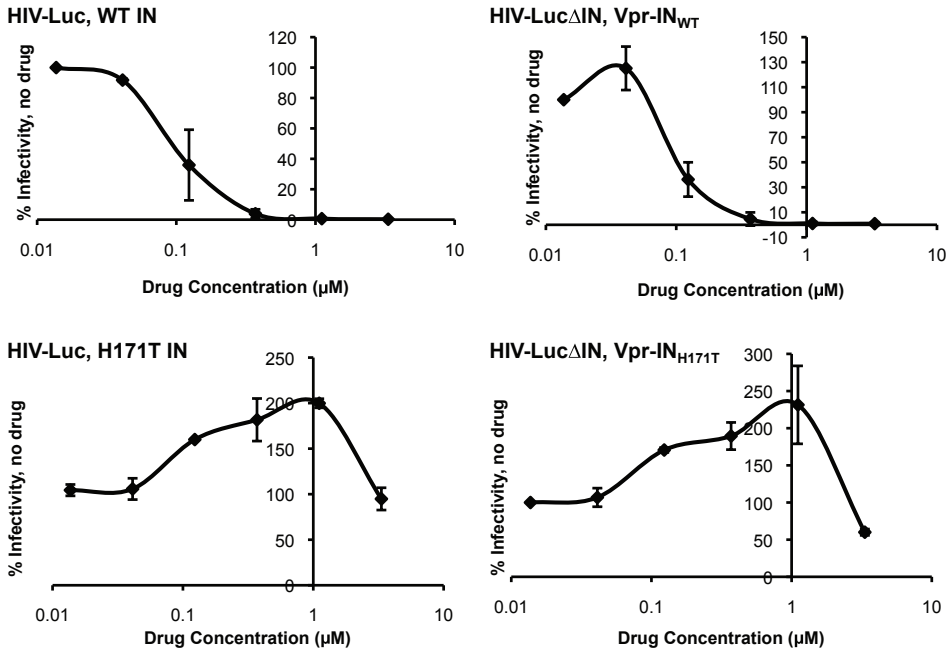

	HIV-Luc		HIV-LucΔIN	
IN	WT	H171T	Vpr-IN$_{WT}$	Vpr-IN$_{H171T}$
EC_{50} (μM)	0.083 ± 0.01[a]	>3	0.065 ± 0.03[a]	>3
Slope	2.4 ± 0.4	NA[b]	2.0 ± 0.3	NA[b]

[a] *P* = 0.33 as determined by a paired sample t-test (two-tailed)
[b] NA, Not applicable

Figure 2-6. IN serves as the BI-D target during HIV-1 production

HEK293T cells expressing HIV-Luc carrying WT or H171T IN, or HIV-LucΔIN transcomplemented with Vpr-IN$_{WT}$ or Vpr-IN$_{H171T}$, were treated with the indicated concentrations of BI-D. Following transduction of SupT1 cells, the resulting levels of luciferase activity were normalized to control viruses constructed in the presence of DMSO. BI-D concentrations in the range of 0.05–1.0 μM, which inhibit WT IN containing viruses, stimulate H171T-expressing viral infectivities by ~2.0–2.5-fold in biphasic fashion. Lower table, calculated EC_{50} values and slope parameters. Results are averages ± SD from three independent experiments.

antiviral activity was not detected. Consistent with its low micromolar virucidal activity (253), the nonnucleoside RT inhibitor (NNRTI) efavirenz (EFV) yielded an EC_{50} of 4.2 ± 3.5 μM (n = 3).

ALLINI potency is independent of LEDGF/p75 expression level during HIV-1 production.

LEDGF/p75 and ALLINIs compete for binding to a pocket formed through the dimerization of the HIV-1 IN CCD (183, 225) (Figure 2-5A). To address if LEDGF/p75 affects BI-D potency, EC_{50} values were assessed in constitutively knocked down versus control HEK293T cells (176) (Figure 2-7). Consistent with results using mouse knockout cells (236), LEDGF/p75 knockdown yielded a significant 29-fold increase in BI-D potency during the acute phase of HIV-1 infection, whereas RAL potency was unaffected (Table 2-2). By contrast, LEDGF/p75 depletion did not significantly alter BI-D potency during HIV-1 production. Potency during the acute phase of HIV-1 infection in LEDGF/p75-depleted cells was moreover similar to BI-D titer during virus production regardless of LEDGF/p75 expression level (Table 2-2).

Purified protein and virion-associated IN are oligomerized by BI-D treatment.

Integration is catalyzed by an IN tetramer (134); in the absence of vDNA, recombinant HIV-1 IN assumes a variety of multimeric forms, from monomer to higher-order oligomers, depending on buffer conditions and protein concentration (254). Resonance transfer-based assays previously demonstrated that ALLINIs promote IN multimerization (230-232). HTRF (232) accordingly yielded an in vitro stimulatory concentration 50% of 0.027 ± 0.003 μM with an

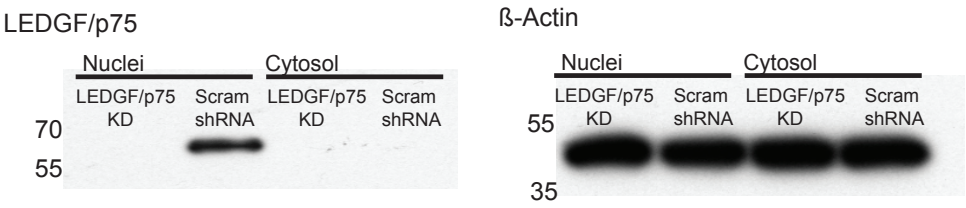

Figure 2-7. Characterization of LEDGF/p75 knockdown cells

Western blot of LEDGF/p75 (60.1 kDa) expression in nuclear and cytoplasmic extracts of constitutively knocked down 293T-si1340/1428 and 293T-siScram control cells. β-Actin (47 kDa) was blotted as a loading control (Right).

Table 2-2. LEDGF/p75 expression level does not influence BI-D titer during the late phase of HIV-1 replication

	RAL		BI-D	
Treatment condition	EC_{50} (μM)	slope	EC_{50} (μM)	slope
293T-si1340/1428 target cell	0.009 ± 0.001[a]	0.86 ± 0.13	0.131 ± 0.003[b,d,e]	0.85 ± 0.05
293T-siScram target cell	0.01 ± 0.001[a]	0.94 ± 0.86	3.8 ± 1.1[b]	1.27 ± 0.67
293T-si1340/1428 producer cell	ND[f]	NA[g]	0.161 ± 0.05[c,d]	2.40 ± 0.41
293T-siScram producer cell	ND[f]	NA[g]	0.144 ± 0.07[c,e]	2.44 ± 0.12

[a] $P = 0.79$
[b] $P = 0.016$
[c] $P = 0.56$
[d] $P = 0.46$
[e] $P = 0.84$
[f] ND, Not determined
[g] NA, Not applicable

accompanying slope of 1.97 ± 0.36 for BI-D (Figure 2-5B), and the compound expectedly cocrystallized in the LEDGF/p75 binding pocket at the CCD dimer interface (Figure 2-5A). Size exclusion chromatography was used to monitor distinct protein species, which revealed that BI-D effectively converted IN tetramers to higher-order oligomers (Figure 2-8A). To assess effects of ALLINI treatment on IN multimerization during virus production, reducing agent was omitted from virion lysates (255), which revealed ~3-fold enhancement of IN dimer formation by BI-D (Figure 2-8B, lanes 1–6). The substitution of Asp at position 124 in the ALLINI binding pocket (Figure 2-5A), which confers ~250-fold resistance to BI-D (226), importantly negated compound-induced IN multimerization in vitro and in virions (Figure 2-8 A and B).

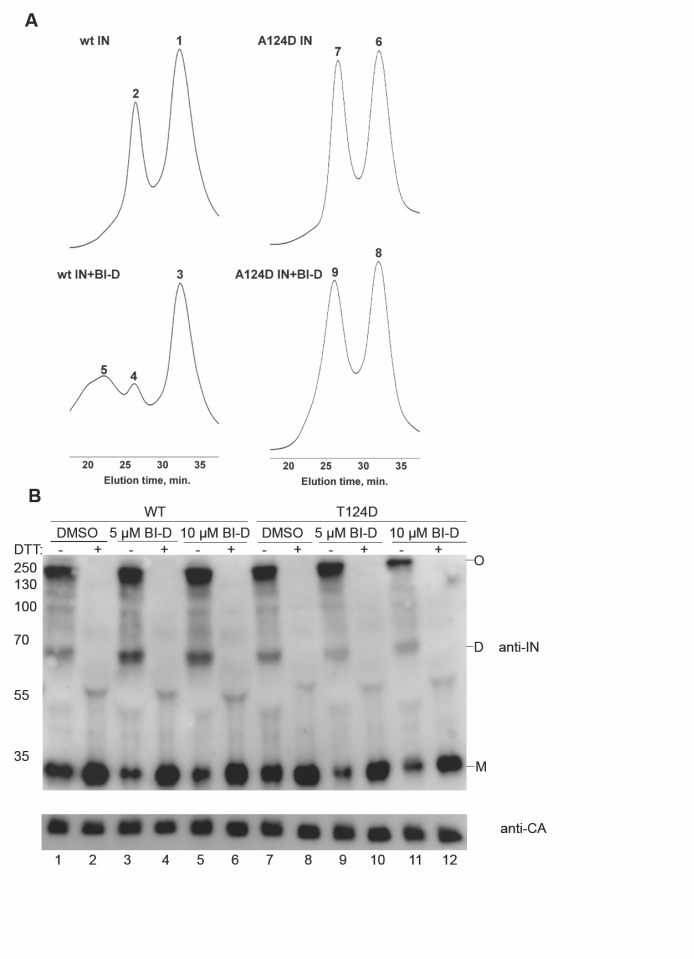

Figure 2-8. BI-D enhances the formation of IN oligomers

(A) Elution profiles of purified wild-type (WT) and A124D mutant IN (20 μM) in the absence of drug (*Upper*) or in the presence of 10 μM BI-D. (B) Wild-type HIV-1_{NL4-3} and IN mutant T124D (position 124 is polymorphic; HIV-1_{HXB2} carries Ala where HIV-1_{NL4-3} harbors Thr) made in the presence of DMSO solvent control or 5 μM or 10 μM BI-D as indicated were prepared with and without DTT reducing agent in the SDS/PAGE sample buffer. Upper, blot was probed with anti-IN monoclonal antibody 8E5; *Lower*, blot probed with anti-p24 antibody. Results are representative of three independent experiments. D, IN dimer; M, IN monomer; O, IN oligomer.

Discussion

Some antiretroviral drugs, like potent NNRTIs, display weak activities (<1% of full potency) against secondary steps in the viral lifecycle (256). Low micromolar styrylquinoline-based IN inhibitors can inhibit recombinant IN nuclear transport in vitro (257) and reverse transcription and integration during HIV-1 infection (258), although the contributions of these different activities to compound potency have remained unclear (259). The results reported here differ starkly from these prior reports: ALLINI potency is determined through the inhibition of viral core maturation, a step in the HIV-1 lifecycle that is clearly distinct from the catalytic requirement for the targeted IN enzyme (Figures 2-1 and 2-3 and Table 2-1). We expect that future allosteric inhibitors of viral targets will similarly unveil the versatile nature of these compounds to primarily inhibit replication in unanticipated ways. Because styrylquinolines harbor the quinoline pharmacophore common to many ALLINIs (Figure 1-6), it will be instructive to ascertain if they too impact late events in HIV-1 replication.

Although there is strong consensus for a role for LEDGF/p75 during the early phase of HIV-1 replication, a potential postintegration role for this protein is less clear. Expression of a LEDGF/ p75-binding peptide in virus producer cells reduced HIV-1 infectivity (260). Overexpression of IBD-containing dominant interfering fragments by contrast potently restricted HIV-1 ingress, but not egress (186). Our finding that BI-D potency is unchanged by depleting LEDGF/p75 from virus producer cells is consistent with the fact that the IBD and ALLINIs engage the same CCD binding pocket on IN. We therefore conclude that ALLINI-mediated multimerization of IN through CCD dimer binding in the absence of competing LEDGF/p75 protein during HIV-1 egress underlies the multimode mechanism of ALLINI action. Although our work indicates that inhibition of the interaction between IN and LEDGF/p75 or its close

relative hepatoma-derived growth factor related-protein (HRP)-2 does not significantly contribute to ALLINI potency (236) (Table 2-2), it nevertheless underscores the utility of searching for inhibitors of protein–protein interactions. ALLINIs can block the interaction between a physiologically relevant host factor and a viral protein dimerization interface, and we speculate that small molecules that block interactions between binding partners and target multimerization interfaces will allosterically alter target function even when the binding partner (e.g., recombinant antibody) plays a limited physiological role.

INSTIs display slope parameters of ~1 because each infectious particle yields a single intasome (129, 245). The underlying theme for steeper slopes, participation of multiple copies of the drug target in the relevant step of the lifecycle (245), is consistent with the results reported here for ALLINIs. The cooperative behavior of ALLINIs in IN multimerization assays (232) (Figure 2-5B), combined with the apparent inability of LEDGF/p75 to engage HIV-1 during virus egress, determines ALLINI potency (EC_{50} and slope parameter). Because LEDGF/p75 depletion from target cells sharply increases BI-D EC_{50} values, the host factor competes with the drug for binding to the CCD dimer interface during the acute phase of infection (236). The slope of the dose–response curve remains close to 1 under this condition (Table 2-2) because only a minor fraction of the IN during viral ingress is required for intasome formation. IN therefore is a monovalent target of INSTIs and ALLINIs during the early phase of HIV-1 replication, where both types of compounds specifically target integration. We consider that inhibition of multiple viral replication steps (core formation, reverse transcription, and integration) could also contribute to the multimode mechanism of ALLINI action.

Whereas INSTIs recapitulate the phenotype of class I IN mutant viruses, our findings highlight that ALLINI treatment during HIV-1 production induces the class II IN mutant viral

phenotype (Figure 2-3 and 2-4). The behavior of certain class II mutant viruses indicated a potential role for IN during the late stage of HIV-1 replication (150), although the underlying mechanism has remained elusive. The particle release defect of IN deletion mutant viruses is overridden by inhibiting PR activity (158), and suboptimal concentrations of PR inhibitors can yield the eccentric core morphology described here (162). One interpretation of our results is an active role for IN in the formation of the electron-dense HIV-1 core. However, structural rearrangements subsequent to Gag and Gag-Pol proteolysis that underlie HIV-1 core formation might by contrast be particularly sensitive to deregulated IN multimerization. Concordantly, a variety of mutations that either enhance or inhibit IN oligomerization confer the class II IN mutant phenotype (261-264). Although we cannot rule out that ALLINIs engage the IN domain of the Gag-Pol precursor protein before proteolysis, the results of Vpr-IN complementation assays indicate that the drug target during HIV-1 production is the postcleavage IN protein (Figure 2-6). ALLINIs lack virucidal activity because mature HIV-1 particles have proceeded past the point in the lifecycle where IN unveils a CCD–CCD Achilles' heel for engagement by small molecule inhibitors. Further evaluation of class II mutant viruses may shed additional light on the multimode mechanism of ALLINI action. Hypersensitivity to multimerization inducing small molecules during viral egress highlights IN as an attractive target for clinical ALLINI development.

Materials and Methods

Plasmids and antivirals

Plasmids pNL43/XmaI (265) and pNLX.Luc.R- (250) encode for HIV-1_{NL4-3} and single-round HIV-Luc, respectively. FLAG-tagged HIV-1_{NL4-3}-based bacterial IN expression vector was described previously (232); pCPH6PHIV1-IN (266) was used to express hexahistidine (His6) tagged HIV-1_{HXB2}-based IN. Position 124 in IN, where notable ALLINI resistance can arise (226), is polymorphic (Thr in HIV-1_{NL4-3}; Ala in HIV-1_{HXB2}). Plasmid pMM310, which expresses the BlaM-Vpr fusion protein, was described (267), as were plasmids for expressing vesicular stomatitis virus G (VSV-G) and HIV-1 Env glycoproteins (250). Plasmid pNL43/XmaI encoding the V165A IN mutation was described (246); ΔIN deletion and T124D missense mutations were made by PCR-directed mutagenesis. The following plasmids were also altered by PCR mutagenesis to confer the associated IN changes: A124D in pCPH6P-HIV1-IN, and H171T in pRL2PVpr-IN (268) and pNLX.Luc.R-. Targeted mutations and absence of unwanted secondary changes were confirmed by dideoxy sequencing.

BI-1001 and BI-D were synthesized as described (232, 236). RAL and EFV were obtained from the National Institutes of Health AIDS Research and Reference Reagent Program.

Cells, viruses, and antiviral assays

HEK293T cells were grown in Dulbecco's modified Eagle medium (DMEM) supplemented to contain 10% (vol/vol) fetal bovine serum (FBS), 100 IU/mL penicillin, and 100 μg/mL streptomycin. HEK293T cells that stably express LEDGF/p75-targeting shRNAs (293Tsi1340/1428) and a scrambled control sequence (293T-siScram) (176) were additionally maintained with 3 μg/mL puromycin–500 μg/mL hygromycin B and 500 μg/mL hygromycin B,

respectively. PBMCs isolated from human blood (Research Blood Components), SupT1 cells, and CEMx174 5.25 M7 indicator cells (269) were maintained in RPMI medium 1640 containing 10% FBS, 100 IU/mL penicillin, and 100 μg/mL streptomycin. PBMCs were stimulated with phytohemagglutinin (5 μg/mL) for 48 h before infection.

HIV-1_{NL4-3} infectivity (0.5 ng p24/mL) was determined using CEMx174 5.25 M7 indicator cells. HIV-Luc was pseudotyped by cotransfecting HEK293T cells with pNLX.Luc.R- and an Env expression vector (HIV-1_{NL4-3} or VSV-G) using FuGENE 9 (Promega) (250). DMSO and ALLINIs were maintained in media throughout transfection procedures. Cell-free virus concentration, typically 500–800 ng/mL, was determined using a commercial p24 ELISA kit (Advanced Biosciences Laboratories). SupT1 (2×10^5/mL), CEMx174 5.25 M7 (2×10^5/mL), and shRNA-expressing HEK293T (1.5×10^5/mL) cells were infected in triplicate with 5 ng/mL p24, unless specified otherwise. Where indicated, compound or DMSO was added to target cells at the time of infection. Luciferase values, expressed as relative light units, were determined 48 h postinfection. Virucidal activity was analyzed after 1 h incubation with drug at 37 °C. Drug was removed before infection via three rounds of successive ultrafiltration in 100 kDa concentrators (Amicon), theoretically yielding a 28,000-fold reduction in the concentration of flow-through molecules. Stimulated PBMCs were infected with HIV-1_{NL4-3} (500 ng/mL p24) for 2 h. Residual virus was removed by washing cells three times. At the peak of replication (7 d postinfection), cells were washed before DMSO control or BI-D (10 μM) addition, and supernatant collected 24 h later was ultrafiltered to remove excess drug.

DNA and RNA analysis

DNA was extracted from SupT1 cells infected with ultrafiltered, DNase-treated (1 h at 37 °C) HIV-Luc (100 ng p24/mL) using the DNeasy blood and tissue kit (Qiagen). Parallel infections were performed in the presence of 10 μM EFV to account for residual plasmid after DNase treatment, and values obtained from separate PCR assays were subtracted from experimental samples. Duplicate PCRs containing 25 ng DNA, 0.2 μM primers, 0.1 μM probe and 1× QuantiTect Probe PCR Master Mix were incubated at 50 °C for 2 min and 95 °C for 15 min, followed by 40 cycles of 94 °C for 15 s, 58 °C for 30 s, and 72 °C for 30 s. Standards were prepared by diluting pNLX.Luc.R- (early and late reverse transcription) or pUC19.2LTR [2-LTR circles] (250) in DNA from uninfected cells. Primers AE2963/AE4422 and probe AE2965 were used to detect late reverse transcripts, whereas primers AE989/AE990 with probe AE995 were used for early reverse transcripts (116); 2–LTR circles were detected using primers AE4450/AE4451 with probe AE4452. Integration efficiency was measured by nested Alu-PCR; first round reactions used primers AE3014/AE1066, and second round real-time reactions contained primers AE3013/AE990 and probe AE995 (105). Integration standards were made by diluting DNAs from cells infected with wildtype virus under DMSO control conditions with DNA from uninfected cells. Values obtained from parallel reactions that omitted Alu-specific AE1066 primer from first round samples were subtracted from experimental Alu-PCR values.

RNA was extracted from DNase-treated HIV-1_{NL4-3} (250 ng p24) made in the presence of DMSO solvent control or 10 μM BI-D using the viral RNA extraction kit (Qiagen). Triplicate PCRs containing 25 ng RNA, 0.2 μM of AE2963 and AE4422 primers, and 1× SYBR green Master Mix (Qiagen) with and without the supplied 1× RT mix were incubated at 50 °C for 30 min and 95 °C for 15 min, followed by 40 cycles of 96 °C for 15 s, 55–90 °C for 30 s, and 72 °C

for 30 s. Genomic standards were made by diluting RNAs from the supernatant of cells transfected with pNL43/XmaI under DMSO control conditions. To account for signal from plasmid DNA that potentially remained from DNA transfection, values obtained in the absence of the RT mix were subtracted from the values obtained in the presence of the RT mix.

Virion analyses

HEK293T cells (9×10^5) were transfected with pNL4-3/XmaI-based plasmids (4.4 μg) using FuGENE 9. Cell-free HIV-1_{NL4-3} was purified from transfected HEK293T cell supernatants by ion exchange and size exclusion chromatography as described (247) before fixation and submission to the Harvard Medical School Electron Microscopy core facility. Images were taken with a JEOL 1200EX microscope equipped with an AMT 2k charge-coupled device camera. Images were visually scanned to count 100 viral particles per virus preparation.

Vpr complementation assays

HIV-1NLX.Luc.R-.ΔIN was transcomplemented with Vpr-IN by cotransfecting HEK293T cells with 1.8 μg pNLX.Luc.R-.ΔIN, 0.4 μg pRL2P-Vpr-IN containing the wild-type IN or H171T mutation, and 0.2 μg VSV-G expression vector. SupT1 cells (2×10^5/mL) were infected in triplicate with 5 ng/mL p24, and luciferase activities in cell extracts were determined at 48 h postinfection. HIV-1 entry was quantified by the Vpr-BlaM assay essentially as previously described (270). SupT1 cells infected for 4 h at 37 °C with 15 ng p24/mL HIV-Luc were washed and brought to room temperature before loading with the fluorogenic CCF2-AM substrate (Promega). Beta-lactamase activity was determined after 18 h via flow cytometry (BD Biosciences).

Radiolabeling and immunoprecipitation.

Transfected HEK293T cells were metabolically labeled with [^{35}S]Cys and [^{35}S]Met (50 μCi/mL each) at 24 h posttransfection for 16 h in Met−Cys− DMEM. BI-D was maintained at 10 μM throughout transfection and labeling. Viral particles were pelleted from cell-free supernatants by ultracentrifugation at 4 °C for 1.5 h in a Beckman SW55 rotor at 27,000 rpm. Pelleted virions and cells were lysed in buffer containing 0.3 M NaCl, 50 mM Tris·HCl, pH 7.5, 0.5% Triton X-100, 0.2 mM 4-(2-aminoethyl)benzenesulfonyl fluoride (AEBSF), and 100 μg/mL leupeptin. Cell lysates were precleared with 50 μL protein A-Sepharose CL-4B beads (GE Healthcare) hydrated in PBS before immunoprecipitation. Viral and cell lysates were immunoprecipitated using antiserum from patients with AIDS (National Institutes of Health AIDS Research and Reference Reagent Program). Following extensive washing, proteins boiled from Sepharose beads were separated by SDS/ PAGE, and images of dried gels were developed using a Storm 820 PhosphorImager; signal intensities were determined using ImageQuant version 1.2 (GE Healthcare).

Western blotting

HEK293T cell supernatants from pNL43/XmaIbased transfections (9×10^5 cells) were pelleted by ultracentrifugation at 4 °C for 1.5 h in a Beckman SW55 rotor at 27,000 rpm. Pelleted virions were lysed in 20 μL SDS/PAGE sample buffer (0.3125 M Tris·HCl pH 6.8, 2% SDS, 10% (wt/vol) glycerol, 0.001% bromophenol blue) ± DTT. Lysed virions were fractionated by SDS/PAGE before immunoblotting IN with mouse monoclonal antibody 8E5 (271) at 1:5,000 dilution. For LEDGF/p75 detection, cells were fractionated as described (272), and cytosolic and

nuclear extract protein concentrations were determined by Bradford assay (Pierce); 2 μg and 10 μg of nuclear and cytoplasmic extract, respectively, was probed using a 1:10,000 dilution of anti LEDGF/p75 antibody A300-848 (Bethyl Laboratories). HRP-conjugated secondary antibodies (Dako) were used at 1:10,000.

Homogeneous time resolved fluorescence and size exclusion chromatography

Recombinant FLAG and His6-tagged HIV-1 IN proteins for HTRF assays were purified following expression in *Escherichia coli* as described previously (232). The IN–IN interaction HTRF assay was performed as described, with signals recorded on a Perkin-Elmer Multimode Enspire plate reader (232). WT and A124D INs for size exclusion chromatography (SEC) experiments were purified according to the method of Pandey et al. (273). SEC was performed over a Superdex 200 10/300 GL column (GE Healthcare) operated at 0.5 mL/min in buffer containing 20 mM Hepes, pH 6.8, 750 mM NaCl, 10 mM $MgSO_4$, 0.2 mM EDTA, 5 mM β-mercaptoethanol and 5% glycerol at 4 °C. IN (20 μM) was preincubated for 30 min with 10 μMBI-D or DMSO solvent control before column injection. Protein elution was monitored by A280.

X-Ray crystallization and structure determination

The HIV-1 IN CCD (residues 50–212) containing the solubilizing F185K substitution was purified following expression in *E. coli* as described (123). The protein, concentrated to 8 mg/mL, was crystallized at 4 °C using hanging drop diffusion against crystallization buffer containing 0.1 M Na cacodylate, pH 6.5, 0.1 M ammonium sulfate, 10% (wt/vol) polyethylene glycol 8000, and 5 mM DTT. Crystals reached 0.1–0.2 mm within 4 wk. Crystals were soaked in

5 mM BI-D dissolved in crystallization buffer containing 10% (vol/vol) DMSO for 8 h before flash freezing in liquid N_2. Diffraction data were collected at 100 F on a Rigaku Raxis 4++ image plate detector at The Ohio State University Crystallography facility. Data intensity integration and reduction were performed using HKL2000 (274). The structure was solved by molecular replacement using Protein Data Bank (pdb) code 1ITG (123) with Phaser (275) in the CCP4 package (276). Coot (277) was used for subsequent refinement and to build the structure. Coordinates have been deposited in the Protein Data Bank under accession number 4ID1.

Statistical analysis. Significant differences between data groups were determined by a paired-sample t test (two-tailed).

Chapter 3

Distribution and redistribution of HIV-1 nucleocapsid protein in immature, mature, and integrase-inhibited virions: a role for integrase in maturation

Distribution and redistribution of HIV-1 nucleocapsid protein in immature, mature, and integrase-inhibited virions: a role for integrase in maturation

Juan Fontana[a]*, Kellie A. Jurado[b]*, Naiqian Cheng[a], Ngoc L. Ly[b], James R. Fuchs[c], Robert J. Gorelick[d], Alan N. Engelman[b], and Alasdair C. Steven[a]

** These authors contributed equally.*

[a]Laboratory of Structural Biology Research, National Institute of Arthritis, Musculoskeletal and Skin Diseases, National Institutes of Health, Bethesda, MD 20892, USA; and [b]Department of Cancer Immunology and AIDS, Dana-Farber Cancer Institute, Boston, MA 02215, USA; and [c]Division of Medicinal Chemistry and Pharmacognosy, College of Pharmacy, The Ohio State University, Columbus, OH 43210, USA; and [4]AIDS and Cancer Virus Program, Leidos Biomedical Research, Inc., Frederick National Laboratory for Cancer Research, Frederick, MD 21702-1201, USA.

** This chapter is adapted from the manuscript:

Fontana J, Jurado KA, Cheng N, Ly NL, Fuchs JR, Gorelick RJ, Engelman A and Steven AC. Distribution and Redistribution of HIV-1 Nucleocapsid Protein in Immature, Mature, and Integrase-inhibited Virions: A Role for Integrase in Maturation. *Journal of Virology,* 89(19):9765-80.

Contributions: I preformed experiments associated with Figures 3-1, 3-4B and C, 3-7 and 3-8. I prepared the HIV-1 virion preparations used for microscopy for all other figures. Juan Fontana, Alasdair Steven, Alan Engelman and I wrote the manuscript.

Abstract

During virion maturation, HIV-1 capsid protein assembles into a conical core containing the vRNP complex, thought to be composed mainly of the vRNA and NC. After infection, the viral RNA is reverse-transcribed into double-stranded DNA, which is then incorporated into host chromosomes by IN catalysis. Certain IN mutations (class II) and antiviral drugs (ALLINIs) adversely affect maturation, resulting in virions that contain "eccentric condensates", spherical electron-dense aggregates located outside electron-translucent cores. Here we demonstrate that in addition to the mislocalization of electron density, a class II IN mutation and ALLINIs each increase the fraction of virions with malformed cores (from ~12% to ~53%). Eccentric condensates have a high NC content as demonstrated by "tomo-bubblegram" imaging, a novel labeling technique that exploits NC's susceptibility to radiation damage. Tomo-bubblegram imaging also localized NC inside wild-type cores and lining the spherical Gag shell in immature virions. We conclude that eccentric condensates represent non-packaged vRNPs and that either genetic or pharmacological inhibition of IN can impair vRNP encapsidation. Supplying IN in trans as part of a Vpr-IN fusion protein partially restored the formation of conical cores with internal electron density and the infectivity of a class II IN deletion mutant virus. Moreover the ability of ALLINIs to induce eccentric condensate formation required both IN and viral RNA. Based on these observations, we propose a role for IN in initiating core morphogenesis and vRNP encapsidation during HIV-1 maturation.

Introduction

The formation of infectious HIV-1 particles starts with the co-assembly of the Gag and Gag-Pol polyproteins into a spherical shell, which buds from the cell to produce an immature virion (251). Following budding, the viral PR is activated and cleaves Gag and Gag-Pol into their component domains, of which the capsid protein CA assembles into a conical capsid shell containing the vRNA genome, NC, and replication enzymes (we use the term CA to denote the assembled protein shell and core for the CA plus whatever it may contain). This transformation is known as HIV-1 maturation. Drawing mainly on studies by cryo-electron tomography (cryo-ET), a technique that allows 3D imaging of individual pleomorphic particles with good preservation of native structure (e.g. (278)), a number of different models explaining how CA can assemble into conical cores have been proposed (59, 60, 279, 280). However, maturation – which is the process targeted not only by protease inhibitors (PIs) (281) but also by 'maturation inhibitors' that act by denying PR access to a key cleavage site (282, 283) – is incompletely understood.

Mutational studies of the viral enzyme IN have demonstrated that the effects of some amino acid substitutions – the so-called class II IN mutations – include defects in particle assembly and reverse transcription (compared to class I IN mutations, which only affect integration) [reviewed in (150)]. Class II IN mutant viruses provided an initial clue for a role of IN in the late stages of replication, including maturation. More recently, a group of investigational compounds, 2-(quinolin-3-yl) acetic acid derivatives, which we refer to as ALLINIs (232) but are also called NCINIs for non-catalytic site IN inhibitor (284), LEDGINs for LEDGF-IN inhibitor (225), INLAIs for IN-LEDGF/p75 allosteric inhibitors (234), and MINIs for multimeric IN inhibitors (228), were found to inhibit HIV-1 infection (225, 229).

ALLINIs engage the interface that is formed by two molecules of the IN catalytic core domain at the binding pocket for the cellular integration co-factor LEDGF/p75 (225, 228, 230, 232-235), which itself guides vDNA integration to active genes [reviewed in (285)]. Inhibition of the LEDGF/p75-IN interaction was initially thought to underlie the mode of ALLINI action (225). However, the compounds were since discovered to affect the late stage of HIV-1 replication in a manner that is independent of LEDGF/p75 expression (180, 228, 233, 284, 286). The compounds are also active during the early stage of HIV-1 replication, but require much higher concentrations to achieve similar potencies as compared to when virus producer cells are treated (180, 228, 233-235, 284, 286). Akin to several class II IN mutant viruses, particles produced in the presence of ALLINIs are reportedly defective for multiple steps of HIV-1 replication, i.e.: maturation (228, 233, 284, 286), reverse transcription (228, 233, 284, 286), nuclear import of the vDNA (286), and integration (225, 228, 230, 233, 234, 284, 286). The ability of ALLINIs to induce higher-order IN oligomerization during virus production underlies their antiviral activity (228, 230-235, 237, 284, 286).

Transmission electron microscopy of thin sections of plastic embeddings (referred to hereafter as TEM) of HIV-1 particles generated in the presence of ALLINIs revealed an apparent uncoupling of the incorporation of the vRNP complex - assumed to be composed primarily of vRNA and NC – from assembly of the capsid (228, 233, 284, 286). Instead of a normal electron-dense core, a relatively electron-translucent core was observed, accompanied by a roughly spherical electron-dense feature, situated between the viral envelope and the translucent core. We refer to this feature as an “eccentric condensate”. It follows that ALLINIs can be useful probes to help understand how IN contributes to maturation, in a similar way that maturation inhibitors (which prevent the scission of the CA-SP1 junction within Gag, the final proteolytic cleavage

that leads to the generation of a mature core (287, 288), or mutations that prevent the cleavage of the Pol polyprotein (289, 290), have provided structural insights.

In this study, we first analyzed the relationships between core formation, reverse transcription, and infectivity of ALLINI-treated particles, and conclude from dose-response curves that inhibition of particle maturation is the process that underlies the potencies of two representative ALLINI compounds. Using cryo-ET, we found that, in addition to affecting vRNP incorporation into the mature core, ALLINIs reduced by a factor of approximately five the efficiency with which conical cores are formed. To demonstrate that the eccentric condensate is indeed composed of NC and RNA, we applied tomo-bubblegram imaging, a novel technique that takes advantage of the acute sensitivity of NC protein to electron irradiation expressed in the generation of bubbles as radiation damage products. The same approach confirmed that NC – and by inference, the vRNP – is present inside wildtype cores, predominantly at the wide end; and that NC lines the inner part of the thick-walled Gag shell in immature virions. Using Vpr-IN to functionally transcomplement particles that lack IN (ΔIN), we also show that IN promotes conical core formation and HIV-1 infectivity in parallel. Furthermore, we implicate vRNA as a necessary component for ALLINI action during virus production. Together, these results imply that IN has a direct role in nucleating the assembly of conical cores and the incorporation of the vRNP into the mature core; and that ALLINI treatment effectively subverts this role(s) of IN during HIV-1 particle maturation.

Results

Inhibition of virion maturation underlies ALLINI potency

ALLINIs have been reported to inhibit multiple aspects of HIV-1 replication including virion maturation, reverse transcription, nuclear import, and integration (see Introduction), suggesting that it may be the combination of multiple inhibitory processes that underlies ALLINI potency. An alternative scenario is that inhibition may be due to a single dominant or bottleneck step, which in this case would be particle maturation, as it is the first step inhibited from the perspective of the virus producer cell. To investigate this possibility, we compiled dose-response curves measuring the first two steps affected by ALLINIs - maturation and reverse transcription - and compared them to overall antiviral activity as assessed by the expression of the luciferase reporter gene in cells infected with drug-treated HIV-Luc particles. If maturation is a bottleneck step, we anticipated that its inhibition would equate with antiviral potency. If inhibition of multiple steps is involved, then the maturation and reverse transcription inhibitory curves would individually be less potent than overall antiviral activity.

HIV-Luc was produced in the presence of two representative ALLINI compounds, BI-D, with an EC_{50} for inhibition of HIV-1 infection of 89 nM, and BIB-2 (also known as ALLINI-2), with an EC_{50} of 630 nM (236, 237) (Figure 1-6), at varying EC_{50} doses (1X, 2X, 4X, and 8X). TEM analysis of virus made in the presence of solvent control DMSO revealed that 87 ± 2% of these particles harbored mature cores with internal density. This value decreased by ~ 50% when virus was produced with unit EC_{50} concentrations of BI-D or BIB-2, with accompanying increases in particles containing eccentric condensates (Figure 3-1A). Higher doses of each compound further reduced the fraction of mature cores and increased the fraction

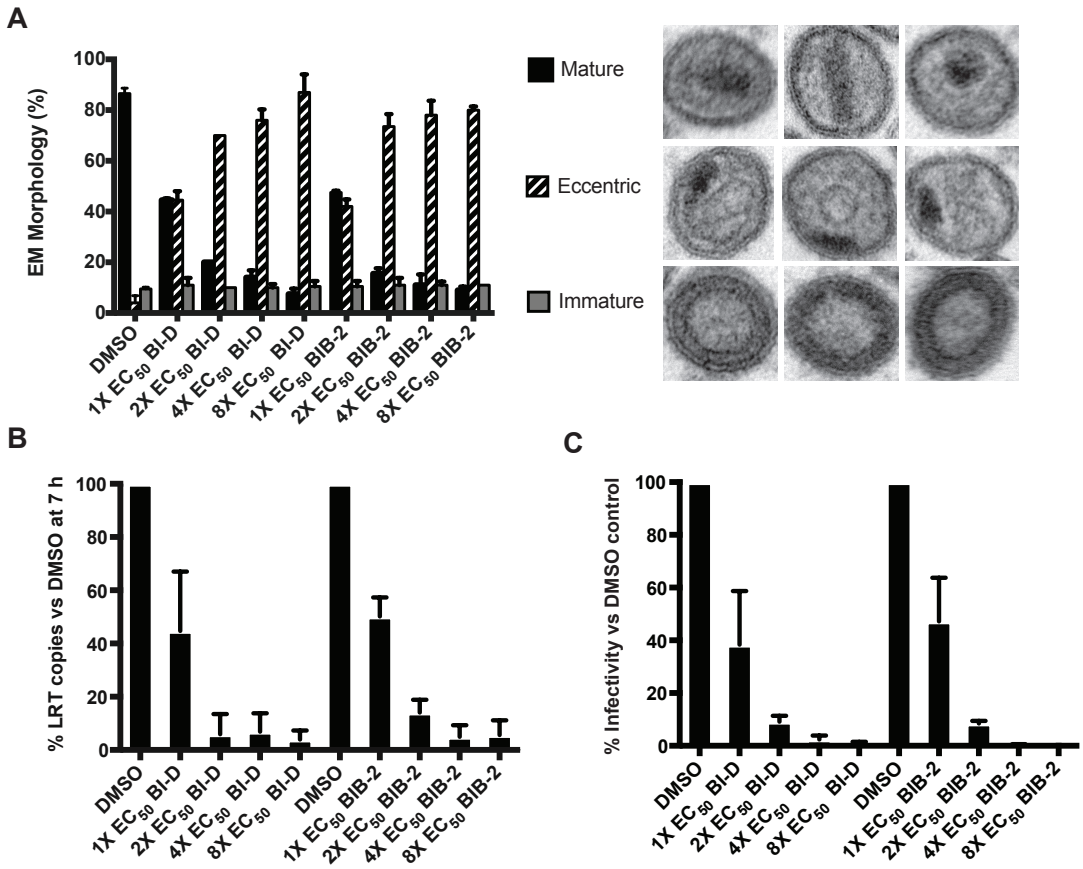

Figure 3-1. Inhibition of virion maturation underlies ALLINI potency

(A) *Left,* quantitation of core morphotype frequencies (average ± SD for 2 independent experiments) for sets of 100 counted HIV-Luc particles. *Right,* representative TEM images of mature, eccentric, and immature virions produced in these experiments. (B) Quantitation of late reverse transcription product formation from infections initiated with samples shown in panel A. (C) Antiviral activity as assessed by bulk luciferase output. Error bars in panels B and C are the variation obtained from three independent experiments.

of eccentric condensate-containing particles. The reverse transcription activity and infectivity (luciferase activity) of the particles were measured in SupT1 cells infected with equal amounts of virus, as quantitated by their CA/p24 content. By comparing the results of Figure 3-1A & B, we determined that the effect of drug treatment on reverse transcription activity closely paralleled the inhibition of mature core formation (Pearson correlation coefficient r^2=0.998 for the two sets of dose-response curves; P <0.001). Inhibition of reverse transcription moreover paralleled overall antiviral activity (Figure 3-1C; Pearson correlation coefficient r^2=0.903 for these two datasets; P <0.001).

ALLINI treatment affects conical core assembly in addition to vRNP incorporation into the mature core

Having determined that the antiviral activity of two independently tested, representative ALLINIs correlates with their inhibition of particle maturation, we performed cryo-ET to further probe the antiviral phenotype. Virions produced with full inhibitory ALLINI concentrations (10X EC_{50} for BIB-2; 10-100X EC_{50} for BI-D; Figure 3-1C) were classified according to core morphology (conical – e.g. Figure 3-2A, B; non-conical – e.g. Fig. 3-2C, D; or no core), and the presence (Figure 3-2B, D) or absence (Figure 3-2A, C) of an eccentric condensate. The eccentric condensate was previously observed by TEM as a compact, darkly staining body common to class II IN mutant viruses (146, 233, 284, 291) and ALLINI-treated virions (228, 233, 284). We used cryo-ET to extend these observations (Figure 3-2B, D). Their compactness and density distinguish condensates from the other material that typically occupies the space between the core and the viral envelope, which we take to be mostly non-polymerized CA (292, 293) and host cell proteins (294). In BI-D-treated particles, the eccentric condensates have ellipsoidal

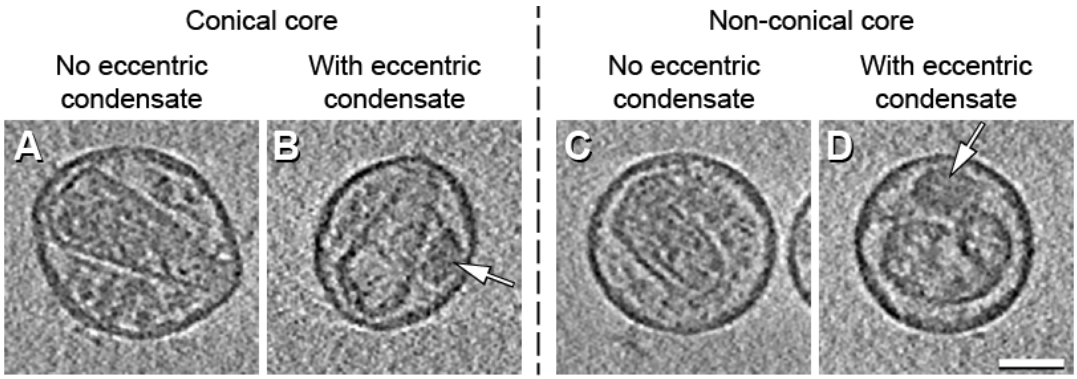

E. Morphological quantitation of HIV samples

	Conical Core		Non-conical core[1]		No core		
	No eccentric conden-sate[2]	With eccentric conden-sate[2]	No eccentric conden-sate[2]	With eccentric conden-sate[2]	No eccentric conden-sate[2]	With eccentric conden-sate[2]	Immature
WT (n=110)	**77**	9	9	3	2	0	0
WT + BI-D (n=121)	12	**22**	8	**53**	0	3	2
WT+BIB-2 (n=120)	8	**38**	4	**37**	2	3	8
V165A (n=153)	7	**29**	8	**48**	1	5	2

[1] Virions with irregular, cylindrical, polyhedral, double-layered or incomplete cores; or with two cores.

[2] Refers to a compact body of density located between the core and the envelope, denser than the material found in WT virions in that region.

Figure 3-2. Classification of HIV-1 particles observed by cryo-ET

(A-D) Tomographic central slices of representative HIV-1 virions classified according to core morphology (conical or non-conical) and the presence or absence of an eccentric condensate

Continued legend for Figure 3-2

(white arrows). Eccentric condensates appear denser than the material lying between the core and the envelope in particles that lack an eccentric condensate. The cores of virions that have an eccentric condensate are relatively empty (e.g. panel B). Bar, 50 nm. (E) Percentages of HIV-1 virions classified according to their core morphology (conical, non-conical, or no core) and presence or absence of an eccentric condensate. The majority species for each sample is given in bold font. According to the chi-square test, significant differences with P-values < 0.00001 were found for comparisons between WT and BIB-2 and between WT and V165A. The difference between WT and BI-D had a P-value of 0.013, whereas the differences between V165A and BI-D or BIB-II were not significant, with P-values > 0.26. The Chi-square test was used to test for equal distribution of compartmentalized data, but should not be used if more of 20% of the bins contain fewer than 5 counts. Therefore, immature virions were not taken into account and virions with no cores were considered a single category, independent of the presence or absence of an eccentric condensate.

shapes with major and minor axes of 58 ± 12 nm and 37 ± 12 nm (n=93), respectively; those present in particles treated with BIB-2 or untreated V165A particles, which was utilized as a class II IN mutant control (233), were similar in size. The incidence of these morphological classes is summarized in Figure 3-2E. Eccentric condensates are relatively rare (~12%) in WT virions but present in ~75% of particles treated with BI-D or BIB-2, or with the V165A IN mutation. We observed no virions with more than one eccentric condensate.

As in earlier studies by cryo-ET (e.g. (59, 279, 287)), most WT virions (~77%) were found to have closed conical cores with internal density (Figure 3-2A), noting that the tomograms would not detect small holes if present (295). Most of the eccentric condensate-containing virions from BI-D or BIB-2 treatment or the V165A IN mutant also have a core (Figure 3-2E), but there are two striking differences between these cores and WT cores. First, they have a much higher incidence of non-conical cores than with WT (the ratios of non-conical to conical cores were 1.8 : 1 for BI-D, 0.9 : 1 for BIB-2, and 1.6 : 1 for V165A, as compared to 1 : 7.2 for WT). Thus, there is marked impairment of capsid morphogenesis. Second, V165A/BI-D/BIB-2 conical cores are relatively empty, as exemplified by comparing Figure 3-2A and B. With WT cores, internal material is generally taken to consist mainly of the vRNP, although this assignment has not been formally demonstrated and is addressed further below. While conical V165A/BI-D/BIB-2 cores have less internal content than the WT ones, they tend to have some internal material (e.g. Figure 3-2D). With this caveat, we estimate that ~50% of them have little or no content vs. 3% for the WT virions. These data suggest that V165A/BI-D/BIB-2 virions are deficient in capsid morphogenesis in addition to incorporation of the vRNP into the mature core.

Bubblegrams detect radiation-sensitive material in filled cores and eccentric condensates

It is plausible that eccentric condensates represent NC-vRNA complexes that failed to be incorporated into the mature core. We obtained supporting evidence for this hypothesis by means of a labeling technique called “bubblegram imaging” (296, 297). Vitrified samples imaged in an electron microscope undergo progressive damage by electron irradiation. This damage is initially expressed as a 'smearing' of the macromolecular density, and for this reason the electron dose is kept as low as possible during imaging (298). When proteinaceous specimens are subjected to relatively high levels of electron irradiation in cryo-EM – perhaps 10-fold higher than the dose used in a typical imaging experiment - bubbles of hydrogen gas are generated (299, 300), which are readily visible due to their low density. Different proteins have different bubbling thresholds (N,C., Weimin Wu, Anastasia Aksyuk, J.F. & A.C.S., unpublished observations). Moreover, proteins intercalated in DNA bubble relatively early because the densely packed DNA impedes the diffusion of radiation products from their sites of origin, accelerating their build-up to a critical concentration for bubbling. Hypothesizing that compact NC-vRNA condensates may have distinctive bubbling behavior, we subjected HIV-1 virions to bubblegram imaging. In “dose-series” micrographs (not shown), small bubbles first appeared after a cumulative dose of 160 - 200 e-/Å^2 and grew in size and number with subsequent exposures. The bubbles co-projected with filled cores and eccentric condensates, and the two structures appeared to have the same bubbling threshold, although in some micrographs the boundaries of these structures were difficult to discern. However, we could not rule out that the bubbles may not be inside these structures but coincidentally lie along the same line-of-sight.

Aiming to eliminate the ambiguity of co-projection, we extended the bubblegram method to 3D imaging by electron tomography. We call this method “tomo-bubblegram imaging”. First,

a regular tilt-series is collected from an area of interest and a tomogram is calculated. This involves a total dose of ~75 e-/Å^2, which is below the bubbling threshold for HIV-1. Second, an untilted dose-series is performed, stopping after the first small bubbles begin to develop (another ~70 e-/Å^2). Third, after waiting ~2 h to allow radiation products to dissipate, a second tilt series is recorded (~70 e-/Å^2) during which larger bubbles appear in the "primed" specimen. These bubbles are visualized in the corresponding tomogram – the "tomo-bubblegram". Finally, comparing the first tomogram (the "before" state with the virions in a close-to-native state) and the second one (the "after" state) allows the sites in which the bubbles nucleated to be mapped in three dimensions. As illustrated in Figure 3-3 and Table 3-1 the bubbles specifically label the core interiors in WT virions, predominantly towards the wide end of the core. They also label the eccentric condensates of V165A and BI-D/BIB-2 virions. Of note, bubbles were never seen only inside cores (i.e. outside the condensates) of V165A or BI-D/BIB-2 virions that also contained eccentric condensates: in these particles, either bubbles were observed only in the condensate (~80% of the condensate-containing particles) or in both the condensate and the core (~20%). In summary, we found that the WT conical core contents and eccentric condensates are more prone to bubbling than the other components of the virion (CA protein, MA protein, envelope glycoprotein) and they are indistinguishable in this respect. In turn, this correlation strongly supports the idea that they are chemically the same and are indeed NC-vRNA complexes.

Bubbles label NC-RNA in immature virions

To further investigate which component of HIV-1 virions is bubbling, we examined immature (PR-defective. i.e. PR–) virions in which, in the absence of proteolysis, the Gag and Gag-Pol domains are radially ordered, with MA in contact with the viral membrane, and CA and

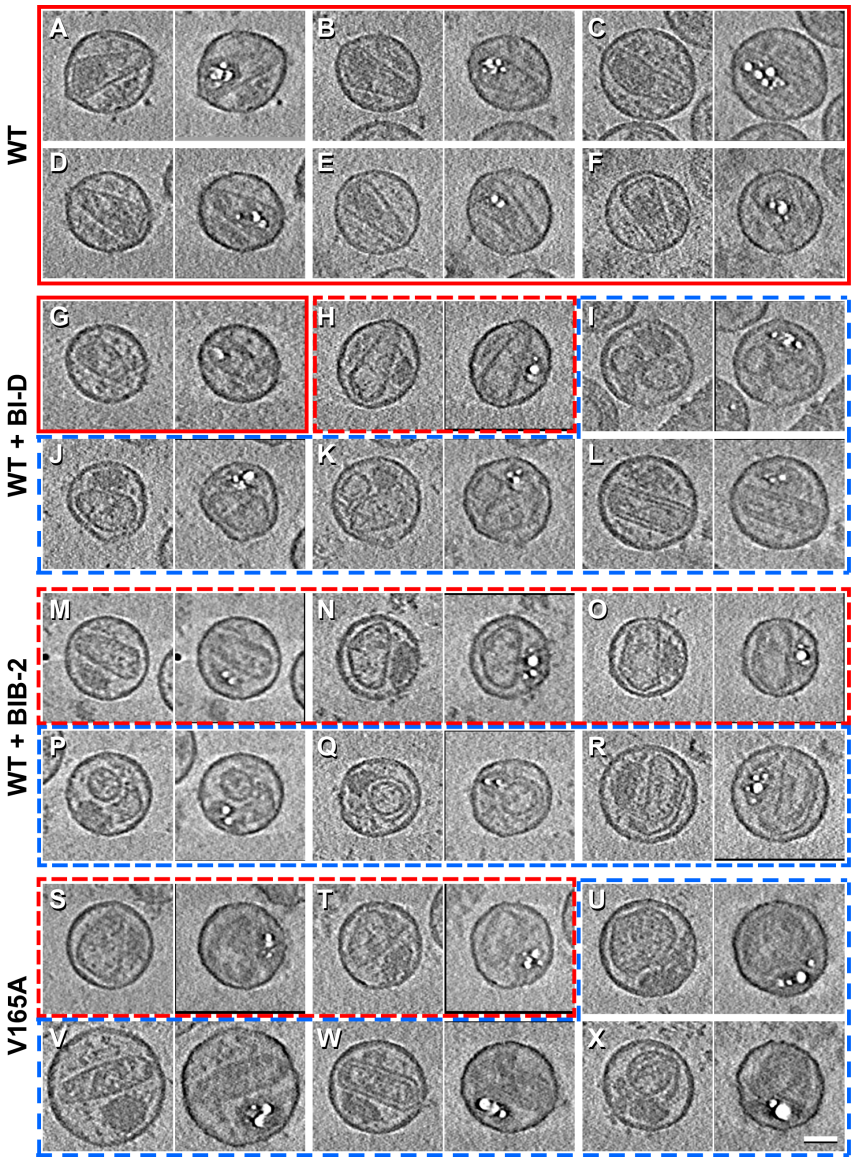

Figure 3-3. Tomo-bubblegrams of HIV-1 particles

(A-X) Each pair of panels shows a central section from an initial tomogram (left) and the corresponding section from the tomo-bubblegram (right). The types of virions analyzed are labeled on the left side of each block. BIB-2 (10X) and BI-D (10X EC_{50} for panels G, I, and L; 100X EC_{50} for panels H, J, and K) were used at full inhibitory concentration. Particles with conical cores are framed in red and those with non-conical cores in blue; particles lacking eccentric condensates are framed with continuous lines and particles that have eccentric condensates, with dashed lines. Bar, 50 nm.

Table 3-1. Tomo-bubblegram labeling of HIV-1 virions

	Conical core, no condensate			Non-conical core, no condensate			Condensate with core (conical or non-conical)		
Bubbles:	**Inside core**	**Outside core**	**Both**	**Inside core**	**Outside core**	**Both**	**Outside condensate**	**Inside condensate**	**Both**
WT (N=78)	**55**	0	**19**	1	3	3	4	4	9
BI-D (N=72)	7	0	7	1	1	6	0	**56**	**21**
BIB-2 (N=64)	8	0	0	0	3	0	0	**77**	**12**
V165A (N=88)	3	0	2	6	0	2	0	**67**	**18**

[a]The data are shown as percentages of virions with bubbles either inside the core, outside the core, or both.

NC/vRNA arranged in successive concentric layers. PR– virions (HIV-1_{NL4-3} with the D25A inactivating mutation in the PR active site) exhibited a similar bubbling threshold as WT virions, although the bubbles appeared in a different location, i.e., within the Gag shell (Figure 3-4Ai, ii). Radially, these bubbles are centered at ~15 nm (average 15 ± 5 nm; n=333) in from the middle of the viral envelope, a position that corresponds to the interface between the CA and NC+vRNA layers (Figure 3-5). In the other two dimensions of the Gag lattice, we did not find a preference for bubbling in any particular location.

Next, immature virions in which vRNA and NC were respectively eliminated from Gag virus-like particles (VLPs) were analyzed to test for the relative contributions of these two components to bubbling phenomena. A VLP construct that lacked the vRNA ψ region (301) reduced the packaging of vRNA relative to total virion RNA by ~20,000-fold (Figure 3-4B, C). Gag/ψ-minus particles bubbled in the same locations as immature (PR–) virions, thus showing that vRNA is not needed for bubbling (Figure 3-4Aiii, iv). We do, however, note that the bubbling appeared to be slightly reduced with this construct (16 ± 10 bubbles/virion in Gag/ψ-minus particles vs. 27 ± 15 bubbles/virion in PR– particles – Table 3-2; the differences are significant at $p < 0.01$ according to the two-tailed student T-test). The difference, such as it is, might arise from the ~2.5-fold reduction in overall RNA content in Gag/ψ-minus particles, as the RNA may impede the dispersal of hydrogen gas generated from NC. To eliminate NC but nevertheless retain structurally similar particles, we used a construct in which the NC domain of Gag was replaced by a leucine zipper (35), in which Gag otherwise retains its immature conformation (302). The Gag-LeuZip VLPs yielded almost no bubbles (Figure 3-4Av, vi; 0.3 bubbles/virion vs. 16 bubbles per Gag/ψ-minus VLP at the same electron doses), and ~94% of

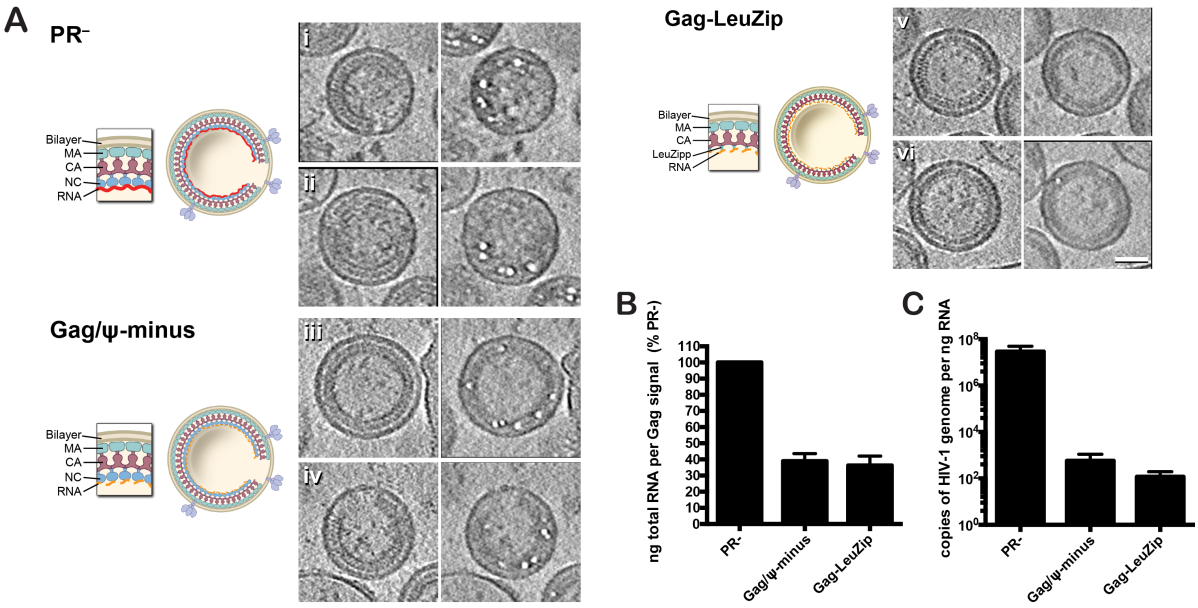

Figure 3-4. Tomo-bubblegrams of immature HIV-1 particles

(A) (i-vi) Central tomographic sections (left) and corresponding tomo-bubblegram sections (right). The diagrams on the left side of the figure convey the composition of each sample. PR^{-} particles contain the Gag and Gag-Pol polyproteins that includes NC and incorporates vRNA. The virions are immature due to the inactivating D25A mutation in the PR active site. Gag/ψ-minus particles are also immature, and additionally their RNA lacks the ψ region and therefore vRNA is not incorporated into particles. The Gag-LeuZip particles replace NC with a leucine zipper; these particles lack NC and vRNA. Bar, 50 nm. (B) Total virion RNA from the particles described in A. RNA concentration was normalized to the Gag signal obtained from anti-p24 western blots of multiple input volumes. Shown are average (± SD) of total RNA (ng) standardized by Gag signal for 4 independent experiments, reported as percentage of PR-. (C) RNA from B was utilized to determine the copy number of vRNA. Values, reported as a percentage of PR-, are the average (± SD) for 4 independent experiments.

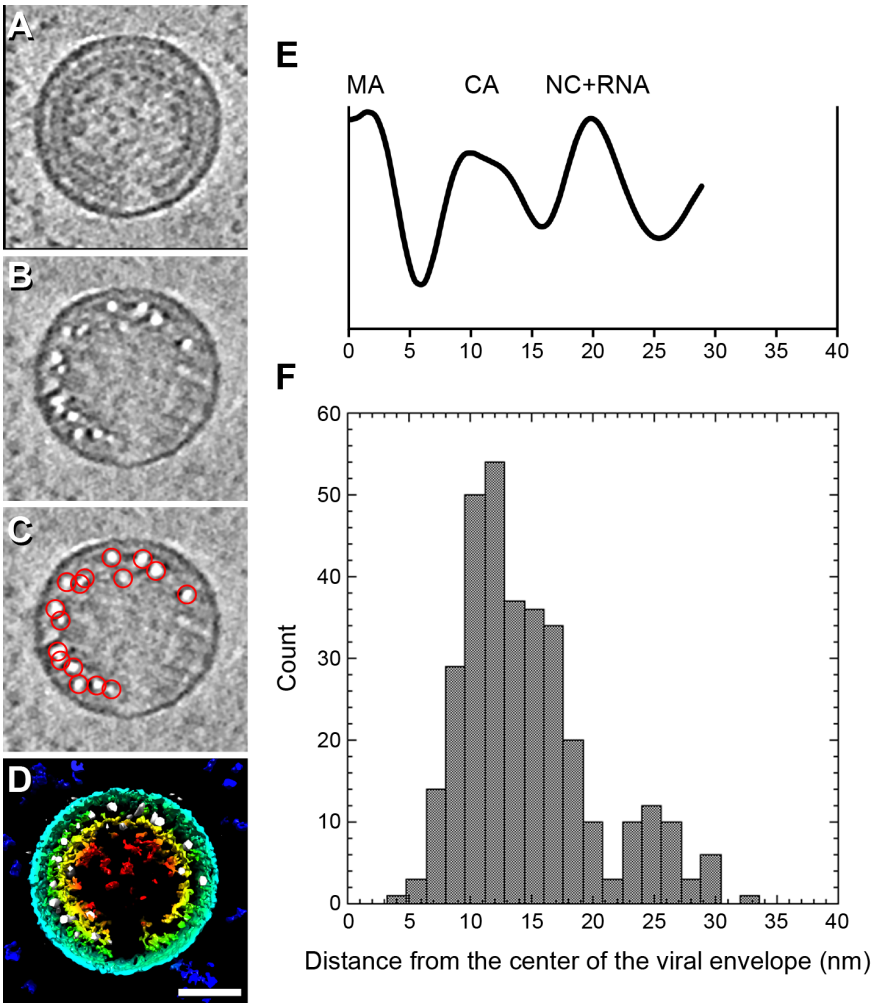

Figure 3-5. Locations of bubbles in PR- virions

(A) Cryo-ET central slice of an immature PR^{-} particle. (B and C) The tomo-bubblegram section corresponding to panel A. In C, bubbles are marked with red circles. (D) Surface rendering of a cutaway slice of the particle shown in panels A-C. Most of the bubbles (white) are located between the CA layer (green) and the NC-vRNA layer (yellow). The viral envelope is in cyan and the internal contents in red. Bar, 50 nm. (E) Radial density profile of subtomogram averaged Gag from immature virions (from (287)). (F) Histogram of the distance from the center of the bubbles to the center of the viral envelope (membrane + MA).

Table 3-2. Bubbles in three kinds of PR- HIV-1 particles

	# of tomograms	Total avg. dose ($e^-/Å^2$)	# virions	# bubbles /virion[1]	% of virions with 2 or more bubbles [1]	% of virions with 1 or no bubbles [1]
PR^-	3	215	65	27 ± 15	100	0
Gag/ψ-minus	4	221	53	16 ± 10	100	0
Gag-LeuZip	4	228	53	0.3 ± 0.6	6	94

[1] For PR^- and Gag/ψ-minus VLPs, the bubbles from 29 and 31 virions were counted respectively. For the Gag-LeuZip, bubbles from all particles imaged were counted.

these particles had 0 or 1 bubble (vs. 100% of the control particles that each had two or more bubbles; Table 3-2). The relative levels of total RNA and vRNA in Gag-LeuZip VLPs were similar to those in Gag/ψ-minus VLPs (Figure 3-4B, C), though we do note that an earlier study failed to detect tangible RNA levels in Gag-LeuZip VLPs (35). Nevertheless, we conclude that, apart from a very low background of bubbles from other sources (as illustrated in Figure 3-4Av, vi), NC protein is the bubbling component.

Purified NC exhibits similar bubbling behavior to that observed in mature and immature virions

Identification of NC protein as the component responsible for bubbling in both mature WT and IN mutant/ALLINI-treated virions and in immature virions led to the prediction that NC protein should also bubble provided that it is suitably concentrated. To test this hypothesis, we examined aggregates of purified NC. Aggregates were similar in diameter to eccentric condensates (average 51 ± 20 nm, n=69, vs. 48 ± 9 nm, n=93), and were found to have a similar bubbling threshold to that of eccentric condensates (average, 154 ± 57 e-/Å2, n=69 vs. 165 ± 42 e-/Å2, n=69). Their bubbling threshold was somewhat dependent on size, with larger aggregates bubbling earlier than smaller ones (Figure 3-6). This is consistent with the greater abundance of NC in larger aggregates providing a richer source of hydrogen gas as a radiation product. Strikingly, bubbling started in the middle of these aggregates and then spread outwards, consistent with the outer layers of molecules impeding the outward diffusion of the gas. Taken together, these observations provide strong evidence that the bubbling component in HIV-1 virions is NC protein, and therefore confirm that ALLINI treatment affects incorporation of the vRNP into the core.

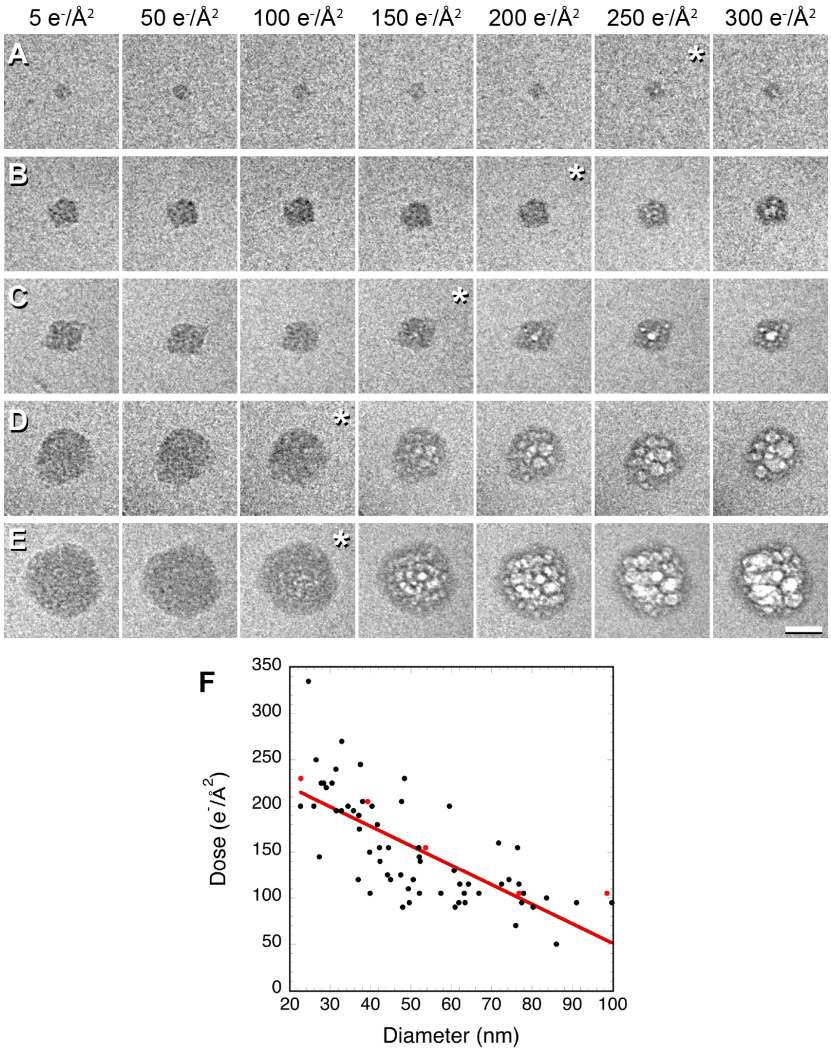

Figure 3-6. Bubblegram imaging of purified NC protein

(A-E) Cryo-EM dose series of five NC aggregates of different sizes. The images in which bubbles first appear are labeled with a white asterisk in each case (although NC is formally soluble, small aggregates of suitable size were consistently found on EM grids). Bar, 50 nm. (F) Plot of the diameters of NC aggregates *vs.* the cumulative electron dose at which they started bubbling. Points corresponding to the aggregates from panels A-E are shown in red. While the data exhibit some stochastic variability in bubbling threshold, there is a clear trend towards larger aggregates requiring less electron radiation to initiate bubbling. A linear fit is shown for reference (red line).

ALLINI-induced eccentric condensate formation requires vRNA

To address whether ALLINI-mediated impairment of vRNP incorporation into the mature core is dependent upon the species of RNA within the virus, we co-transfected pHI-Luc, which expresses a minimal HIV-1 transfer vector that harbors ~45% of the full-length vRNA genome, with pHP-dl-N/A that expresses the Gag and Pol proteins required to package HI-Luc vRNA in trans. As a transfection control for pHI-Luc, we utilized the promoter-less pGL3-basic (GL3-B) construct that carries the luciferase gene but lacks HIV-1-related sequences and the capacity to express RNA. Total RNA levels of pelleted virions nevertheless did not vary significantly between those made in the presence of pHI-Luc or GL3-B, although, as expected, the HIV-1 genome was selectively incorporated into HI-Luc particles (Figure 3-7A, B). We also note that HI-Luc total and vRNA levels were similar to those of the HIV-Luc virions characterized in Figure 3-1. TEM revealed that ~30% of HI-Luc viruses harbored WT-like conical cores, ~22% harbored cores as well as eccentric aggregates, ~25% had a previously unseen morphology wherein dual electron density (dual ED) appeared both inside and outside the core, ~15% had empty cores, and ~15% contained immature-like spherical shells (Figure 3-7C). The baseline phenotype of virions made in the presence of GL3-B did not differ dramatically from that of virions that harbored HI-Luc vRNA (Figure 3-7C). As expected, BI-D treatment increased the frequency of HI-Luc virions with eccentric aggregates (~60%), with accompanying decreases in mature (~5%) and dual ED (~1%) cores. By contrast, the fraction of virions with eccentric aggregates did not significantly change when sham virus made in the presence of GL3-B was treated with BI-D (Figure 3-7C).

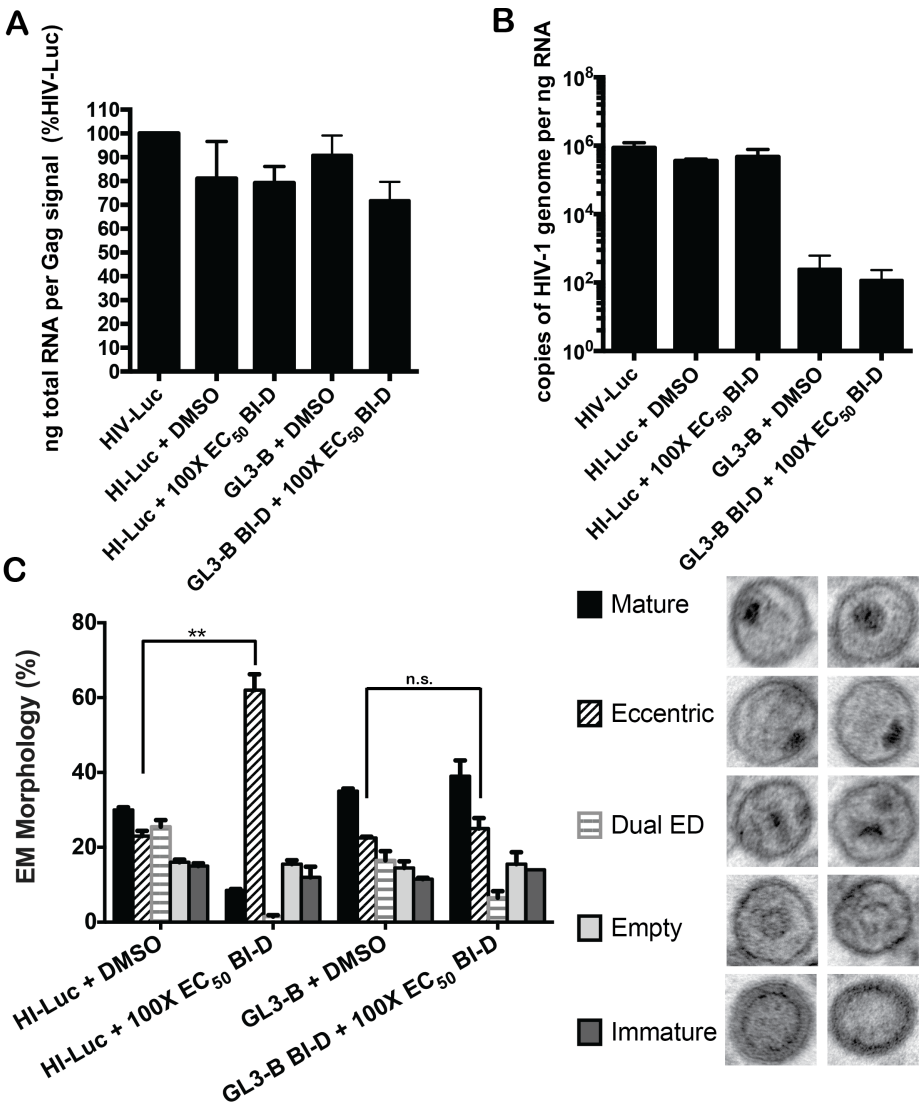

Figure 3-7. Viral RNA requirement for eccentric condensate formation

(A) Total RNA (ng) of concentrated virion preparations. RNA concentration was standardized by the p24 signal obtained from western blots of multiple input volumes. Shown are averages (± SD) from 4 independent experiments reported as percentages of untreated HIV-Luc virions. (B) Average (± SD) copies of vRNA per ng total RNA (n=4) determined for the samples described in A. (C) *Left,* core morphology frequencies in sets of 100 counted virions (average ± SD) from two independent isolates of particles prepared as described in A. **, $P < 0.01$; n.s., not significant ($P = 0.37$). *Right,* representative images of the mature, eccentric, dual electron density (ED), empty, and immature virions observed in these experiments.

Partial recovery of WT core formation by IN in trans

TEM classification of ΔIN virions revealed that the majority (~61%) contained eccentric condensates while ~9% harbored WT-like conical cores and ~30% were immature (233). To assess the role of IN in HIV-1 maturation and the impact of ALLINI treatment on this role, ΔIN virions were functionally trans-complemented by IN fused to the viral accessory protein Vpr. IN_{H171T}, which confers ~44-fold resistance to BI-D (226), was utilized as a control. Although class II IN mutations such as ΔIN can impede CA/p24 release in a cell type-dependent manner (158, 250), the ΔIN virus used here yielded supernatant p24 values similar to the WT control virus (233). Vpr-IN boosted the infectivity of the highly defective ΔIN virions ~100-fold, to a level equal to ~5-10% of the infectivity of the parental HIV-Luc virus (Figure 3-8A). As expected (233), a 10X EC_{50} dose of BI-D abolished the infectivity of ΔIN virions trans-complemented with Vpr-IN_{WT} but not with Vpr-IN_{H171T}. Concomitant with the gain in infectivity, the incidence of conical cores rose from ~9% to ~30% upon Vpr-IN transcomplementation (Figure 3-8B). With Vpr-IN_{WT}, ALLINI treatment restored this phenotype to the non-complemented ΔIN value of ~9%, whereas virions trans-complemented by Vpr-IN_{H171T} harbored ~30% mature cores, regardless of ALLINI treatment.

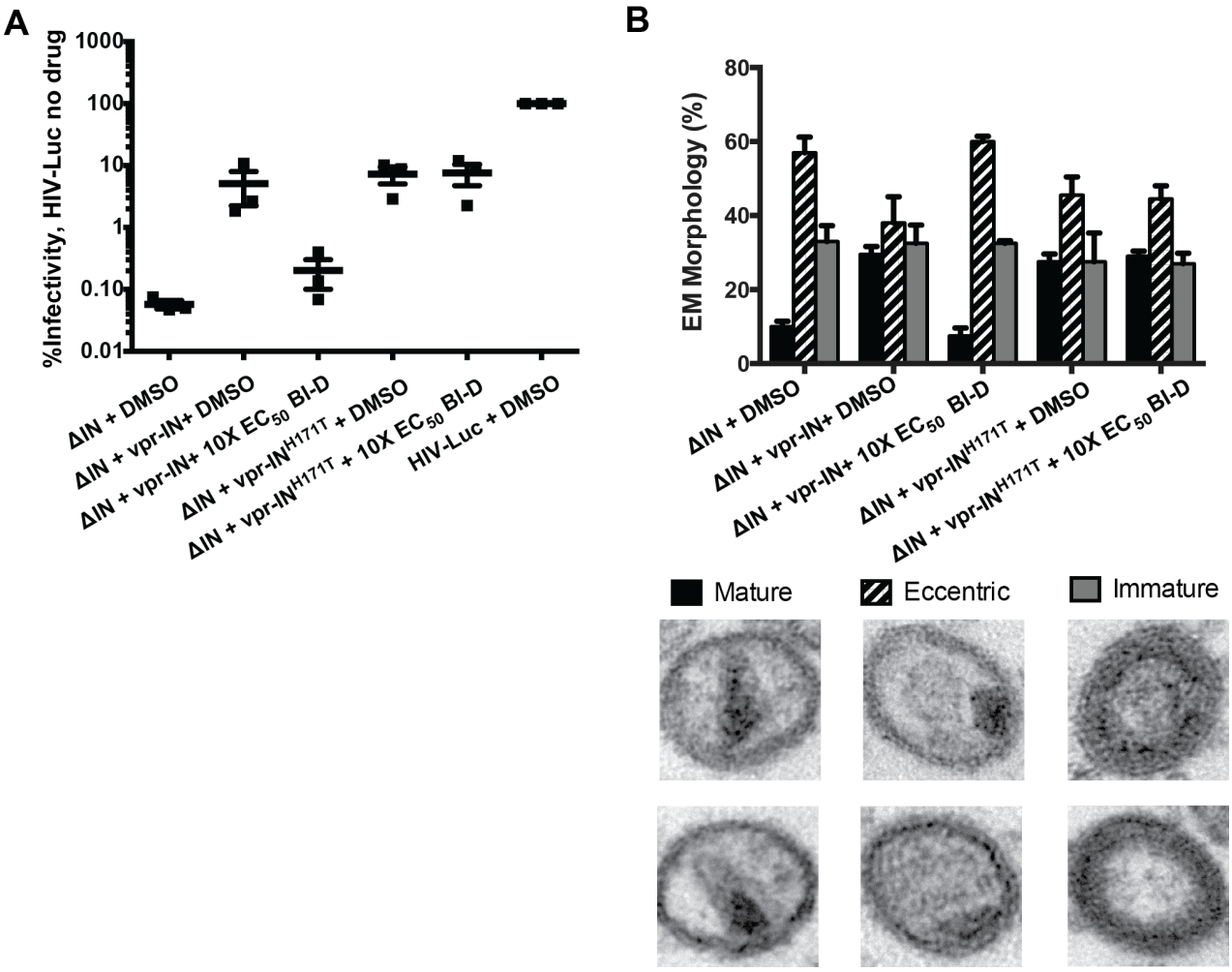

Figure 3-8. IN *in trans* stimulates WT core formation in ΔIN virions

(A) Infectivity of HIV-Luc.ΔIN transcomplemented with Vpr-IN_{WT} or Vpr-IN_{H171T} made in the presence of BI-D or DMSO. Values were normalized to control HIV-Luc virus constructed in the presence of DMSO. (B) *Upper,* quantitation of core morphology frequencies of 100 counted virions (the ΔIN mutation yields more immature particles than does other class II (e.g., missense) mutations (233, 303)). Shown are average ± SD for 2 independent experiments for the transcomplemented preparations described in A. *Lower,* representative images of the mature, eccentric, and immature virions observed within experiments.

Discussion

In this study we have utilized the recently discovered antiviral activity of ALLINIs to assess the role of IN in HIV-1 maturation. Of virions assembled in ALLINI-treated cells, the fraction that acquires a closed conical capsid (taken to be a requirement for infectivity - (82)) is markedly reduced. Many of these capsids are malformed. Moreover, in most of these virions, the vRNP is not incorporated into the mature core but remains outside the capsid as an "eccentric condensate" – even if a closed conical capsid is assembled. These phenotypes are reproduced by various class II IN mutations, including the V165A point mutation or IN deletion. IN supplied in trans partially rescued the fraction of ΔIN virions that harbored WT cores with internal electron density, a recovery that could be abolished by ALLINI treatment (Figure 3-8B). As vRNA was required for ALLINI-induced eccentric condensate formation, we suggest a model wherein disruption of an IN-vRNA interaction, either by genetic or pharmacological means, results in the inability to properly incorporate the vRNP into the capsid during HIV-1 core morphogenesis.

ALLINI antiviral activity is due to inhibition of HIV-1 particle maturation

ALLINIs have been shown to inhibit several steps of the HIV-1 replication cycle (see Introduction). However, it has been unclear whether inhibition of multiple steps combines to determine drug potency, or whether ALLINs inhibit a single bottleneck step in the replication cycle. To address this issue we correlated dose-response curves from inhibiting maturation and reverse transcription – the first two steps that are inhibited from the perspective of the drug-treated virus-producer cells – to overall antiviral activity. As all three curves (percentage of mature cores, reverse transcription activity, infectivity) effectively superposed with highly

significant correlations for two representative inhibitors, we conclude that inhibition of HIV-1 maturation determines the antiviral potency of these compounds.

Similar to PIs (245), ALLINIs display relatively steep dose response curves (232, 233). Two mutually non-exclusive models for this behavior posit that such compounds inhibit multiple copies of the drug target at the relevant step of the replication cycle (245) or that they inhibit multiple steps in the replication cycle (304). Whereas inhibition of multiple replication steps appears to underlie the cooperative behavior of PIs (304), we conclude from our data that ALLINIs mainly if not exclusively target IN during HIV-1 maturation and, by inference, that multiple copies of IN, if not the full virion complement of the protein, are affected. We accordingly note similar slopes of BI-D dose response curves for stimulation of purified IN multimerization in vitro (m ~2) and inhibition of HIV-1 replication (m ~2.8) (233).

Tomo-bubblegram imaging labels NC-containing complexes in 3D

Cryo-ET and tomo-bubblegram imaging have given a clearer account of the substructure of HIV-1 virions whose maturation was subverted by a class II mutation in IN or by ALLINI treatment. First, we confirmed earlier TEM data (228, 233, 284, 286) that ALLINI treatment yields a high proportion of virions with eccentric condensates. This property reoccurs in the class II IN mutant control virus. Second, being able to visualize the 3D structures of complete virions in greater detail, we additionally found an adverse effect of the V165A mutation and ALLINIs on capsid morphogenesis.

We now consider the density inside conical capsids of mature WT virions. This density has been interpreted as the vRNP, composed primarily of NC and vRNA. The vRNP also contains the RT and IN enzymes and some other viral and host cell components (82, 305-307).

Serendipitously, NC turned out to be highly susceptible to irradiation-induced bubbling and we exploited this property to demonstrate that NC is indeed a major internal component of WT cores; moreover, the NC is primarily at the wide end of the core (see Figure 3-3A-F; also (58)). Because few bubbles are seen elsewhere in virions, it seems that most if not all of the NC protein goes into the core. These data directly support earlier evidence that most or all of NC is in the core, whereby the ratio of NC to CA was found to be significantly higher in isolated cores than in virions (308), in keeping with the property that only about half of the CA present in an immature virion assembles into a mature capsid (292, 293). Similarly, our tomo-bubblegrams have shown that eccentric condensates are rich in NC, with few bubbles seen anywhere else in condensate-containing virions.

The typical dimensions of the material enclosed in the wide end of a WT core are similar to those of an eccentric condensate. It appears therefore that when NC and the attached genomes are released from the Gag shell in a maturing virion, they condense into one or the other of these aggregates. A heuristic calculation supports this inference. If one takes an eccentric condensate to have major axes of 55 x 55 x 35 nm (see above), its volume is ~55,000 nm^3. Assuming ~50% of this volume to be occupied by protein (a value typical for a protein crystal) and a protein density of 0.78 kDa/nm^3, a mass of 21.5 MDa results. Alternatively, an NC copy number of ~2000 - 2500 per virion (251) and a subunit mass of 7.2 kDa gives a total mass of ~14 - 18 MDa. Therefore, the eccentric condensates are large enough to account for all of the NC plus the two copies of the vRNA genome, which remain associated with NC after virion maturation (24, 309). Our analysis also shows that ~12% of WT virions contain eccentric condensate: of these, 75% have conical cores and 25% have non-conical cores. The existence of such particles demonstrates miscarried vRNP incorporation into mature cores under the otherwise unperturbed WT situation

of HIV-1 clade B strain NL4-3 assembly from transfected HEK293T cells. Additional work with other viral clades and cell types would be needed to discern how broadly applicable this observation may be.

Implications for core assembly

In order to assemble a core, PR must dissect Gag and Gag-Pol, with their component domains being separated in a tightly regulated cleavage sequence (310). Finally, CA is released from the maturing Gag shell into a pool whence it assembles to form the mature core, leaving about 50% unassembled (59, 288, 292, 293). During core assembly, NC together with the vRNA and IN and RT enzymes becomes situated into the mature core (see above).

Several models have been proposed for how capsid assembly takes place (59, 279). They differ on whether assembly starts at the wide end (279) or the narrow end (59) and are couched primarily in terms of self-assembly properties attributed to CA protein, since conical capsids similar to the ones observed inside HIV-1 virions can be assembled from purified components in vitro (311). It has also been suggested that the vRNP may help to nucleate assembly (58, 60, 279), ensuring its incorporation into the capsid, and that MA or the inner surface of the viral membrane could direct the closure of the core (59). A related idea for coupling capsid assembly with vRNA packaging was advanced for Rous sarcoma virus in that some unprocessed or incompletely processed copies of Gag in the Gag shell may form a nucleation complex that binds via the NC moieties to a genomic packaging site and, via the CA moieties, nucleates outgrowth of the capsid shell (312). Although IN has been implicated in regulating PR activity during HIV-1 assembly and particle release (158), a role for the viral enzyme in core morphogenesis has not been proposed. Based on our data, we propose an active role for IN in initiating vRNP

incorporation into the mature core, which then nucleates capsid formation around the enclosed vRNA-NC complex (Figure 3-9). This scenario could in theory apply to pre-cleavage IN as a domain of Gag-Pol or post-cleavage IN that has remained in essentially the same position. Supporting a model for an IN-vRNA interaction(s) in core morphogenesis, our data reveal a role for vRNA in ALLINI-induced eccentric condensate formation (Figure 3-7) and high affinity binding of purified HIV-1 IN to RNA has been observed in vitro (161). Linkage between IN and CA changes has moreover been noted among strains in drug-naive and drug-experienced AIDS patients (313), indicating a potential biological role for an IN-CA interaction. IN-RNA and IN-CA interactions are two avenues that we are currently pursuing to investigate the mechanistic basis of IN in HIV-1 core formation and vRNP incorporation into the mature core.

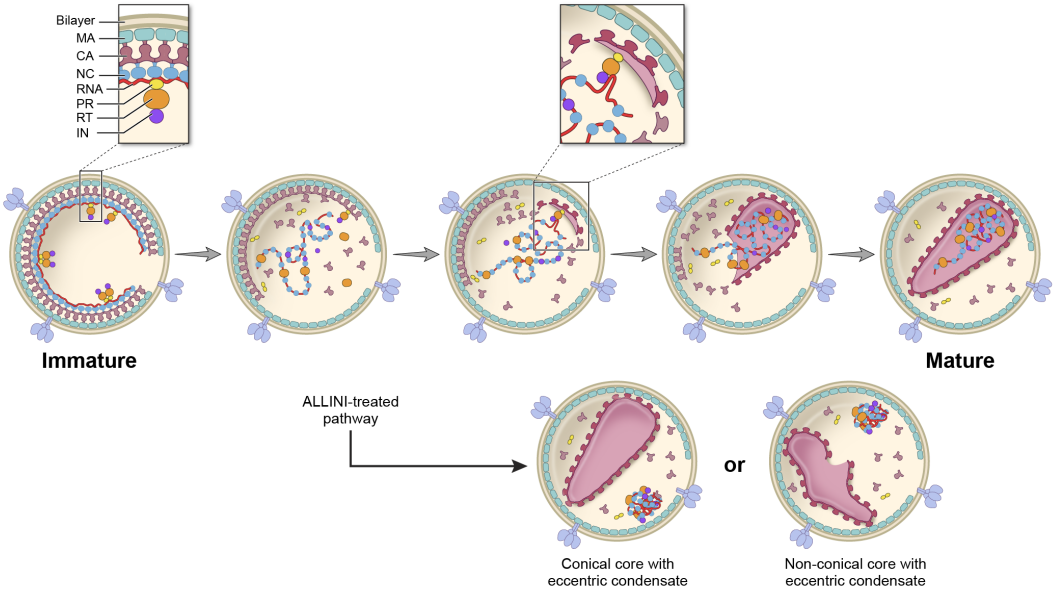

Figure 3-9 Model for the role of IN in during HIV-1 maturation

Maturation starts with activation of the PR and dissection of the Gag and Gag-Pol polyproteins and release of the vRNP/NC from the Gag shell. The key element of this model is that it envisages a molecular complex containing one or several copies of Gag-Pol that initiates both assembly of the capsid by an outgrowth of CA subunits and packaging of the vRNA through binding to IN or to RT as conformationally influenced by IN. The cartoon shows RT and IN associated with the eccentric condensate for which there is currently no evidence although they do remain, mostly or totally, inside the wild-type capsid (307). A variant of this model in the Rous sarcoma virus system envisages participation of the cytoplasmic domain of Env (312). The virion and core also contain other components (e.g. Vpr in the core; some host proteins somewhere in the virion), which are not shown.

Materials and Methods

Plasmids and antivirals

HIV-1_{NL4-3} carrying WT IN was expressed from pNL43/Xmal (265) whereas the V165A IN mutant was expressed from pNL43/XmaI.V165A (29) (246). Single-round derivatives HIV-Luc and HIV-Luc.ΔIN were expressed from pNLX.Luc.R- (250) and pNLX.Luc.R-.ΔIN (233), respectively. The D25A mutation in PR was introduced into pNL43/XmaI using PCR-directed mutagenesis. Gag/ψ-minus VLPs were expressed from pRR359 (301) whereas Gag-LeuZip was expressed from pRR546 (35). HIV-1-based pHP-dI-N/A packaging plasmid (314) was cotransfected with pHI-Luc transfer vector (315) or pGL3-Basic control plasmid (Promega). Vpr fused to the IN protein from HIV-1SG3 (WT or H171T) was expressed from pRL2PVpr-IN (233, 268) whereas the VSV-G glycoprotein was expressed using pCG-VSV-G (250). BI-D and BIB-2 were synthesized as described (236, 237). EFV was obtained from the National Institutes of Health AIDS Research and Reference Reagent Program.

Cells, viruses, and antiviral assays

Transformed HEK293T cells (American Type Tissue Collection item number CRL-3216) were grown in Dulbecco's modified Eagle medium while human SupT1 T cells (NIH AAARP item number 100) were maintained in RPMI medium 1640, both supplemented to contain 10% (vol/vol) fetal bovine serum, 100 IU/mL penicillin, and 100 μg/mL streptomycin. HIV-Luc was produced by cotransfecting HEK293T cells (8 x 105) with 3.5 μg pNLX.Luc.R- and 0.35 μg pCG-VSV-G using PolyJet transfection reagent (SignaGen Laboratories). HIV-1NLX.Luc.R-ΔIN was transcomplemented with Vpr-IN by cotransfecting HEK293T cells (3 x 106) with 4.5 μg pNLX.Luc.R-.ΔIN, 1.25 μg pRL2P-Vpr-IN containing WT or H171T IN, and 0.5 μg pCG-

VSV-G. DMSO or ALLINIs were added with fresh media at ~17- 20 h post transfection, and cell supernatants were collected 24 h later. Cell-free virus concentration, typically 500-1000 ng/mL, was determined using a commercial p24 ELISA kit (Advanced Biosciences Laboratories). For Vpr-IN complementation experiments, SupT1 cells were infected in quadruplicate with 5 ng/mL p24. Luciferase values, expressed as relative light units, were determined 48 h postinfection.

DNA analysis and quantitative PCR

SupT1 cells (2 x 10^6) infected with DNase-treated (1 h at 37 °C) HIV-Luc (50 ng p24/mL) for 2 h were washed and split into two samples. DNA was isolated from one set of samples 5 h later using the DNeasy blood and tissue kit (Qiagen). The other set of samples was seeded in quadruplicate in 96-well plates, and luciferase activity was determined 48 h from the start of infection. Duplicate PCRs containing 50 ng DNA, 0.2 μM primers (AE2963/AE4422), 0.1 μM probe (AE2965), and 1X QuantiText Probe PCR Master Mix were incubated at 50 °C for 2 min and 95 °C for 15 min, followed by 40 cycles of 94 °C for 15 s, 59 °C for 30 s, and 72 °C for 30 s (116). Standards were prepared by end-point diluting pNLX.Luc.R- into DNA from uninfected cells. To account for potential residual plasmid carryover from transfection, parallel infections were preformed in the presence of 10 μM EFV, and the values obtained from these PCR assays were subtracted from the experimental samples.

RNA isolation and analysis

Total RNA was extracted from concentrated virus preparations after a 30 min incubation with 0.05 μg/mL proteinase K (Life Technologies) and 0.40% SDS at 56 ºC. Following phenol chloroform extraction, RNA was precipitated using isopropanol and GenElute-LPA (Sigma-

Aldrich) as carrier. RNA concentration was determined by the Ribogreen (Invitrogen) assay, which was completed according to the manufacturer's instructions. PCRs to determine vRNA copy number per ng total RNA were completed as previously described (233), utilizing 2 μL of purified RNA and primer sets AE2963/AE2964 for Figure 3-7 (excluding HIV-Luc) and AE2961/AE4422 for Figure 3-8 samples and HIV-Luc.

TEM

Viruses produced from transfected HEK293T cells were pelleted at 30,000 rpm at 4°C for 1.5 h using a Beckman SW41 rotor. Pelleted virus was resuspended in a small volume of phosphate-buffered saline. An equal volume of 4% EM-grade paraformaldehyde (Electron Microscopy Sciences) was added and samples were incubated at 4 °C before embedding in epon resin. Thin (75-100 nm) sections were applied to 200-mesh carbon-coated copper grids, stained with 0.2% lead citrate, and observed using either a Tecnai-12 (FEI) or JEOL 1200EX microscope equipped with a Gatan or AMT 2k CCD camera, respectively. Images were captured at 37,500X magnification and were visually scanned to count 100 viral particles per preparation.

Cryo-ET

HIV-1 carrying the V165A mutation, WT virons produced with the indicated concentration of ALLINIs or DMSO control, PR– virions, Gag/ψ-minus VLPs, and Gag-LeuZip VLPs were pelleted as described above and were imaged by cryo-ET as described previously (316). In brief, purified fixed virus was mixed (2:1) with a suspension of colloidal gold particles (Electron Microscopy Sciences), applied to Quantifoil R2/2 holey carbon grids (Structure Probe, Inc.), and plunge-frozen in a Vitrobot (FEI). For data acquisition, grids were transferred to a

cryoholder (type 626; Gatan), and single-axis tilt series were recorded on a Tecnai-12 electron microscope equipped with an energy filter (GIF 2002; Gatan) operated at 120 keV in zero-loss mode with an energy slit width of 20 eV. Images were acquired on a 2,048- by 2,048-pixel CCD camera (Gatan) using SerialEM (317). Tilt-series projections were acquired at 2º intervals from ~ -66º to ~ 66º, at 38,500x magnification (0.78-nm/pixel) and a defocus of -4 μm. The electron dose per projection was ~1.1 e-/Å^2, giving a total cumulative dose of ~75 e-/Å^2. Tilt209 series were reconstructed using the Bsoft package (318), and virions were extracted as subtomograms and denoised by 20 iterations of anisotropic nonlinear diffusion (319).

Bubblegram and tomo-bubblegram Imaging

Dose-series of HIV-1 particles were acquired either on a CM200-FEG TEM (FEI), operating at 120 keV with doses of ~17 e-/Å^2 per exposure; or in a Tecnai-12 TEM operating at 120 keV at ~5e-/Å^2 per exposure. All images were collected on 2,048- by 2,048-pixel CCD cameras. Filled cores and eccentric aggregates bubbled at average doses of 165 ± 40 e-/Å^2, n=109. The procedure used to collect and analyze data for tomo-bubblegram imaging is described in the Results section. The distances from the bubble centers to the center of the viral Env were measured using Bsoft programs. Briefly, after extracting and centering a virion, its radius was estimated: First, to eliminate the missing wedge, particles were symmetrized (icosahedral symmetry, which is not present in HIV-1 virions, was used for ease of analysis; this symmetry renders an almost spherical particle, like the ones selected for this analysis, into a featureless sphere). Then the radius was estimated from a density profile of the averaged particle. The bubble centers were then selected manually in the tomo-bubblegram, using the BshowX utility, and the distances of the bubbles from the Env were calculated by subtracting the distance

from the center of the bubble to the center of the particle from the particle radius at the middle of the Env. Isosurface rendering of viral particles was done in Chimera (320). NC was purified as previously described (321) and lyophilized after adding one equivalent Zn^{2+} per zinc finger. NC was then resuspended in buffer (25 mM HEPES, 30 mM NaCl, 1 mM $MgCl_2$, 3 mM DTT and 10% of glycerol at pH 7.5) at a concentration of 10 μM, aliquoted, and immediately frozen and stored at -80ºC until used. For cryo-EM, thawed aliquots (25 μl) were centrifuged at maximum speed for 5 min in a tabletop centrifuge and the top 20 μl were discarded. The remaining 5 μl was applied to a 400 mesh copper grid covered with a thin carbon film supported by a thick lacey carbon film, washed with buffer (25 mM HEPES, 10 mM NaCl, 1 mM $MgCl_2$, pH 7.5) to remove the glycerol and plunge-frozen and imaged in a Tecnai-12 EM as described above.

Chapter 4

Allosteric integrase inhibitors cause retargeting of HIV-1 integration site distribution

Allosteric integrase inhibitors cause retargeting of HIV-1 integration site distribution

Kellie A. Jurado[1], Erik Serrao[1], Andrea L. Ferris[2], Xiaolin Wu[3], Hind Fadel[4,5], Eric Poeschla[4], Stephen H. Hughes[2], and Alan N Engelman[1]

[1]Department of Cancer Immunology and AIDS, Dana-Farber Cancer Institute, Boston, MA 02215, USA; [2]Retroviral Replication Laboratory and HIV Drug Resistance Program, National Cancer Institute, National Institutes of Health, Frederick, MD, USA; [3]Leidos Biomedical Research Inc, Frederick National Laboratory for Cancer Research, Frederick, MD, USA; [4]Division of Infectious Diseases, University of Colorado School of Medicine, Denver, CO, USA; [5]Division of Infectious Diseases, Mayo Clinic, Rochester, MN, USA

Contributions: I preformed virus preparations, infections and DNA extractions associated with Figure 4-1, 4-2 and 4-3.

Abstract

HIV-1 selectively integrates into the bodies of active genes as opposed to within promoters. This preference is largely manifested through interaction of the HIV-1 intasome (IN tetramer and vDNA) with host cellular co-factor LEDGF/p75. ALLINIs, which inhibit HIV-1 replication, target the interface of two IN molecules within the same binding pocket that LEDGF/p75 engages. Consistently, ALLINIs have been found to compete for LEDGF/p75 binding in vitro and to display weak antiviral activity when integration occurs within the early stages of HIV-1 replication. Yet, the main antiviral activity of ALLINIs occurs at the late stage of the viral lifecycle through inhibition of maturation. Therefore, we were interested in determining whether compound-treated viruses would result in altered integration site distribution within the subsequent infection. We found that ALLINI treatment did indeed cause changes in integration site distributions, an effect that was not dependent upon time of exposure to the compounds (drug exposure limited to early versus late phase of the lifecycle), but rather to the percent of inhibition of infection and the particular ALLINI utilized. Since a potent ALLINI used at inhibiting concentration demonstrated a tendency to alter integration site distribution, further attention concerning this phenotype should be provided to ALLINI compounds within the pipeline for clinical development.

Introduction

Despite HIV-1 unstintingly integrating vDNA into the genome of a susceptible host cell within an infected individual, an HIV-1 infection is not associated with directly causing cancer (322). The propensity for HIV-1 to target integration into the bodies of active genes is thought to be one reason as to why the DNA-integrating virus is specifically able to avoid insertional activation of proto-oncogenes (323). Four molecules of the viral protein IN will interact with vDNA to form an intasome-- the catalytically active entity responsible for mediating retroviral integration (129, 134, 144). Interaction of the intasome with host cellular cofactor LEDGF/p75, specifically within a defined pocket formed by the interface of two IN molecules, plays a critical role in directing HIV-1 integration into active transcription units (reviewed in (241, 242)). This defined pocket has recently been established as a feasible drug target (reviewed in (324)).

ALLINIs are a promising group of small molecule compounds that inhibit HIV-1 replication through modifying IN oligomerization (230-235, 284, 286). Surprisingly, although maintaining a weak activity during the early stages of HIV-1 replication in which integration occurs, the primary antiviral activity of ALLINIs occurs through stabilizing higher-ordered IN multimers during HIV-1 maturation (228, 233-235, 284, 286). Viruses made in the presence of the small molecules are unable to properly encapsidate their vRNP complex within a protective capsid core (325). These aberrant viruses are then defective for reverse transcription (228, 233, 284, 286) and integration (225, 228, 230, 233, 234, 284, 286) within the subsequent infection. ALLINIs engage IN within the same defined pocket as LEDGF/p75, essentially mimicking the exact covalent bond interactions as those of the host factor (reviewed in (324)). As ALLINIs compete for LEDGF/p75 binding in vitro (230, 232) and display weak activity during the early phase of HIV-1 replication, it is plausible that they could influence integration site distribution.

Since an alteration of integration site distribution could influence the propensity to avoid insertional activation, precaution should be taken when attempting to modify an interaction(s) that may influence the signature HIV-1 integration site pattern.

Prior studies on the influence of ALLINIs on HIV-1 integration site distribution have reported conflicting results. One study found a significant alteration of HIV-1 integration patterns, as defined by a change in the percent integration into genes, when cells were treated during the early phase of replication (228), whereas a separate study did not (235). Infections initiated with compound-treated virions have additionally not shown an effect on integration site distribution within either of the two reports (228, 235). Because of the differences within the literature, we sequenced integration sites following ALLINI exposure during both the early phase of HIV-1 infection and during virus production.

Results

ALLINIs can alter HIV-1 integration site patterns under certain infection conditions

To further investigate the impact of ALLINI treatment on integration site distribution in an attempt to understand the discrepancies within the literature, we first completed infections where drug treatment was limited to the early stages of virus replication by exposing target cells to different doses of two representative ALLINIs: BI-D (236) and ALLINI-2, which is also known as BIB-2 (236) (Figure 1-6). We found that the percentage of integration sites in genes was modified by both inhibitors under this condition of drug exposure (Figure 4-1A and B). Interestingly, ALLINI-2 caused a decrease in the percentage of integrations into genes with an inhibitor dose as low as EC_{60} (Figure 4-1B), whereas BI-D did not show a difference in integration site distribution patterns at an EC_{60} drug dose, but did at the next tested drug dose where 85% of the infection was inhibited (Figure 4-1A).

We next completed infections where drug exposure was limited to the late stages of virus replication by providing various drug doses of ALLINI-2 or BI-D during virus production and then exposing these viruses to susceptible host cells. Since the two previous integration site sequencing studies (228, 235) did not find an effect on integration site distribution under a single drug dose, we decided to complete a wide range of inhibitor doses in order to determine whether the percentage inhibited could contribute to the ability to see an effect as it did with BI-D when drug exposure was limited to the early phases of replication. Interestingly, we found that ALLINI-2 did not demonstrate a difference in integration site distribution under any drug dose tested (Figure 4-2B), whereas BI-D showed a decrease in the percentage of integrations into genes only with high inhibitor doses of EC_{95} or EC_{99} (Figure 4-2A). Although this finding was

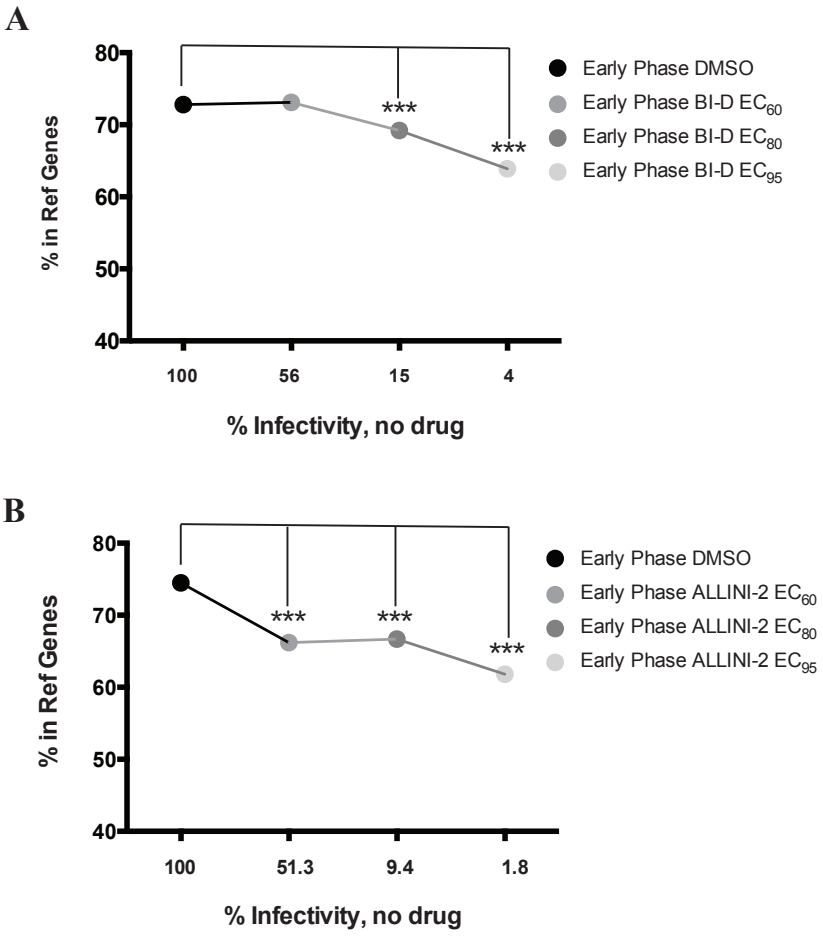

Figure 4-1. Representative ALLINIs BI-D and ALLINI-2 retarget HIV-1 integration when exposure is limited to the early stages of the HIV-1 replication lifecycle

Percent integrations into reference genes (n=1) determined from DNA extracted from SupT1 cell cultures 5-days postinfection with HIV-Luc that was made from HEK293T cells in the presence of DMSO, or EC_{60}, EC_{80} or EC_{95} doses of BI-D (A) or ALLINI-2 (B). Realized percent infectivity at 48 h postinfection is reported on the x-axis (normalized to DMSO control). The percentage of integrations into reference genes of a computationally generated, matched random control sites would be 44.7%. P-values were determined utilizing Fisher's extact test: * = $p < 0.01$ and *** = $p < 0.00001$.

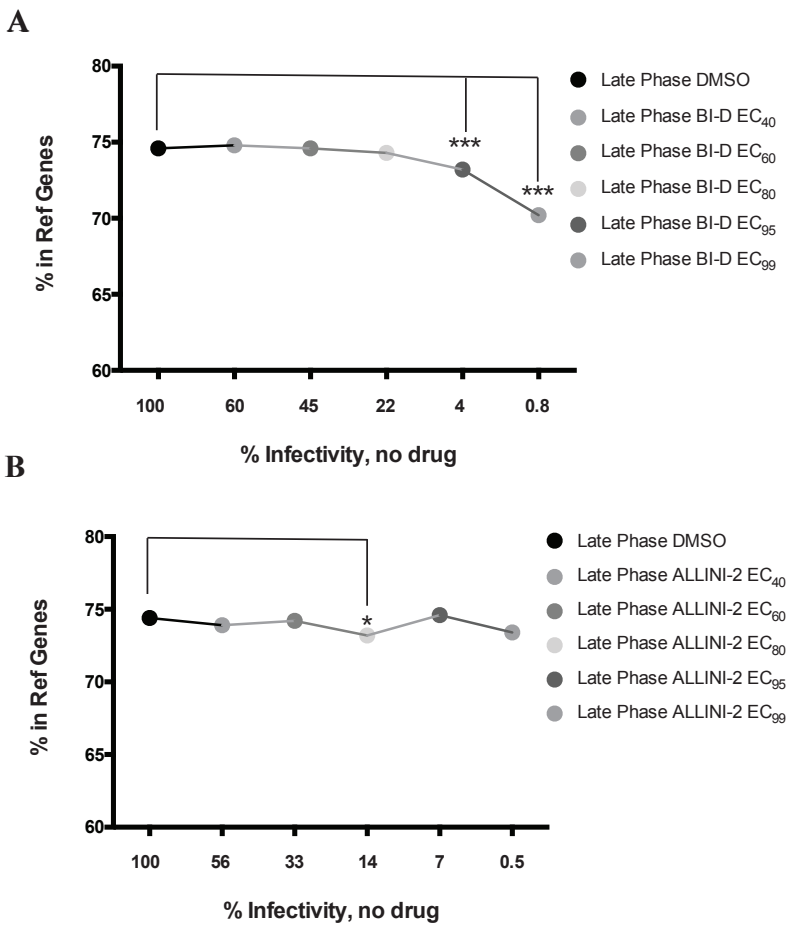

Figure 4-2. ALLINI BI-D retargets HIV-1 integration sites when exposure is limited to production under high percentage of inhibition

Percent integrations into reference genes determined from DNA extracted from SupT1 cell cultures 5-days postinfection with HIV-Luc that was made from HEK293T cells in presence of DMSO or EC_{40}, EC_{60}, EC_{80}, EC_{95} and EC_{99} doses of BI-D (A: representative data of 1 experiment; n=6 for some data points) or ALLINI-2 (B). Realized percent infectivity at 48 h postinfection is reported on the x-axis (normalized to DMSO control). The percentage of integrations into reference genes of a computationally generated, matched random control sites would be 44.7%. P-values were determined utilizing Fisher's extact test: * = $p < 0.01$ and *** = $p < 0.00001$.

reproducible, 2 out of the 6 experiments failed to detect considerable differences in integration site distribution under these high inhibitor doses.

The influence of LEDGF/p75 on integration retargeting by BI-D during HIV-1 production.

Since we (233) and others (180, 228, 284, 326) have shown that LEDGF/p75 does not influence ALLINI potency during production, we were interested in determining whether LEDGF/p75 within the virus-producing cell played a role in the BI-D-induced alteration of HIV-1 integration site distribution utilizing LEDGF/p75 knockout cells (LKOs) (180). We found that, independent of whether the target cells were LEDGF/p75 competent or depleted for the host factor, when LEDGF/p75 was not present in the producer cell (LKO virus; B1 versus B2 and B5 versus B6) that we lost the ability for the drug to promote retargeting of integration into genes since there was not a difference between integration into reference genes when the virus was made in the presence of BI-D (B2 and B6) or was made in the presence of the DMSO control (B1 and B5) (Figure 4-3). By contrast when the virus was made from a cell that is LEDGF/p75 competent (293T virus; B3 versus B4 and B7 versus B8), we regained the ability to influence retargeting within the subsequent target cell, as there was a considerable difference when virus was made in the presence (B4 and B8) or absence (B3 and B7) of BI-D. Consistently, this result was independent of whether the target cells were LEDGF/p75 competent or depleted for the host factor.

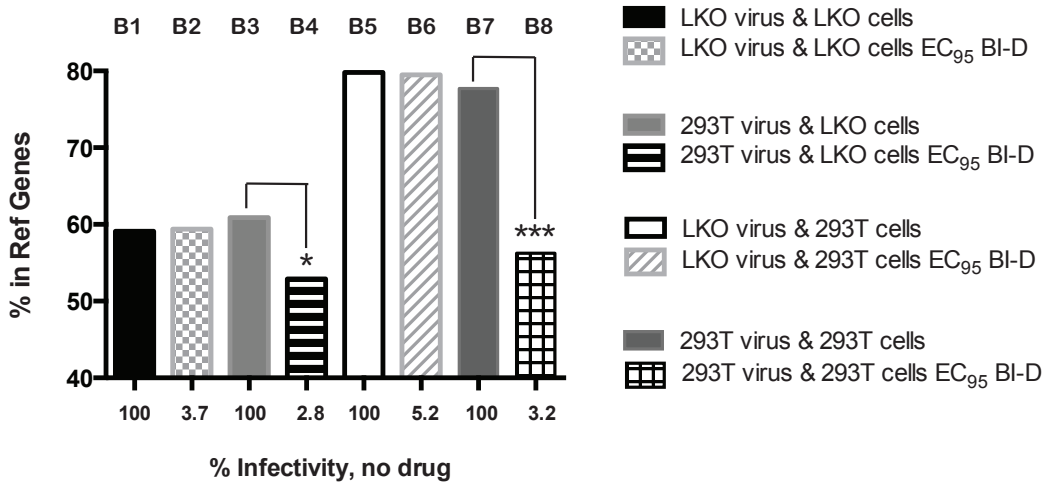

Figure 4-3. Retargeting of HIV-1 integration site distribution by BI-D exposure during virus production is dependent upon the expression of LEDGF/p75 within the virus-producing cell

Percent integrations in reference genes were determined in DNA extracted from cell cultures that were LEDGF/p75 depleted (LKO) or competent that had been infected with HIV-Luc virus that was produced in either LKO or 293T cells in the presence or absence of an EC_{50} dose of BI-D. Realized percent infectivity at 48 h postinfection is reported on the x-axis (normalized to DMSO control). The percentage of integrations into reference genes of a computationally generated, matched random control sites would be 44.7%. P-values were determined utilizing Fisher's extact test: * = $p < 0.05$ and *** = $p < 0.00001$.

Discussion

Because of conflicting results within the literature on the influences of ALLINIs on HIV-1 integration site distribution (228, 235), we determined whether integration sites under infection conditions where ALLINI exposure was limited to either the early phase of HIV-1 infection or the late stages of the virus lifecycle— viral production. We found alterations of HIV-1 integration site patterns to occur independent of time of drug exposure for one highly potent ALLINI, BI-D (Figure 4-1 and 4-2) (236). Although this finding was reproducible, only 4 out of the 6 experiments we completed determined considerable differences in integration site distribution. This inconsistency of results indicates that there may be an unconsidered infection property that is contributing to the ability to observe differences in integration site distribution and signifies that more work must be completed before definitive conclusions can be made. Similar to Sharma et al. (228), we found disruptions in integration site distribution to only occur when drug exposure was limited to the early stages of HIV-1 replication with another representative compound, ALLINI-2 (Figure 4-1 and 4-2) (237). Therefore, our results are supportive of Sharma et al. (228) who found an alteration of integration site patterns associated with HIV-1 when drug exposure was limited to the early stages of virus replication. In contrast to their work we also found an effect of inhibitor on the late stages of virus replication with 1 of 2 representative ALLINI inhibitors in the majority of experiments completed.

Because we completed multiple infections with a titration curve of BI-D exposure during virus production, we were able to determine the role that percentage of inhibition could be contributing to the discrepancies within the literature. In fact, the main differences between the different methods of infections was the percentage of inhibition achieved via the amount of inhibitor provided (~EC_{95} versus ~EC_{75} (228)). Interestingly, we found that integration site

patterns of BI-D treated viruses were only modified under infection conditions where the percentage of inhibition was 95-99% (Figure 4-2). The high level of inhibition needed to observe an effect indicates that compound treatment during production only influences a very small minority of virions, whose effects on integration sites can easily be masked by viruses that are not manipulated upon infections with less inhibitor/inhibition.

We (233) and others (180, 228, 284, 326) have shown that LEDGF/p75 does not influence ALLINI potency during production. Therefore, in order to determine whether the critical host factor within virus-producing cells played a role in the BI-D-induced alteration of HIV-1 integration site distribution we observed when drug exposure was limited to production, we utilized LKOs as virus producer and/or susceptible target cells (180). Surprisingly, we found that the ability to retarget integration sites under infection conditions where a BI-D dose of EC_{95} was provided during virus production was dependent upon the presence of LEDGF/p75 (Figure 4-3). Therefore, our deep sequencing results indicate that LEDGF/p75 expression within the virus-producer cell appears to be especially important in the ability for BI-D to influence integration site distribution under infection conditions with a high percentage of inhibition during the late stage of HIV-1 replication.

Beyond a recent study that found LEDGF/p75 to be incorporated into HIV-1 viral particles (326), a role for LEDGF/p75 within the late stages of viral replication is not widely accepted within integration community. Established to be a substrate for HIV-1 protease, LEDGF/p75 is degraded after incorporation (326). Whether there is a proper role for LEDGF/p75 incorporation into the viral particle or rather incorporation is just a mere consequence of being an interacting partner with HIV-1 IN within the context of Gag-Pol is uncertain and requires further experimentation. Regardless, our results indicate that within a

minority of virus particles, BI-D-induced retargeting of the HIV-1 integration pattern seen within a subsequent infection is apparently dependent upon the LEDGF/p75 that is incorporated into the viral particle.

Since BI-D and not ALLINI-2 repeatedly, albeit within only 4 out of 6 experiments, yielded differences in integration patterns when exposure was limited to production suggests that a particular characteristic of the ALLINI inhibitor appears to be principally important in yielding effects on integration patterns. Because a relatively potent ALLINI may result in altered integration sites independent of the time of compound exposure, our results suggest that a more thorough investigation of this property should be mandatory prior to clinical application of these small molecule inhibitors.

Materials and Methods

Plasmids, antivirals, and cells

Single-round HIV-Luc was co-expressed from pNLX.Luc.R- (250) and the VSV-G glycoprotein was expressed using pCG-VSV-G (250). BI-D and ALLINI-2 were synthesized as described (236, 237). LEDGF/p75 knockout HEK293T cells were constructed as described (180). Transformed HEK293T cells (ATTC: CRL-3216) and LEDGF/p75 knockout HEK293T cells were grown in DMEM while human SupT1 T cells (NIH ARRRP item number 100) were maintained in RPMI medium 1640, both supplemented to contain 10% (vol/vol) FBS, 100 IU/mL penicillin, and 100 μg/mL streptomycin.

Viruses and antiviral assays

HIV-Luc was produced by cotransfecting HEK293T cells (8×10^6) with 9 μg pNLX.Luc.R- and 1 μg pCG-VSV-G using PolyJet transfection reagent (SignaGen Laboratories). DMSO or ALLINIs were added with fresh media at ~17-20 h post transfection, and cell supernatants were collected 24 h later. Cell-free viruses were concentrated by ultracentrifugation (30,000 rpm at 4°C for 1.5 h using a Beckman SW41 rotor) and DNase-treated for 1 h at 37 °C. Virus concentrations were determined using a commercial p24 ELISA kit (Advanced Biosciences Laboratories). SupT1 cells (3×10^6) and HEK293T cells (3×10^5) were infected with 500 ng/mL p24 for 2 hours, after which infected cells were washed 1X in phosphate buffered saline solution and then replenished with fresh media. Luciferase values, expressed as relative light units, were determined 48 h postinfection and cells were harvested 5 days postinfection for DNA extraction.

Deep sequencing of HIV-1 integration sites

DNA was extracted from SupT1 and HEK293T cells infected with ultrafiltered, DNase-treated (1 h at 37 °C) HIV-Luc (100 ng p24/mL) using the DNeasy blood and tissue kit (Qiagen) 5 days post-infection using the DNeasy Blood and Tissue Kit (Qiagen). Extracted DNA (20 μg) was then subjected to overnight digestion with MseI and BglII and subsequently purified using the QIAquick PCR Purification Kit (Qiagen). Double-stranded asymmetric linker DNA (1.5 μM) was made as described (327) and ligated with digested cellular DNA (1 μg) overnight at 16°C in four parallel reactions. The DNAs were then pooled and re-purified using the QIAquick PCR Purification Kit. Viral LTR-host genomic DNA junctions were amplified by seminested PCR. PCRs multiplexed into eight separate samples each contained 1 μg DNA substrate and first-round HIV-1 LTR specific PCR primer and the linker specific primer in Advantage 2 PCR Buffer. The linker-specific primer is complementary to the annealed linker and contains the Illumina P7 adapter sequence. Completed PCR reactions were then pooled, PCR purified and subjected to the seminested PCR where the same linker-specific primer was utilized along with a second-round HIV-1 LTR specific PCR primer that additionally contained the Illumina P5 adapter sequence. PCRs were then incubated at 94°C for 4 min, followed by six cycles at 94°C for 15 sec, 60°C for 30 sec, and 68°C for 45 sec. Reactions were then PCR cycled 24 times at 94°C for 15 sec, 55°C for 30 sec, and 68°C for 45 sec, that was finally followed by an extension for 10 min at 68°C. Pooled PCRs were then purified using the QIAquick PCR Purification Kit and sequenced on the Illumina MiSeq platform at the Dana-Farber Cancer Institute Molecular Biology Core Facilities.

Bioinformatics analysis of integration sites

Illumina reads were parsed for LTR-containing sequences. LTR sequences were then trimmed from each read with duplicates being removed from the trimmed reads and the resulting sequences were aligned to human reference genome hg19 by BLAT (328). Alignments with e values less than 0.05 and that matched starting from the first nucleotide after the LTR were selected. Bit scores (differences <0.0001) were used to remove multiple genomic sequences in order to identify unique alignments. The start position of the alignment on the positive strand was chosen as the insertion site, while 4 nucleotides were subtracted from the start position of alignments on the negative strand. Bedtools were used to calculate the gene densities for each insertion (329). An MRC dataset of 282,824 sites was created by selecting random genomic positions in proximity (<500 bp) of a AvrII, NheI or SpeI recognition site.

Chapter 5

Discussion

Mechanism of action for 2-(quinolin-3-yl) acetic acid derivatives

X-ray co-crystallography (225, 228, 230, 232-235) and selection of resistance mutations (225, 226, 228, 230) within IN have revealed the binding site of ALLINIs to be at the interface of two IN monomers. ALLINIs specifically bind within a cavity formed by two IN CCDs in which the host factor LEDGF/p75 normally engages. Small molecule contact is accomplished through mirroring the critical interactions formed by LEDGF/p75 (hydrogen bonds formed from LEDGF/p75 residue Asp 366; Figure 1-5 and Figure 2-5). Although there is strong evidence that the molecular target of the compounds is IN, selection of ALLINI-resistance outside of IN could indirectly occur since multiple steps of the viral lifecycle are blocked (Chapter 2) and/or multiple viral proteins could be involved in the step inhibited (Figure 3-9). PR inhibitors have provided precedent for trans-protein drug resistance. PR inhibitors also cause replication blocks at multiple steps of the viral lifecycle, but the inhibitory potential appears to be especially important at entry (304). Consistently, in addition to finding PR inhibitor drug resistance mutations within PR, resistance mutations could also be found within the cytoplasmic tail of Env (304). Determining whether ALLINI resistance mutations can arise outside of the IN reading frame could be important in further elucidating the functional role of IN during maturation.

By limiting compound exposure to a particular phase of HIV-1 replication through use of a single-round virus infection system, we were able to separate the effects of the investigational inhibitor on the *early* versus *late* stages of the virus lifecycle. Upon this analysis we found that the main antiviral activity of ALLINIs occurred during a late stage event; as drug potency of a spreading replication was retained only when the virus was produced in the presence of the inhibitor (during the *late* phase) (Figure 2-1 and Table 2-1) (233). This differs from INSTIs where drug potency of a spreading replication is retained when drug exposure is limited to the

acute phase of infection (during the *early* phase of replication) (Table 2-1) (233). Several other groups have since corroborated this conclusion with various ALLINI derivatives utilizing similar methodology (228, 235, 284) or through time of addition experiments (234, 286). This was somewhat of an unanticipated finding since the catalytic activity of IN occurs within the *early* phase of virus replication.

Class II IN mutations: A foreshadowing for a role for IN within maturation

IN amino acid substitutions in or around the LEDGF/p75 binding pocket, which resulted in disruption of the IN-LEDGF/p75 interaction, also demonstrated decreased viral fitness (114, 184). Prior to detection of the dominant role for LEDGF/p75 during HIV-1 integration, the block in replication of these IN mutant viruses was originally proposed as evidence for the importance of the host factor during an infection (114). Yet, upon further breakdown, the block in replication was instead mapped to preintegrative steps (184). Rather than catalytic activity being defective, blocks in the ability to properly undergo reverse transcription were instead discovered (184). These findings indicated that introduction of missense mutations in or around the LEDGF/p75 binding pocket resulted in the class II IN mutant virus phenotype, leading to the prediction a number of years ago that small molecule inhibitors that target this region may induce the class II IN phenotype— and cause pleiotropic perturbations within the HIV-1 lifecycle (183, 184). Thus, the *late* stage block of HIV-1 replication elicited by a small molecule that targets IN within the LEDGF/p75-binding pocket of ALLINIs was resonant of the preintegrative blocks induced by class II IN mutations.

ALLINIs exposure during production induces the class II IN mutant virus phenotype

In addition to blocking the integration step, ALLINI-treated viruses exhibited several defects along the HIV-1 replication pathway. As predicted, these replication blocks virtually mirrored those of class II IN mutant viruses: maturation/assembly (228, 233, 284, 286), reverse transcription (228, 233, 284, 286), and integration (225, 228, 230, 233, 234, 284, 286). Although multiple steps were inhibited, we found inhibitory potential was manifested at the maturation step (Figure 3-1). This finding indicates that when drug exposure is limited to production, the defects seen within reverse transcription and integration are a mere consequence of the aberrant/eccentric viral particle formed. The fact that ALLINIs only induce reverse transcription defects when exposure is limited to production (Figure 2-4), suggests that the influence on vDNA synthesis seems to occur prior to or immediately upon virus entry into target cells. ALLINIs do not inhibit RNA incorporation (233, 330), RT enzymatic activity (284, 330), its association with vRNA within the virion (284) or the placement of the tRNA primer on the vRNA genome (330). Therefore, we hypothesize that upon entry into the subsequent target cell, the lack of protective encasing provided by the capsid core leaves the vRNA, RT enzymes and/or the vDNA intermediates more vulnerable to diffusion into the milieu of the host cell cytoplasm. The absence of the protective capsid encapsidation around the vRNA within eccentric virions therefore directly affects reverse transcription efficacy within the subsequent infection-- resulting in the observed defects in early and late reverse transcript products (Figure 2-4). In addition to the lack of vDNA production limiting substrate availability for integration, without the protective capsid encasement IN would also face the diffusion challenge prior to association with the completed vDNA genome. This would account for our finding that the block of maturation of viruses made in the presence of ALLINIs serves as a bottleneck to the subsequent steps within

the HIV-1 replication lifecycle. With the wide range and large number of single point mutations that result in the class II IN phenotype (157), determining whether maturation underlies the HIV-1 replication block of all class II IN mutants, could help to delineate whether all class II mutants are "alike" or if there can be further organization within the class.

The one block of HIV-1 replication known to be associated with the class II IN mutant phenotype that was not found to be defective upon ALLINI exposure during production was virus release. Although virus release has been reported with some class II IN mutants, detection appears to be sensitive to cell-type used to produce the mutant viruses (157, 158, 250). The most common cell-type utilized to produce ALLINI treated viruses, HEK293T (180, 228, 233-235, 284, 330), also does not elicit the virus release defect seen within some class II IN mutant viruses (157). However, defects in virus release upon ALLINI exposure were not observed using PBMCs (233), MT2 (284) or Jurkat cells (180), cell cultures that are more relevant than HEK293T cells when inferring results for HIV-1 replication within infected human hosts.

LEDGF/p75 does not play a role in the potency of ALLINI

ALLINI potency is realized because LEDGF/p75 does not compete for IN-binding during virus production. Since ALLINIs engage the IN dimer interface within the LEDGF/p75 binding pocket, the host factor can serve as a competitive threat to binding of the small molecule inhibitors. When the integration host factor is removed through knockdown (233, 284, 326) or knockout (180, 228), the strength of the compounds is modified during the *early,* but not the *late* stage of HIV-1 replication (where potency of a spreading replication is already realized) (Table 2-1 & Table 2-2). This finding indicates that LEDGF/p75 only plays a competitive role with the inhibitors during the *early* stages of the viral lifecycle. LEDGF/p75 is a protein that is

constitutively bound to chromatin; therefore it is reasonable that it would primarily serve as a compromise to ALLINI potency only when in the same location-- after the PIC enters into the nucleus, but prior to strand transfer. Since potency is determined at the *late* stage of HIV-1 replication, the mechanism of action of ALLINIs is LEDGF/p75 independent.

There is a recent report that LEDGF/p75 *can* be incorporated into the HIV-1 particle through a direct interaction with the Gag-Pol polyprotein (326). Although the finding that ALLINI potency is LEDGF/p75-independent during the *late* stages of the virus lifecycle (180, 228, 233, 284, 326) suggests that LEDGF/p75 incorporation during virus production must either be unstable (through quick degradation (326)) or not incorporated into particles at substantial levels. Interestingly, LEDGF/p75 overexpression within the virus-producing cell also did not result in a change of ALLINI potency (284). This finding further supports that there must be a particular block to the competitive role of LEDGF/p75 during virus production. This could potentially be explained through quick degradation upon PR activation within the maturing virion or a lack of substantial incorporation due to: 1. immediate localization of the surplus protein into the nucleus thereby limiting interaction opportunity or 2. lack of IN dimer interface of Gag-Pol within cellular milieu. Understanding whether overexpression of LEDGF/p75 results in increased incorporation into the HIV-1 particle could be insightful into understanding the discrepancy that despite the apparent incorporation of LEDGF/p75 during virus production, there is no effect on ALLINI potency.

ALLINIs function through inducing higher-ordered IN multimerization

Consistent with in vitro work demonstrating ALLINI enhancement of the multimeric state of recombinant IN (230-232, 234, 235), compound treatment of virus-producing cells

stabilized an oligomeric form of IN within nascent virions (233, 284, 286). Regions within the CCD and CTD of IN promote stabilization of the aberrant higher ordered IN multimers in ALLINI-induced multimerization (235, 331). This differs from the IN tetramerization driven by LEDGF/p75, where interactions occur at interfaces within the CCD and NTD of IN (332, 333). Although the exact multimeric state of IN within untreated HIV-1 particles is unknown, the estimated concentration of IN within virions is 20 mg/mL (324) suggesting that IN would likely exist within an oligomeric form. Our findings, along with others, indicate that stabilization of a higher-ordered form of IN upon ALLINI exposure during virus production results in disruption of proper RNP positioning within the capsid core, generating the observed eccentric morphology.

Complete genetic removal of IN from the virus (HIV-Luc.ΔIN) also causes an increase in the incidence of the eccentric morphology (Figure 2-3) (233). In an attempt to demonstrate the direct role of IN in the mislocalization of the RNP seen within eccentric viruses, we extended TEM analysis of Vpr-IN transcomplemented HIV-Luc.ΔIN viruses. The partial rescue of the electron-dense core indicates that IN indeed has a direct role in normal core formation (Figure 3-8). The protein-processing defects associated with HIV-Luc.ΔIN progeny (Figure 2-2) (233), likely precludes complete rescue of electron-dense cores. Consistently, ALLINI treatment of transcomplemented viruses then reversed the partial rescue of electron-dense cores, resulting in a phenocopy of untranscomplemented HIV-Luc.ΔIN. This result indicates that ALLINI exposure during production results in phenotypic removal or "barring" of IN within the virion (Figure 3-8).

ALLINI stabilization of higher-ordered IN multimers could result in a physical obstruction within the virion that instigates disruptive maturation, which is ultimately shown in the mislocalization of the RNP seen within eccentric viruses. Or perhaps by phenotypic removal of IN through formation of ALLINI-induced higher-order multimers, IN is no longer able to

interact with an IN-binding partner(s) that is critical for proper RNP encapsidation to proceed. In support of the second model, we found the ability for the small molecules to induce the eccentric morphology during virus production to be dependent upon the HIV-1 vRNA substrate incorporated within the virion (Figure 3-7). This suggests that IN must be interacting with the HIV-1 RNA genome in a specific manner and disruption of this interaction through stabilization of higher-order IN results in the lack of proper core encapsidation. Therefore, I predict IN plays an active role in vRNA incorporation into the mature CA core.

In summary, through engaging the IN-IN interface within the LEDGF/p75 binding pocket, ALLINIs promote higher-order IN multimerization within the maturing virion in a LEDGF/p75-independent manner. This uncouples IN from its presumed usual role during maturation, and ultimately results in a mislocalized RNP to outside of the mature CA core. This aberrant, eccentric virion form is then incapable of proper reverse transcription and integration within the subsequent infection.

ALLINIs perturb proper integration site distribution

Conflicting results have been published concerning the effect of ALLINIs on HIV-1 integration site distribution. One report indicated a perturbation of integration site distribution only when drug exposure limited to the *early* stages of virus replication (228), whereas the other found no effect of ALLINIs despite time of compound exposure (235). We have continued to add to the dissimilarity of results, but in a manner that may resolve the inconsistencies within the literature. We find alterations of HIV-1 integration site patterns to occur independent of time of drug exposure within the majority of experiments (Figure 4-1 and 4-2). Therefore, our results are

supportive of the Sharma et al. (228) finding of disruptive integration site patterns when drug exposure is limited to the *early* stages of virus replication, but in contrast to their work we also found an effect of inhibitor on the *late* stages of virus replication for 1 of 2 representative ALLINIs (Figure 4-2). Although, in order to observe a *late* stage effect on integration patterns, we found the percentage of inhibition along with the particular ALLINI derivative utilized to be important. We specifically needed the percentage of inhibition through compound treatment during production to be 95-99% to observe a substantial effect on integration site distribution within the *late* stages of replication (Figure 4-2). Both previously published reports (228, 235) did not achieve this level of inhibition, which could potentially explain the discrepancy between our finding and the past two studies in regards to ALLINI treatment during production. The high level of inhibition needed in order to observe an effect indicates that ALLINI treatment during production only influences a very small minority of virions, whose influences on integration sites can easily be masked by viruses that are not affected upon infections with less inhibitor/inhibition (Figure 4-2). Further, only one of the two inhibitors examined yielded differences of integration patterns within 4 of 6 experiments, indicating that a particular characteristic of the ALLINI appears to be principally important in yielding effects on integration patterns within the subsequent cell when treatment is administered during virus production. Further experimentation must be taken in order to determine mechanistic aspects/compound characteristics/infection conditions that contribute to uncovering a meaningful difference in integration site distribution upon ALLINI drug treatment during virus production prior to definitive conclusions being drawn. Regardless, because a relatively potent ALLINI resulted in altered integration sites independent of the time of compound exposure in the

majority of experiments completed, our results suggest attention should be paid to modifications of integration site distributions when considering compounds for clinical development.

Through use of LEDGF/p75 knockout cells we were able to pinpoint LEDGF/p75 expression within the producer cell to be especially important in ALLINI influence of integration site distribution during the late stage of HIV-1 replication (Figure 4-3). This was a particularly surprising finding since we and others have shown that ALLINI potency is not affected through LEDGF/p75 depletion (180, 228, 233, 284, 326) or overexpression (284). Although a role for LEDGF/p75 in HIV-1 replication beyond integration has yet to be found, LEDGF/p75 is incorporated into the HIV-1 particle through a direct interaction with the Gag-Pol polyprotein, but is degraded by HIV-1 PR within the virion (326). Interestingly, LEDGF/p75 was found to reverse ALLINI-induced aberrant higher-ordered IN multimerization, likely through competitive binding (332). Thereby perhaps within a minority of cases, by competing for the LEDGF/p75 binding site at the interface of the IN dimer, incorporation of LEDGF/p75 provides protection and/or destabilizes the ALLINI-induced IN multimer resulting in a subset of IN molecules still capable of interacting with vDNA. As LEDGF/p75 has been identified as a substrate for HIV-1 PR (326), the host factor bound to the IN dimer interface may still be subject to PR degradation. This could potentially lead to an inactivated form of the IBD remaining within the LEDGF/p75 binding pocket and ultimately result in preclusion of LEDGF/p75 binding to an IN dimer. The precluded IN dimer may still be capable of interaction with vDNA within the subsequent target cell and ultimately result in disruption of the normal HIV-1 integration pattern. Analysis of in vitro PR cleaved IN-LEDGF/p75 could be helpful in determining the validity of this working model for describing how ALLINI exposure during production influences integration site distribution within a LEDGF/p75-dependent manner in a minority of cases.

Outlook for current allosteric integrase inhibitors

The primary weakness of the current repertoire of reported ALLINI derivatives is the tendency for viruses to quickly develop resistance mutations to the compounds in vitro. In reported ALLINI resistance studies to-date only five to six serial passages of HIV-1 virus in the presence of the small molecule compound were needed to select for inhibitor-resistant viruses (225, 228, 230). Since ALLINIs target an allosteric region as opposed to a catalytic site, a mutation within the host-factor binding pocket may be more tolerable as opposed to a mutation that directly influences catalytic activity.

An HIV-1 infection does not directly cause cancer (323). The propensity for HIV-1 to target integration into the bodies of active genes is thought to be one reason as to why the DNA-integrating virus is specifically able to avoid insertional activation of proto-oncogenes (323). Since alteration of integration site distribution could influence the propensity to avoid insertional activation and a relatively potent ALLINI resulted in altered site distribution independent of the time of compound exposure with infections of high ALLINI inhibition within the majority of experiment completed (Figure 4-1 and 4-2), concern should likely be paid when determining whether a compound would be an appropriate candidate for translation into the clinic.

MINIs are modified ALLINIs (pyridine- versus quinoline-based compounds) that selectively inhibit the maturation step of replication as opposed to blocking the LEDGF/p75-IN interaction (228). Since inhibitory concentrations of MINIs do not influence LEDGF/p75 binding in vitro, these compounds should not alter integration site distribution regardless of drug exposure during *early* or *late* stages of virus replication. Although Sharma et al. failed to use a clinically relevant inhibitory concentration, as expected, there was no effect of inhibitor on HIV-

1 integration site distribution at the concentration utilized (~EC_{75}). Since inhibitory concentrations would be needed for use within an infected patient, further MINI studies would need to be completed on infections with higher percentages of inhibition to ensure integration site distribution remains the signature HIV-1 pattern. Regardless, since MINIs selectively inhibit the maturation step as opposed to blocking LEDGF/p75 binding (228), pyridine-based ALLINI compounds are likely the most promising, reported ALLINI to-date for continued development toward clinical use.

Boehringer Ingelheim (BI) advanced the first ALLINI, BI 224436, to phase Ia clinical trials (229, 334, 335). Single rising doses of BI 224436 were administered in a randomized, double-blind study to determine the safety and pharmokinetics of the small molecule within healthy male volunteers (336). The placebo-controlled study demonstrated adequate plasma concentrations with doses up to 200 mg and compound administration was concluded to be safe (336). BI 224436 was then enrolled within Phase Ib trial in order to determine safety and pharmokinetics with multiple rising doses, but was withdrawn prior to completion with the specified safety issue being identified as a "change in clinical laboratory test parameters" (337). As clinical trials progressed, key optimization of BI 224436 by BI was focused on improving the low in vivo clearance seen within rats (338). Utilizing scaffold hopping through modifying the quinoline group to a pyridine-based compound, BI decreased biliary recirculation in rats, thereby successfully improving in vivo clearance (338). MINIs are also pyridine-based compounds (228) therefore the BI-developed group of pyridine-based compounds likely possess the similar property of selectively inhibiting the late stage events of HIV-1 replication as opposed to inhibiting LEDGF/p75 binding. Interestingly, Fader et al. (338) found that the modified pyridine-based compounds appear to bind tighter to tetrameric IN substrates as opposed to dimeric IN

entities. This finding could potentially provide insight into the multimeric form of greater prevalence at the particular stages of replication (*early* versus *late*).

Model for the role of IN during HIV-1 particle maturation

The pleiotropic perturbations of class II IN mutant viruses were the first indication that IN may have a role that extends beyond its catalytic activity. The preintegrative defects at multiple steps of the viral lifecycle of class II IN mutant viruses have been understood for years (146), but the underlying aspects of IN within the *late* phase of replication has remained undefined. The large amount of mutations within all domains of IN that yield the class II phenotype (157) limited the deductive exploration for the role(s) of IN during production. Our findings (233), quickly followed by others (228, 234, 235, 284, 286), have reinvigorated the proposal and pursuit that IN may perform a role during maturation.

We were the first in the literature to propose a direct role for IN during core morphogenesis (Figure 3-9). Based on data described within this dissertation, we predict that IN serves to nucleate vRNA incorporation into the mature core, specifically through nucleating CA formation around genomic vRNA. A role for the viral enzyme within core morphogenesis has yet to be properly established, yet high affinity binding of IN to RNA has previously been observed in vitro (161). In support for an IN-vRNA interaction(s) in core morphogenesis as hypothesized within our model, our data revealed a role for vRNA in ALLINI-induced eccentric condensate formation (Figure 3-7). Additionally, a potential biological role for an IN-CA interaction has been suggested through the discovery of a linkage between IN and CA sequences changes among HIV-1 strains within AIDS patients (313).

Cryo-ET work completed by de Maro et al. (290) utilized single-point mutations that prevent complete PR processing and revealed a link between the condensed NC-RNA and the immature CA lattice. This finding suggests that the NC-RNA remains attached to the CA lattice after PR processing-- implying the presence of a potential interaction or link between the partially cleaved lattice and the condensed NC-RNA. It is an attractive hypothesis to propose that IN is involved in the formation and/or stabilization of the link. Determining whether the link between the condensed NC-RNA and the immature CA lattice can still be formed under conditions that pharmacologically (ALLINI treatment during virus production) or genetically (use of a ΔIN mutant virus manipulation of IN by) manipulate IN within a manner that disrupts the *late stage* role of IN would be extremely informative in addressing whether the described link is indeed representative of the CA-IN-vRNA complex within our model.

There are many unknowns that remain associated with our model: Are other viral particle components involved in the putative CA-IN-vRNA complex? Does the IN involved within the initiation model use IN within the context of Gag-Pol or is it post-cleavage IN? Does CA assembly begin at the wide or narrow end of the CA core? We hypothesize that IN alone as opposed to IN as a part of Gag-Pol is the responsible entity nucleating CA formation around genomic vRNA, since the compounds appear to functionally target post-cleavage IN (Figure 2-6). We also prefer the model where assembly begins at the wide end since the electron density is predominately found within this region of the virus particle (58) as well as initiation at the wide end would narrow down to give a CA cone of about the right length, as demonstrated by CA in the absence of a membrane in vitro (311). Further experimentation is needed to provide clarification to our model that poses an active role for IN in vRNA encapsidation during HIV-1 maturation.

Concluding remarks

Data described within this thesis have provided a somewhat unexpected answer that has rooted an even larger question. Through describing an unanticipated mechanism of action of a new class of small molecule inhibitor, we have reinstated the significance of a phenotype previously described primarily through genetics through now demonstrating that a pharmacological avenue can also lead to a similar phenotype. Our work has reinvigorated efforts on further uncovering the role of IN within the late stage of viral replication. With ALLINIs to continue to serve as biological probes and complement genetic work, we anticipate the role of IN during the *late* stage of virus replication to soon be fully elucidated.

References

1. UNAIDS (2013) UNAIDS Report on the Global AIDS Epidemic.
2. Barre-Sinoussi F, Chermann JC, Rey F, Nugeyre MT, Chamaret S, Gruest J, Dauguet C, Axler-Blin C, Vezinet-Brun F, Rouzioux C, Rozenbaum W, & Montagnier L (1983) Isolation of a T-lymphotropic retrovirus from a patient at risk for acquired immune deficiency syndrome (AIDS). *Science* 220(4599):868-871.
3. Gallo RC, Sarin PS, Gelmann EP, Robert-Guroff M, Richardson E, Kalyanaraman VS, Mann D, Sidhu GD, Stahl RE, Zolla-Pazner S, Leibowitch J, & Popovic M (1983) Isolation of human T-cell leukemia virus in acquired immune deficiency syndrome (AIDS). *Science* 220(4599):865-867.
4. Gelmann EP, Popovic M, Blayney D, Masur H, Sidhu G, Stahl RE, & Gallo RC (1983) Proviral DNA of a retrovirus, human T-cell leukemia virus, in two patients with AIDS. *Science* 220(4599):862-865.
5. Anonymous (1982) Epidemiologic aspects of the current outbreak of Kaposi's sarcoma and opportunistic infections. *The New England journal of medicine* 306(4):248-252.
6. CDC (1981) Kaposi's sarcoma and Pneumocystis pneumonia among homosexual men--New York City and California. *MMWR. Morbidity and mortality weekly report* 30(25):305-308.
7. CDC (1982) A cluster of Kaposi's sarcoma and Pneumocystis carinii pneumonia among homosexual male residents of Los Angeles and Orange Counties, California. *MMWR. Morbidity and mortality weekly report* 31(23):305-307.
8. Administration USFaD (2014) Antiretroviral drugs used in the treatment of HIV infection.

9. Fischl MA, Richman DD, Grieco MH, Gottlieb MS, Volberding PA, Laskin OL, Leedom JM, Groopman JE, Mildvan D, & Schooley RT (1987) The efficacy of azidothymidine (AZT) in the treatment of patients with AIDS and AIDS-related complex. A double-blind, placebo-controlled trial. *The New England journal of medicine* 317(4):185-191.

10. Larder BA & Kemp SD (1989) Multiple mutations in HIV-1 reverse transcriptase confer high-level resistance to zidovudine (AZT). *Science* 246(4934):1155-1158.

11. James JS (1995) Major study shows AZT monotherapy inferior. *AIDS treatment news* (no 231):3-4.

12. CDC (2011) HIV Surveillance --- United States, 1981-2008. in *MMWR. Morbidity and mortality weekly report* (Center for Disease Control and Prevention), pp 689-693.

13. Coffin J, Haase A, Levy JA, Montagnier L, Oroszlan S, Teich N, Temin H, Toyoshima K, Varmus H, Vogt P, & et al. (1986) Human immunodeficiency viruses. *Science* 232(4751):697.

14. Ratner L, Haseltine W, Patarca R, Livak KJ, Starcich B, Josephs SF, Doran ER, Rafalski JA, Whitehorn EA, Baumeister K, & et al. (1985) Complete nucleotide sequence of the AIDS virus, HTLV-III. *Nature* 313(6000):277-284.

15. Wain-Hobson S, Sonigo P, Danos O, Cole S, & Alizon M (1985) Nucleotide sequence of the AIDS virus, LAV. *Cell* 40(1):9-17.

16. Muesing MA, Smith DH, Cabradilla CD, Benton CV, Lasky LA, & Capon DJ (1985) Nucleic acid structure and expression of the human AIDS/lymphadenopathy retrovirus. *Nature* 313(6002):450-458.

17. Chen J, Nikolaitchik O, Singh J, Wright A, Bencsics CE, Coffin JM, Ni N, Lockett S, Pathak VK, & Hu WS (2009) High efficiency of HIV-1 genomic RNA packaging and

heterozygote formation revealed by single virion analysis. *Proceedings of the National Academy of Sciences of the United States of America* 106(32):13535-13540.

18. Swanson CM & Malim MH (2008) SnapShot: HIV-1 proteins. *Cell* 133(4):742, 742 e741.

19. Jacks T, Power MD, Masiarz FR, Luciw PA, Barr PJ, & Varmus HE (1988) Characterization of ribosomal frameshifting in HIV-1 gag-pol expression. *Nature* 331(6153):280-283.

20. Wilson W, Braddock M, Adams SE, Rathjen PD, Kingsman SM, & Kingsman AJ (1988) HIV expression strategies: ribosomal frameshifting is directed by a short sequence in both mammalian and yeast systems. *Cell* 55(6):1159-1169.

21. Gheysen D, Jacobs E, de Foresta F, Thiriart C, Francotte M, Thines D, & De Wilde M (1989) Assembly and release of HIV-1 precursor Pr55gag virus-like particles from recombinant baculovirus-infected insect cells. *Cell* 59(1):103-112.

22. Accola MA, Strack B, & Gottlinger HG (2000) Efficient particle production by minimal Gag constructs which retain the carboxy-terminal domain of human immunodeficiency virus type 1 capsid-p2 and a late assembly domain. *Journal of virology* 74(12):5395-5402.

23. Gelderblom HR, Hausmann EH, Ozel M, Pauli G, & Koch MA (1987) Fine structure of human immunodeficiency virus (HIV) and immunolocalization of structural proteins. *Virology* 156(1):171-176.

24. Kutluay SB, Zang T, Blanco-Melo D, Powell C, Jannain D, Errando M, & Bieniasz PD (2014) Global changes in the RNA binding specificity of HIV-1 gag regulate virion genesis. *Cell* 159(5):1096-1109.

25. Gottlinger HG, Sodroski JG, & Haseltine WA (1989) Role of capsid precursor processing and myristoylation in morphogenesis and infectivity of human immunodeficiency virus

type 1. *Proceedings of the National Academy of Sciences of the United States of America* 86(15):5781-5785.

26. Bryant M & Ratner L (1990) Myristoylation-dependent replication and assembly of human immunodeficiency virus 1. *Proceedings of the National Academy of Sciences of the United States of America* 87(2):523-527.

27. Zhou W, Parent LJ, Wills JW, & Resh MD (1994) Identification of a membrane-binding domain within the amino-terminal region of human immunodeficiency virus type 1 Gag protein which interacts with acidic phospholipids. *Journal of virology* 68(4):2556-2569.

28. Carlson LA, de Marco A, Oberwinkler H, Habermann A, Briggs JA, Krausslich HG, & Grunewald K (2010) Cryo electron tomography of native HIV-1 budding sites. *PLoS pathogens* 6(11):e1001173.

29. von Schwedler UK, Stray KM, Garrus JE, & Sundquist WI (2003) Functional surfaces of the human immunodeficiency virus type 1 capsid protein. *Journal of virology* 77(9):5439-5450.

30. Cimarelli A, Sandin S, Hoglund S, & Luban J (2000) Basic residues in human immunodeficiency virus type 1 nucleocapsid promote virion assembly via interaction with RNA. *Journal of virology* 74(7):3046-3057.

31. Bowzard JB, Bennett RP, Krishna NK, Ernst SM, Rein A, & Wills JW (1998) Importance of basic residues in the nucleocapsid sequence for retrovirus Gag assembly and complementation rescue. *Journal of virology* 72(11):9034-9044.

32. Muriaux D, Mirro J, Harvin D, & Rein A (2001) RNA is a structural element in retrovirus particles. *Proceedings of the National Academy of Sciences of the United States of America* 98(9):5246-5251.

33. Dawson L & Yu XF (1998) The role of nucleocapsid of HIV-1 in virus assembly. *Virology* 251(1):141-157.

34. Zhang Y, Qian H, Love Z, & Barklis E (1998) Analysis of the assembly function of the human immunodeficiency virus type 1 gag protein nucleocapsid domain. *Journal of virology* 72(3):1782-1789.

35. Crist RM, Datta SA, Stephen AG, Soheilian F, Mirro J, Fisher RJ, Nagashima K, & Rein A (2009) Assembly properties of human immunodeficiency virus type 1 Gag-leucine zipper chimeras: implications for retrovirus assembly. *Journal of virology* 83(5):2216-2225.

36. Gorelick RJ, Nigida SM, Jr., Bess JW, Jr., Arthur LO, Henderson LE, & Rein A (1990) Noninfectious human immunodeficiency virus type 1 mutants deficient in genomic RNA. *Journal of virology* 64(7):3207-3211.

37. Dannull J, Surovoy A, Jung G, & Moelling K (1994) Specific binding of HIV-1 nucleocapsid protein to PSI RNA in vitro requires N-terminal zinc finger and flanking basic amino acid residues. *The EMBO journal* 13(7):1525-1533.

38. Berkowitz RD, Ohagen A, Hoglund S, & Goff SP (1995) Retroviral nucleocapsid domains mediate the specific recognition of genomic viral RNAs by chimeric Gag polyproteins during RNA packaging in vivo. *Journal of virology* 69(10):6445-6456.

39. Moore MD, Nikolaitchik OA, Chen J, Hammarskjold ML, Rekosh D, & Hu WS (2009) Probing the HIV-1 genomic RNA trafficking pathway and dimerization by genetic recombination and single virion analyses. *PLoS pathogens* 5(10):e1000627.

40. Kutluay SB & Bieniasz PD (2010) Analysis of the initiating events in HIV-1 particle assembly and genome packaging. *PLoS pathogens* 6(11):e1001200.

41. Ivanchenko S, Godinez WJ, Lampe M, Krausslich HG, Eils R, Rohr K, Brauchle C, Muller B, & Lamb DC (2009) Dynamics of HIV-1 assembly and release. *PLoS pathogens* 5(11):e1000652.

42. Aldovini A & Young RA (1990) Mutations of RNA and protein sequences involved in human immunodeficiency virus type 1 packaging result in production of noninfectious virus. *Journal of virology* 64(5):1920-1926.

43. Jouvenet N, Bieniasz PD, & Simon SM (2008) Imaging the biogenesis of individual HIV-1 virions in live cells. *Nature* 454(7201):236-240.

44. Garrus JE, von Schwedler UK, Pornillos OW, Morham SG, Zavitz KH, Wang HE, Wettstein DA, Stray KM, Cote M, Rich RL, Myszka DG, & Sundquist WI (2001) Tsg101 and the vacuolar protein sorting pathway are essential for HIV-1 budding. *Cell* 107(1):55-65.

45. VerPlank L, Bouamr F, LaGrassa TJ, Agresta B, Kikonyogo A, Leis J, & Carter CA (2001) Tsg101, a homologue of ubiquitin-conjugating (E2) enzymes, binds the L domain in HIV type 1 Pr55(Gag). *Proceedings of the National Academy of Sciences of the United States of America* 98(14):7724-7729.

46. Martin-Serrano J, Zang T, & Bieniasz PD (2001) HIV-1 and Ebola virus encode small peptide motifs that recruit Tsg101 to sites of particle assembly to facilitate egress. *Nature medicine* 7(12):1313-1319.

47. Strack B, Calistri A, Craig S, Popova E, & Gottlinger HG (2003) AIP1/ALIX is a binding partner for HIV-1 p6 and EIAV p9 functioning in virus budding. *Cell* 114(6):689-699.

48. Gottlinger HG, Dorfman T, Sodroski JG, & Haseltine WA (1991) Effect of mutations affecting the p6 gag protein on human immunodeficiency virus particle release.

Proceedings of the National Academy of Sciences of the United States of America 88(8):3195-3199.

49. Fuller SD, Wilk T, Gowen BE, Krausslich HG, & Vogt VM (1997) Cryo-electron microscopy reveals ordered domains in the immature HIV-1 particle. *Current biology : CB* 7(10):729-738.

50. Wilk T, Gross I, Gowen BE, Rutten T, de Haas F, Welker R, Krausslich HG, Boulanger P, & Fuller SD (2001) Organization of immature human immunodeficiency virus type 1. *Journal of virology* 75(2):759-771.

51. Kaplan AH, Manchester M, & Swanstrom R (1994) The activity of the protease of human immunodeficiency virus type 1 is initiated at the membrane of infected cells before the release of viral proteins and is required for release to occur with maximum efficiency. *Journal of virology* 68(10):6782-6786.

52. Debouck C, Gorniak JG, Strickler JE, Meek TD, Metcalf BW, & Rosenberg M (1987) Human immunodeficiency virus protease expressed in Escherichia coli exhibits autoprocessing and specific maturation of the gag precursor. *Proceedings of the National Academy of Sciences of the United States of America* 84(24):8903-8906.

53. Tang C, Louis JM, Aniana A, Suh JY, & Clore GM (2008) Visualizing transient events in amino-terminal autoprocessing of HIV-1 protease. *Nature* 455(7213):693-696.

54. Krausslich HG, Ingraham RH, Skoog MT, Wimmer E, Pallai PV, & Carter CA (1989) Activity of purified biosynthetic proteinase of human immunodeficiency virus on natural substrates and synthetic peptides. *Proceedings of the National Academy of Sciences of the United States of America* 86(3):807-811.

55. Tritch RJ, Cheng YE, Yin FH, & Erickson-Viitanen S (1991) Mutagenesis of protease cleavage sites in the human immunodeficiency virus type 1 gag polyprotein. *Journal of virology* 65(2):922-930.

56. Prabu-Jeyabalan M, Nalivaika E, & Schiffer CA (2002) Substrate shape determines specificity of recognition for HIV-1 protease: analysis of crystal structures of six substrate complexes. *Structure* 10(3):369-381.

57. Lee SK, Potempa M, Kolli M, Ozen A, Schiffer CA, & Swanstrom R (2012) Context surrounding processing sites is crucial in determining cleavage rate of a subset of processing sites in HIV-1 Gag and Gag-Pro-Pol polyprotein precursors by viral protease. *The Journal of biological chemistry* 287(16):13279-13290.

58. Briggs JA, Wilk T, Welker R, Krausslich HG, & Fuller SD (2003) Structural organization of authentic, mature HIV-1 virions and cores. *The EMBO journal* 22(7):1707-1715.

59. Briggs JA, Grunewald K, Glass B, Forster F, Krausslich HG, & Fuller SD (2006) The mechanism of HIV-1 core assembly: insights from three-dimensional reconstructions of authentic virions. *Structure* 14(1):15-20.

60. Woodward CL, Cheng SN, & Jensen GJ (2015) Electron cryotomography studies of maturing HIV-1 particles reveal the assembly pathway of the viral core. *Journal of virology* 89(2):1267-1277.

61. Saphire AC, Bobardt MD, Zhang Z, David G, & Gallay PA (2001) Syndecans serve as attachment receptors for human immunodeficiency virus type 1 on macrophages. *Journal of virology* 75(19):9187-9200.

62. Arthos J, Cicala C, Martinelli E, Macleod K, Van Ryk D, Wei D, Xiao Z, Veenstra TD, Conrad TP, Lempicki RA, McLaughlin S, Pascuccio M, Gopaul R, McNally J, Cruz CC, Censoplano N, Chung E, Reitano KN, Kottilil S, Goode DJ, & Fauci AS (2008) HIV-1 envelope protein binds to and signals through integrin alpha4beta7, the gut mucosal homing receptor for peripheral T cells. *Nature immunology* 9(3):301-309.

63. Cicala C, Martinelli E, McNally JP, Goode DJ, Gopaul R, Hiatt J, Jelicic K, Kottilil S, Macleod K, O'Shea A, Patel N, Van Ryk D, Wei D, Pascuccio M, Yi L, McKinnon L, Izulla P, Kimani J, Kaul R, Fauci AS, & Arthos J (2009) The integrin alpha4beta7 forms a complex with cell-surface CD4 and defines a T-cell subset that is highly susceptible to infection by HIV-1. *Proceedings of the National Academy of Sciences of the United States of America* 106(49):20877-20882.

64. Geijtenbeek TB, Kwon DS, Torensma R, van Vliet SJ, van Duijnhoven GC, Middel J, Cornelissen IL, Nottet HS, KewalRamani VN, Littman DR, Figdor CG, & van Kooyk Y (2000) DC-SIGN, a dendritic cell-specific HIV-1-binding protein that enhances trans-infection of T cells. *Cell* 100(5):587-597.

65. Dalgleish AG, Beverley PC, Clapham PR, Crawford DH, Greaves MF, & Weiss RA (1984) The CD4 (T4) antigen is an essential component of the receptor for the AIDS retrovirus. *Nature* 312(5996):763-767.

66. Klatzmann D, Champagne E, Chamaret S, Gruest J, Guetard D, Hercend T, Gluckman JC, & Montagnier L (1984) T-lymphocyte T4 molecule behaves as the receptor for human retrovirus LAV. *Nature* 312(5996):767-768.

67. Maddon PJ, Dalgleish AG, McDougal JS, Clapham PR, Weiss RA, & Axel R (1986) The T4 gene encodes the AIDS virus receptor and is expressed in the immune system and the brain. *Cell* 47(3):333-348.

68. McDougal JS, Kennedy MS, Sligh JM, Cort SP, Mawle A, & Nicholson JK (1986) Binding of HTLV-III/LAV to T4+ T cells by a complex of the 110K viral protein and the T4 molecule. *Science* 231(4736):382-385.

69. Weiss CD, Levy JA, & White JM (1990) Oligomeric organization of gp120 on infectious human immunodeficiency virus type 1 particles. *Journal of virology* 64(11):5674-5677.

70. Zarr M & Siliciano R (2015) Stoichiometric parameters of HIV-1 entry. *Virology* 474:1-9.

71. Wu L, Gerard NP, Wyatt R, Choe H, Parolin C, Ruffing N, Borsetti A, Cardoso AA, Desjardin E, Newman W, Gerard C, & Sodroski J (1996) CD4-induced interaction of primary HIV-1 gp120 glycoproteins with the chemokine receptor CCR-5. *Nature* 384(6605):179-183.

72. Trkola A, Dragic T, Arthos J, Binley JM, Olson WC, Allaway GP, Cheng-Mayer C, Robinson J, Maddon PJ, & Moore JP (1996) CD4-dependent, antibody-sensitive interactions between HIV-1 and its co-receptor CCR-5. *Nature* 384(6605):184-187.

73. Deng H, Liu R, Ellmeier W, Choe S, Unutmaz D, Burkhart M, Di Marzio P, Marmon S, Sutton RE, Hill CM, Davis CB, Peiper SC, Schall TJ, Littman DR, & Landau NR (1996) Identification of a major co-receptor for primary isolates of HIV-1. *Nature* 381(6584):661-666.

74. Alkhatib G, Combadiere C, Broder CC, Feng Y, Kennedy PE, Murphy PM, & Berger EA (1996) CC CKR5: a RANTES, MIP-1alpha, MIP-1beta receptor as a fusion cofactor for macrophage-tropic HIV-1. *Science* 272(5270):1955-1958.

75. Dragic T, Litwin V, Allaway GP, Martin SR, Huang Y, Nagashima KA, Cayanan C, Maddon PJ, Koup RA, Moore JP, & Paxton WA (1996) HIV-1 entry into CD4+ cells is mediated by the chemokine receptor CC-CKR-5. *Nature* 381(6584):667-673.

76. Choe H, Farzan M, Sun Y, Sullivan N, Rollins B, Ponath PD, Wu L, Mackay CR, LaRosa G, Newman W, Gerard N, Gerard C, & Sodroski J (1996) The beta-chemokine receptors CCR3 and CCR5 facilitate infection by primary HIV-1 isolates. *Cell* 85(7):1135-1148.

77. Doranz BJ, Rucker J, Yi Y, Smyth RJ, Samson M, Peiper SC, Parmentier M, Collman RG, & Doms RW (1996) A dual-tropic primary HIV-1 isolate that uses fusin and the beta-chemokine receptors CKR-5, CKR-3, and CKR-2b as fusion cofactors. *Cell* 85(7):1149-1158.

78. Feng Y, Broder CC, Kennedy PE, & Berger EA (1996) HIV-1 entry cofactor: functional cDNA cloning of a seven-transmembrane, G protein-coupled receptor. *Science* 272(5263):872-877.

79. Weissenhorn W, Dessen A, Harrison SC, Skehel JJ, & Wiley DC (1997) Atomic structure of the ectodomain from HIV-1 gp41. *Nature* 387(6631):426-430.

80. Chan DC, Fass D, Berger JM, & Kim PS (1997) Core structure of gp41 from the HIV envelope glycoprotein. *Cell* 89(2):263-273.

81. Fitzon T, Leschonsky B, Bieler K, Paulus C, Schroder J, Wolf H, & Wagner R (2000) Proline residues in the HIV-1 NH2-terminal capsid domain: structure determinants for proper core assembly and subsequent steps of early replication. *Virology* 268(2):294-307.

82. Forshey BM, von Schwedler U, Sundquist WI, & Aiken C (2002) Formation of a human immunodeficiency virus type 1 core of optimal stability is crucial for viral replication. *Journal of virology* 76(11):5667-5677.

83. Rouzina I & Bruinsma R (2014) DNA confinement drives uncoating of the HIV Virus. *The European Physical Journal Special Topics* 223(9):1745-1754.

84. Arhel NJ, Souquere-Besse S, Munier S, Souque P, Guadagnini S, Rutherford S, Prevost MC, Allen TD, & Charneau P (2007) HIV-1 DNA Flap formation promotes uncoating of the pre-integration complex at the nuclear pore. *The EMBO journal* 26(12):3025-3037.

85. Hulme AE, Perez O, & Hope TJ (2011) Complementary assays reveal a relationship between HIV-1 uncoating and reverse transcription. *Proceedings of the National Academy of Sciences of the United States of America* 108(24):9975-9980.

86. Hu WS & Hughes SH (2012) HIV-1 reverse transcription. *Cold Spring Harbor perspectives in medicine* 2(10).

87. Barat C, Lullien V, Schatz O, Keith G, Nugeyre MT, Gruninger-Leitch F, Barre-Sinoussi F, LeGrice SF, & Darlix JL (1989) HIV-1 reverse transcriptase specifically interacts with the anticodon domain of its cognate primer tRNA. *The EMBO journal* 8(11):3279-3285.

88. Mak J, Jiang M, Wainberg MA, Hammarskjold ML, Rekosh D, & Kleiman L (1994) Role of Pr160gag-pol in mediating the selective incorporation of tRNA(Lys) into human immunodeficiency virus type 1 particles. *Journal of virology* 68(4):2065-2072.

89. Huang Y, Wang J, Shalom A, Li Z, Khorchid A, Wainberg MA, & Kleiman L (1997) Primer tRNA3Lys on the viral genome exists in unextended and two-base extended forms within mature human immunodeficiency virus type 1. *Journal of virology* 71(1):726-728.

90. Zack JA, Haislip AM, Krogstad P, & Chen IS (1992) Incompletely reverse-transcribed human immunodeficiency virus type 1 genomes in quiescent cells can function as intermediates in the retroviral life cycle. *Journal of virology* 66(3):1717-1725.

91. Kim SY, Byrn R, Groopman J, & Baltimore D (1989) Temporal aspects of DNA and RNA synthesis during human immunodeficiency virus infection: evidence for differential gene expression. *Journal of virology* 63(9):3708-3713.

92. Barbosa P, Charneau P, Dumey N, & Clavel F (1994) Kinetic analysis of HIV-1 early replicative steps in a coculture system. *AIDS research and human retroviruses* 10(1):53-59.

93. Bukrinsky MI, Sharova N, McDonald TL, Pushkarskaya T, Tarpley WG, & Stevenson M (1993) Association of integrase, matrix, and reverse transcriptase antigens of human immunodeficiency virus type 1 with viral nucleic acids following acute infection. *Proceedings of the National Academy of Sciences of the United States of America* 90(13):6125-6129.

94. Karageorgos L, Li P, & Burrell C (1993) Characterization of HIV replication complexes early after cell-to-cell infection. *AIDS research and human retroviruses* 9(9):817-823.

95. Miller MD, Farnet CM, & Bushman FD (1997) Human immunodeficiency virus type 1 preintegration complexes: studies of organization and composition. *Journal of virology* 71(7):5382-5390.

96. Heinzinger NK, Bukrinsky MI, Haggerty SA, Ragland AM, Kewalramani V, Lee MA, Gendelman HE, Ratner L, Stevenson M, & Emerman M (1994) The Vpr protein of human immunodeficiency virus type 1 influences nuclear localization of viral nucleic

acids in nondividing host cells. *Proceedings of the National Academy of Sciences of the United States of America* 91(15):7311-7315.

97. Pauza CD (1990) Two bases are deleted from the termini of HIV-1 linear DNA during integrative recombination. *Virology* 179(2):886-889.

98. Sherman PA & Fyfe JA (1990) Human immunodeficiency virus integration protein expressed in Escherichia coli possesses selective DNA cleaving activity. *Proceedings of the National Academy of Sciences of the United States of America* 87(13):5119-5123.

99. Bushman FD & Craigie R (1991) Activities of human immunodeficiency virus (HIV) integration protein in vitro: specific cleavage and integration of HIV DNA. *Proceedings of the National Academy of Sciences of the United States of America* 88(4):1339-1343.

100. Engelman A, Mizuuchi K, & Craigie R (1991) HIV-1 DNA integration: mechanism of viral DNA cleavage and DNA strand transfer. *Cell* 67(6):1211-1221.

101. Bukrinsky MI, Stanwick TL, Dempsey MP, & Stevenson M (1991) Quiescent T lymphocytes as an inducible virus reservoir in HIV-1 infection. *Science* 254(5030):423-427.

102. Zack JA, Arrigo SJ, Weitsman SR, Go AS, Haislip A, & Chen IS (1990) HIV-1 entry into quiescent primary lymphocytes: molecular analysis reveals a labile, latent viral structure. *Cell* 61(2):213-222.

103. Schaller T, Ocwieja KE, Rasaiyaah J, Price AJ, Brady TL, Roth SL, Hue S, Fletcher AJ, Lee K, KewalRamani VN, Noursadeghi M, Jenner RG, James LC, Bushman FD, & Towers GJ (2011) HIV-1 capsid-cyclophilin interactions determine nuclear import pathway, integration targeting and replication efficiency. *PLoS pathogens* 7(12):e1002439.

104. Di Nunzio F, Danckaert A, Fricke T, Perez P, Fernandez J, Perret E, Roux P, Shorte S, Charneau P, Diaz-Griffero F, & Arhel NJ (2012) Human nucleoporins promote HIV-1 docking at the nuclear pore, nuclear import and integration. *PloS one* 7(9):e46037.

105. Matreyek KA & Engelman A (2011) The requirement for nucleoporin NUP153 during human immunodeficiency virus type 1 infection is determined by the viral capsid. *Journal of virology* 85(15):7818-7827.

106. Luban J, Bossolt KL, Franke EK, Kalpana GV, & Goff SP (1993) Human immunodeficiency virus type 1 Gag protein binds to cyclophilins A and B. *Cell* 73(6):1067-1078.

107. Zhou L, Sokolskaja E, Jolly C, James W, Cowley SA, & Fassati A (2011) Transportin 3 promotes a nuclear maturation step required for efficient HIV-1 integration. *PLoS pathogens* 7(8):e1002194.

108. Valle-Casuso JC, Di Nunzio F, Yang Y, Reszka N, Lienlaf M, Arhel N, Perez P, Brass AL, & Diaz-Griffero F (2012) TNPO3 is required for HIV-1 replication after nuclear import but prior to integration and binds the HIV-1 core. *Journal of virology* 86(10):5931-5936.

109. Krishnan L, Matreyek KA, Oztop I, Lee K, Tipper CH, Li X, Dar MJ, Kewalramani VN, & Engelman A (2010) The requirement for cellular transportin 3 (TNPO3 or TRN-SR2) during infection maps to human immunodeficiency virus type 1 capsid and not integrase. *Journal of virology* 84(1):397-406.

110. Lee K, Ambrose Z, Martin TD, Oztop I, Mulky A, Julias JG, Vandegraaff N, Baumann JG, Wang R, Yuen W, Takemura T, Shelton K, Taniuchi I, Li Y, Sodroski J, Littman DR,

Coffin JM, Hughes SH, Unutmaz D, Engelman A, & KewalRamani VN (2010) Flexible use of nuclear import pathways by HIV-1. *Cell host & microbe* 7(3):221-233.

111. Price AJ, Fletcher AJ, Schaller T, Elliott T, Lee K, KewalRamani VN, Chin JW, Towers GJ, & James LC (2012) CPSF6 defines a conserved capsid interface that modulates HIV-1 replication. *PLoS pathogens* 8(8):e1002896.

112. Cherepanov P, Maertens G, Proost P, Devreese B, Van Beeumen J, Engelborghs Y, De Clercq E, & Debyser Z (2003) HIV-1 integrase forms stable tetramers and associates with LEDGF/p75 protein in human cells. *The Journal of biological chemistry* 278(1):372-381.

113. Turlure F, Devroe E, Silver PA, & Engelman A (2004) Human cell proteins and human immunodeficiency virus DNA integration. *Frontiers in bioscience : a journal and virtual library* 9:3187-3208.

114. Emiliani S, Mousnier A, Busschots K, Maroun M, Van Maele B, Tempe D, Vandekerckhove L, Moisant F, Ben-Slama L, Witvrouw M, Christ F, Rain JC, Dargemont C, Debyser Z, & Benarous R (2005) Integrase mutants defective for interaction with LEDGF/p75 are impaired in chromosome tethering and HIV-1 replication. *The Journal of biological chemistry* 280(27):25517-25523.

115. Ciuffi A, Llano M, Poeschla E, Hoffmann C, Leipzig J, Shinn P, Ecker JR, & Bushman F (2005) A role for LEDGF/p75 in targeting HIV DNA integration. *Nature medicine* 11(12):1287-1289.

116. Shun MC, Raghavendra NK, Vandegraaff N, Daigle JE, Hughes S, Kellam P, Cherepanov P, & Engelman A (2007) LEDGF/p75 functions downstream from preintegration complex formation to effect gene-specific HIV-1 integration. *Genes & development* 21(14):1767-1778.

117. Marshall HM, Ronen K, Berry C, Llano M, Sutherland H, Saenz D, Bickmore W, Poeschla E, & Bushman FD (2007) Role of PSIP1/LEDGF/p75 in lentiviral infectivity and integration targeting. *PloS one* 2(12):e1340.

118. Ocwieja KE, Brady TL, Ronen K, Huegel A, Roth SL, Schaller T, James LC, Towers GJ, Young JA, Chanda SK, Konig R, Malani N, Berry CC, & Bushman FD (2011) HIV integration targeting: a pathway involving Transportin-3 and the nuclear pore protein RanBP2. *PLoS pathogens* 7(3):e1001313.

119. Koh Y, Wu X, Ferris AL, Matreyek KA, Smith SJ, Lee K, KewalRamani VN, Hughes SH, & Engelman A (2013) Differential effects of human immunodeficiency virus type 1 capsid and cellular factors nucleoporin 153 and LEDGF/p75 on the efficiency and specificity of viral DNA integration. *Journal of virology* 87(1):648-658.

120. Di Nunzio F, Fricke T, Miccio A, Valle-Casuso JC, Perez P, Souque P, Rizzi E, Severgnini M, Mavilio F, Charneau P, & Diaz-Griffero F (2013) Nup153 and Nup98 bind the HIV-1 core and contribute to the early steps of HIV-1 replication. *Virology* 440(1):8-18.

121. Lelek M, Casartelli N, Pellin D, Rizzi E, Souque P, Severgnini M, Di Serio C, Fricke T, Diaz-Griffero F, Zimmer C, Charneau P, & Di Nunzio F (2015) Chromatin organization at the nuclear pore favours HIV replication. *Nature communications* 6:6483.

122. Bushman FD, Fujiwara T, & Craigie R (1990) Retroviral DNA integration directed by HIV integration protein in vitro. *Science* 249(4976):1555-1558.

123. Dyda F, Hickman AB, Jenkins TM, Engelman A, Craigie R, & Davies DR (1994) Crystal structure of the catalytic domain of HIV-1 integrase: similarity to other polynucleotidyl transferases. *Science* 266(5193):1981-1986.

124. Engelman A & Craigie R (1992) Identification of conserved amino acid residues critical for human immunodeficiency virus type 1 integrase function in vitro. *Journal of virology* 66(11):6361-6369.

125. Kulkosky J, Jones KS, Katz RA, Mack JP, & Skalka AM (1992) Residues critical for retroviral integrative recombination in a region that is highly conserved among retroviral/retrotransposon integrases and bacterial insertion sequence transposases. *Molecular and cellular biology* 12(5):2331-2338.

126. Drelich M, Wilhelm R, & Mous J (1992) Identification of amino acid residues critical for endonuclease and integration activities of HIV-1 IN protein in vitro. *Virology* 188(2):459-468.

127. Goldgur Y, Dyda F, Hickman AB, Jenkins TM, Craigie R, & Davies DR (1998) Three new structures of the core domain of HIV-1 integrase: an active site that binds magnesium. *Proceedings of the National Academy of Sciences of the United States of America* 95(16):9150-9154.

128. Maignan S, Guilloteau JP, Zhou-Liu Q, Clement-Mella C, & Mikol V (1998) Crystal structures of the catalytic domain of HIV-1 integrase free and complexed with its metal cofactor: high level of similarity of the active site with other viral integrases. *Journal of molecular biology* 282(2):359-368.

129. Hare S, Gupta SS, Valkov E, Engelman A, & Cherepanov P (2010) Retroviral intasome assembly and inhibition of DNA strand transfer. *Nature* 464(7286):232-236.

130. Krishnan L, Li X, Naraharisetty HL, Hare S, Cherepanov P, & Engelman A (2010) Structure-based modeling of the functional HIV-1 intasome and its inhibition.

Proceedings of the National Academy of Sciences of the United States of America 107(36):15910-15915.

131. McKee CJ, Kessl JJ, Shkriabai N, Dar MJ, Engelman A, & Kvaratskhelia M (2008) Dynamic modulation of HIV-1 integrase structure and function by cellular lens epithelium-derived growth factor (LEDGF) protein. *The Journal of biological chemistry* 283(46):31802-31812.

132. Engelman A, Bushman FD, & Craigie R (1993) Identification of discrete functional domains of HIV-1 integrase and their organization within an active multimeric complex. *The EMBO journal* 12(8):3269-3275.

133. van Gent DC, Vink C, Groeneger AA, & Plasterk RH (1993) Complementation between HIV integrase proteins mutated in different domains. *The EMBO journal* 12(8):3261-3267.

134. Li M, Mizuuchi M, Burke TR, Jr., & Craigie R (2006) Retroviral DNA integration: reaction pathway and critical intermediates. *The EMBO journal* 25(6):1295-1304.

135. Guiot E, Carayon K, Delelis O, Simon F, Tauc P, Zubin E, Gottikh M, Mouscadet JF, Brochon JC, & Deprez E (2006) Relationship between the oligomeric status of HIV-1 integrase on DNA and enzymatic activity. *The Journal of biological chemistry* 281(32):22707-22719.

136. Baranova S, Tuzikov FV, Zakharova OD, Tuzikova NA, Calmels C, Litvak S, Tarrago-Litvak L, Parissi V, & Nevinsky GA (2007) Small-angle X-ray characterization of the nucleoprotein complexes resulting from DNA-induced oligomerization of HIV-1 integrase. *Nucleic acids research* 35(3):975-987.

137. Hare S, Maertens GN, & Cherepanov P (2012) 3'-processing and strand transfer catalysed by retroviral integrase in crystallo. *The EMBO journal* 31(13):3020-3028.

138. Engelman A & Cherepanov P (2014) Retroviral Integrase Structure and DNA Recombination Mechanism. *Microbiology spectrum* 2(6):1-22.

139. Vink C, Yeheskiely E, van der Marel GA, van Boom JH, & Plasterk RH (1991) Site-specific hydrolysis and alcoholysis of human immunodeficiency virus DNA termini mediated by the viral integrase protein. *Nucleic acids research* 19(24):6691-6698.

140. Katzman M, Mack JP, Skalka AM, & Leis J (1991) A covalent complex between retroviral integrase and nicked substrate DNA. *Proceedings of the National Academy of Sciences of the United States of America* 88(11):4695-4699.

141. Holman AG & Coffin JM (2005) Symmetrical base preferences surrounding HIV-1, avian sarcoma/leukosis virus, and murine leukemia virus integration sites. *Proceedings of the National Academy of Sciences of the United States of America* 102(17):6103-6107.

142. Wu X, Li Y, Crise B, Burgess SM, & Munroe DJ (2005) Weak palindromic consensus sequences are a common feature found at the integration target sites of many retroviruses. *Journal of virology* 79(8):5211-5214.

143. Serrao E, Ballandras-Colas A, Cherepanov P, Maertens GN, & Engelman AN (2015) Key determinants of target DNA recognition by retroviral intasomes. *Retrovirology* 12(1):39.

144. Maertens GN, Hare S, & Cherepanov P (2010) The mechanism of retroviral integration from X-ray structures of its key intermediates. *Nature* 468(7321):326-329.

145. Shin CG, Taddeo B, Haseltine WA, & Farnet CM (1994) Genetic analysis of the human immunodeficiency virus type 1 integrase protein. *Journal of virology* 68(3):1633-1642.

146. Engelman A, Englund G, Orenstein JM, Martin MA, & Craigie R (1995) Multiple effects of mutations in human immunodeficiency virus type 1 integrase on viral replication. *Journal of virology* 69(5):2729-2736.

147. Wiskerchen M & Muesing MA (1995) Human immunodeficiency virus type 1 integrase: effects of mutations on viral ability to integrate, direct viral gene expression from unintegrated viral DNA templates, and sustain viral propagation in primary cells. *Journal of virology* 69(1):376-386.

148. Leavitt AD, Robles G, Alesandro N, & Varmus HE (1996) Human immunodeficiency virus type 1 integrase mutants retain in vitro integrase activity yet fail to integrate viral DNA efficiently during infection. *Journal of virology* 70(2):721-728.

149. Masuda T, Planelles V, Krogstad P, & Chen IS (1995) Genetic analysis of human immunodeficiency virus type 1 integrase and the U3 att site: unusual phenotype of mutants in the zinc finger-like domain. *Journal of virology* 69(11):6687-6696.

150. Engelman A (1999) In vivo analysis of retroviral integrase structure and function. *Advances in virus research* 52:411-426.

151. Shank PR, Hughes SH, Kung HJ, Majors JE, Quintrell N, Guntaka RV, Bishop JM, & Varmus HE (1978) Mapping unintegrated avian sarcoma virus DNA: termini of linear DNA bear 300 nucleotides present once or twice in two species of circular DNA. *Cell* 15(4):1383-1395.

152. Shoemaker C, Goff S, Gilboa E, Paskind M, Mitra SW, & Baltimore D (1980) Structure of a cloned circular Moloney murine leukemia virus DNA molecule containing an inverted segment: implications for retrovirus integration. *Proceedings of the National Academy of Sciences of the United States of America* 77(7):3932-3936.

153. Hazuda DJ, Felock P, Witmer M, Wolfe A, Stillmock K, Grobler JA, Espeseth A, Gabryelski L, Schleif W, Blau C, & Miller MD (2000) Inhibitors of strand transfer that prevent integration and inhibit HIV-1 replication in cells. *Science* 287(5453):646-650.

154. Wu X, Liu H, Xiao H, Conway JA, Hehl E, Kalpana GV, Prasad V, & Kappes JC (1999) Human immunodeficiency virus type 1 integrase protein promotes reverse transcription through specific interactions with the nucleoprotein reverse transcription complex. *Journal of virology* 73(3):2126-2135.

155. Zhu K, Dobard C, & Chow SA (2004) Requirement for integrase during reverse transcription of human immunodeficiency virus type 1 and the effect of cysteine mutations of integrase on its interactions with reverse transcriptase. *Journal of virology* 78(10):5045-5055.

156. Wilkinson TA, Januszyk K, Phillips ML, Tekeste SS, Zhang M, Miller JT, Le Grice SF, Clubb RT, & Chow SA (2009) Identifying and characterizing a functional HIV-1 reverse transcriptase-binding site on integrase. *The Journal of biological chemistry* 284(12):7931-7939.

157. Engelman A (2011) The pleiotropic nature of human immunodeficiency virus integrase mutations. *HIV-1 Integrase: Mechanism and Inhibitor Design*, ed Neamati N (John Wiley & Sons, Inc., Hoboken, N.J.), pp 67-81.

158. Bukovsky A & Gottlinger H (1996) Lack of integrase can markedly affect human immunodeficiency virus type 1 particle production in the presence of an active viral protease. *Journal of virology* 70(10):6820-6825.

159. Shehu-Xhilaga M, Hill M, Marshall JA, Kappes J, Crowe SM, & Mak J (2002) The conformation of the mature dimeric human immunodeficiency virus type 1 RNA genome requires packaging of pol protein. *Journal of virology* 76(9):4331-4340.

160. Buxton P, Tachedjian G, & Mak J (2005) Analysis of the contribution of reverse transcriptase and integrase proteins to retroviral RNA dimer conformation. *Journal of virology* 79(10):6338-6348.

161. Allen P, Worland S, & Gold L (1995) Isolation of high-affinity RNA ligands to HIV-1 integrase from a random pool. *Virology* 209(2):327-336.

162. Moore MD, Fu W, Soheilian F, Nagashima K, Ptak RG, Pathak VK, & Hu WS (2008) Suboptimal inhibition of protease activity in human immunodeficiency virus type 1: effects on virion morphogenesis and RNA maturation. *Virology* 379(1):152-160.

163. Vendrame D, Sourisseau M, Perrin V, Schwartz O, & Mammano F (2009) Partial inhibition of human immunodeficiency virus replication by type I interferons: impact of cell-to-cell viral transfer. *Journal of virology* 83(20):10527-10537.

164. Ohishi M, Nakano T, Sakuragi S, Shioda T, Sano K, & Sakuragi J (2011) The relationship between HIV-1 genome RNA dimerization, virion maturation and infectivity. *Nucleic acids research* 39(8):3404-3417.

165. Engelman A (2007) Host cell factors and HIV-1 integration. *Future HIV Therapy* 1:415-426.

166. Schroder AR, Shinn P, Chen H, Berry C, Ecker JR, & Bushman F (2002) HIV-1 integration in the human genome favors active genes and local hotspots. *Cell* 110(4):521-529.

167. Wu X, Li Y, Crise B, & Burgess SM (2003) Transcription start regions in the human genome are favored targets for MLV integration. *Science* 300(5626):1749-1751.

168. Mitchell RS, Beitzel BF, Schroder AR, Shinn P, Chen H, Berry CC, Ecker JR, & Bushman FD (2004) Retroviral DNA integration: ASLV, HIV, and MLV show distinct target site preferences. *PLoS biology* 2(8):E234.

169. Han Y, Lassen K, Monie D, Sedaghat AR, Shimoji S, Liu X, Pierson TC, Margolick JB, Siliciano RF, & Siliciano JD (2004) Resting CD4+ T cells from human immunodeficiency virus type 1 (HIV-1)-infected individuals carry integrated HIV-1 genomes within actively transcribed host genes. *Journal of virology* 78(12):6122-6133.

170. Liu H, Dow EC, Arora R, Kimata JT, Bull LM, Arduino RC, & Rice AP (2006) Integration of human immunodeficiency virus type 1 in untreated infection occurs preferentially within genes. *Journal of virology* 80(15):7765-7768.

171. Nishizawa Y, Usukura J, Singh DP, Chylack LT, Jr., & Shinohara T (2001) Spatial and temporal dynamics of two alternatively spliced regulatory factors, lens epithelium-derived growth factor (ledgf/p75) and p52, in the nucleus. *Cell and tissue research* 305(1):107-114.

172. Ge H, Si Y, & Roeder RG (1998) Isolation of cDNAs encoding novel transcription coactivators p52 and p75 reveals an alternate regulatory mechanism of transcriptional activation. *The EMBO journal* 17(22):6723-6729.

173. Cherepanov P, Devroe E, Silver PA, & Engelman A (2004) Identification of an evolutionarily conserved domain in human lens epithelium-derived growth factor/transcriptional co-activator p75 (LEDGF/p75) that binds HIV-1 integrase. *The Journal of biological chemistry* 279(47):48883-48892.

174. Cherepanov P, Pluymers W, Claeys A, Proost P, De Clercq E, & Debyser Z (2000) High-level expression of active HIV-1 integrase from a synthetic gene in human cells. *FASEB journal : official publication of the Federation of American Societies for Experimental Biology* 14(10):1389-1399.

175. Maertens G, Cherepanov P, Pluymers W, Busschots K, De Clercq E, Debyser Z, & Engelborghs Y (2003) LEDGF/p75 is essential for nuclear and chromosomal targeting of HIV-1 integrase in human cells. *The Journal of biological chemistry* 278(35):33528-33539.

176. Llano M, Vanegas M, Fregoso O, Saenz D, Chung S, Peretz M, & Poeschla EM (2004) LEDGF/p75 determines cellular trafficking of diverse lentiviral but not murine oncoretroviral integrase proteins and is a component of functional lentiviral preintegration complexes. *Journal of virology* 78(17):9524-9537.

177. Vandegraaff N, Devroe E, Turlure F, Silver PA, & Engelman A (2006) Biochemical and genetic analyses of integrase-interacting proteins lens epithelium-derived growth factor (LEDGF)/p75 and hepatoma-derived growth factor related protein 2 (HRP2) in preintegration complex function and HIV-1 replication. *Virology* 346(2):415-426.

178. Vandekerckhove L, Christ F, Van Maele B, De Rijck J, Gijsbers R, Van den Haute C, Witvrouw M, & Debyser Z (2006) Transient and stable knockdown of the integrase cofactor LEDGF/p75 reveals its role in the replication cycle of human immunodeficiency virus. *Journal of virology* 80(4):1886-1896.

179. Llano M, Saenz DT, Meehan A, Wongthida P, Peretz M, Walker WH, Teo W, & Poeschla EM (2006) An essential role for LEDGF/p75 in HIV integration. *Science* 314(5798):461-464.

180. Fadel HJ, Morrison JH, Saenz DT, Fuchs JR, Kvaratskhelia M, Ekker SC, & Poeschla EM (2014) TALEN knockout of the PSIP1 gene in human cells: analyses of HIV-1 replication and allosteric integrase inhibitor mechanism. *Journal of virology* 88(17):9704-9717.

181. Schrijvers R, De Rijck J, Demeulemeester J, Adachi N, Vets S, Ronen K, Christ F, Bushman FD, Debyser Z, & Gijsbers R (2012) LEDGF/p75-independent HIV-1 replication demonstrates a role for HRP-2 and remains sensitive to inhibition by LEDGINs. *PLoS pathogens* 8(3):e1002558.

182. Cherepanov P, Sun ZY, Rahman S, Maertens G, Wagner G, & Engelman A (2005) Solution structure of the HIV-1 integrase-binding domain in LEDGF/p75. *Nature structural & molecular biology* 12(6):526-532.

183. Cherepanov P, Ambrosio AL, Rahman S, Ellenberger T, & Engelman A (2005) Structural basis for the recognition between HIV-1 integrase and transcriptional coactivator p75. *Proceedings of the National Academy of Sciences of the United States of America* 102(48):17308-17313.

184. Rahman S, Lu R, Vandegraaff N, Cherepanov P, & Engelman A (2007) Structure-based mutagenesis of the integrase-LEDGF/p75 interface uncouples a strict correlation between in vitro protein binding and HIV-1 fitness. *Virology* 357(1):79-90.

185. Busschots K, Voet A, De Maeyer M, Rain JC, Emiliani S, Benarous R, Desender L, Debyser Z, & Christ F (2007) Identification of the LEDGF/p75 binding site in HIV-1 integrase. *Journal of molecular biology* 365(5):1480-1492.

186. De Rijck J, Vandekerckhove L, Gijsbers R, Hombrouck A, Hendrix J, Vercammen J, Engelborghs Y, Christ F, & Debyser Z (2006) Overexpression of the lens epithelium-

derived growth factor/p75 integrase binding domain inhibits human immunodeficiency virus replication. *Journal of virology* 80(23):11498-11509.

187. Hombrouck A, De Rijck J, Hendrix J, Vandekerckhove L, Voet A, De Maeyer M, Witvrouw M, Engelborghs Y, Christ F, Gijsbers R, & Debyser Z (2007) Virus evolution reveals an exclusive role for LEDGF/p75 in chromosomal tethering of HIV. *PLoS pathogens* 3(3):e47.

188. Caliendo AM & Hirsch MS (1994) Combination therapy for infection due to human immunodeficiency virus type 1. *Clinical infectious diseases : an official publication of the Infectious Diseases Society of America* 18(4):516-524.

189. Coffin JM (1995) HIV population dynamics in vivo: implications for genetic variation, pathogenesis, and therapy. *Science* 267(5197):483-489.

190. Roberts JD, Bebenek K, & Kunkel TA (1988) The accuracy of reverse transcriptase from HIV-1. *Science* 242(4882):1171-1173.

191. Preston BD, Poiesz BJ, & Loeb LA (1988) Fidelity of HIV-1 reverse transcriptase. *Science* 242(4882):1168-1171.

192. Mansky LM & Temin HM (1995) Lower in vivo mutation rate of human immunodeficiency virus type 1 than that predicted from the fidelity of purified reverse transcriptase. *Journal of virology* 69(8):5087-5094.

193. O'Neil PK, Sun G, Yu H, Ron Y, Dougherty JP, & Preston BD (2002) Mutational analysis of HIV-1 long terminal repeats to explore the relative contribution of reverse transcriptase and RNA polymerase II to viral mutagenesis. *The Journal of biological chemistry* 277(41):38053-38061.

194. Abram ME, Ferris AL, Shao W, Alvord WG, & Hughes SH (2010) Nature, position, and frequency of mutations made in a single cycle of HIV-1 replication. *Journal of virology* 84(19):9864-9878.

195. Perelson AS, Neumann AU, Markowitz M, Leonard JM, & Ho DD (1996) HIV-1 dynamics in vivo: virion clearance rate, infected cell life-span, and viral generation time. *Science* 271(5255):1582-1586.

196. Frost SD & McLean AR (1994) Quasispecies dynamics and the emergence of drug resistance during zidovudine therapy of HIV infection. *AIDS* 8(3):323-332.

197. Nowak MA, Bonhoeffer S, Shaw GM, & May RM (1997) Anti-viral drug treatment: dynamics of resistance in free virus and infected cell populations. *Journal of theoretical biology* 184(2):203-217.

198. Stengel RF (2008) Mutation and control of the human immunodeficiency virus. *Mathematical biosciences* 213(2):93-102.

199. Engelman A & Cherepanov P (2012) The structural biology of HIV-1: mechanistic and therapeutic insights. *Nature reviews. Microbiology* 10(4):279-290.

200. Hammer SM, Squires KE, Hughes MD, Grimes JM, Demeter LM, Currier JS, Eron JJ, Jr., Feinberg JE, Balfour HH, Jr., Deyton LR, Chodakewitz JA, & Fischl MA (1997) A controlled trial of two nucleoside analogues plus indinavir in persons with human immunodeficiency virus infection and CD4 cell counts of 200 per cubic millimeter or less. AIDS Clinical Trials Group 320 Study Team. *The New England journal of medicine* 337(11):725-733.

201. Gulick RM, Mellors JW, Havlir D, Eron JJ, Gonzalez C, McMahon D, Richman DD, Valentine FT, Jonas L, Meibohm A, Emini EA, & Chodakewitz JA (1997) Treatment

with indinavir, zidovudine, and lamivudine in adults with human immunodeficiency virus infection and prior antiretroviral therapy. *The New England journal of medicine* 337(11):734-739.

202. Palella FJ, Jr., Delaney KM, Moorman AC, Loveless MO, Fuhrer J, Satten GA, Aschman DJ, & Holmberg SD (1998) Declining morbidity and mortality among patients with advanced human immunodeficiency virus infection. HIV Outpatient Study Investigators. *The New England journal of medicine* 338(13):853-860.

203. Arts EJ & Hazuda DJ (2012) HIV-1 antiretroviral drug therapy. *Cold Spring Harbor perspectives in medicine* 2(4):a007161.

204. Grobler JA, Stillmock K, Hu B, Witmer M, Felock P, Espeseth AS, Wolfe A, Egbertson M, Bourgeois M, Melamed J, Wai JS, Young S, Vacca J, & Hazuda DJ (2002) Diketo acid inhibitor mechanism and HIV-1 integrase: implications for metal binding in the active site of phosphotransferase enzymes. *Proceedings of the National Academy of Sciences of the United States of America* 99(10):6661-6666.

205. Espeseth AS, Felock P, Wolfe A, Witmer M, Grobler J, Anthony N, Egbertson M, Melamed JY, Young S, Hamill T, Cole JL, & Hazuda DJ (2000) HIV-1 integrase inhibitors that compete with the target DNA substrate define a unique strand transfer conformation for integrase. *Proceedings of the National Academy of Sciences of the United States of America* 97(21):11244-11249.

206. Fransen S, Gupta S, Danovich R, Hazuda D, Miller M, Witmer M, Petropoulos CJ, & Huang W (2009) Loss of raltegravir susceptibility by human immunodeficiency virus type 1 is conferred via multiple nonoverlapping genetic pathways. *Journal of virology* 83(22):11440-11446.

207. Goethals O, Clayton R, Van Ginderen M, Vereycken I, Wagemans E, Geluykens P, Dockx K, Strijbos R, Smits V, Vos A, Meersseman G, Jochmans D, Vermeire K, Schols D, Hallenberger S, & Hertogs K (2008) Resistance mutations in human immunodeficiency virus type 1 integrase selected with elvitegravir confer reduced susceptibility to a wide range of integrase inhibitors. *Journal of virology* 82(21):10366-10374.

208. Marinello J, Marchand C, Mott BT, Bain A, Thomas CJ, & Pommier Y (2008) Comparison of raltegravir and elvitegravir on HIV-1 integrase catalytic reactions and on a series of drug-resistant integrase mutants. *Biochemistry* 47(36):9345-9354.

209. Metifiot M, Vandegraaff N, Maddali K, Naumova A, Zhang X, Rhodes D, Marchand C, & Pommier Y (2011) Elvitegravir overcomes resistance to raltegravir induced by integrase mutation Y143. *AIDS* 25(9):1175-1178.

210. Kobayashi M, Yoshinaga T, Seki T, Wakasa-Morimoto C, Brown KW, Ferris R, Foster SA, Hazen RJ, Miki S, Suyama-Kagitani A, Kawauchi-Miki S, Taishi T, Kawasuji T, Johns BA, Underwood MR, Garvey EP, Sato A, & Fujiwara T (2011) In Vitro antiretroviral properties of S/GSK1349572, a next-generation HIV integrase inhibitor. *Antimicrobial agents and chemotherapy* 55(2):813-821.

211. Hightower KE, Wang R, Deanda F, Johns BA, Weaver K, Shen Y, Tomberlin GH, Carter HL, 3rd, Broderick T, Sigethy S, Seki T, Kobayashi M, & Underwood MR (2011) Dolutegravir (S/GSK1349572) exhibits significantly slower dissociation than raltegravir and elvitegravir from wild-type and integrase inhibitor-resistant HIV-1 integrase-DNA complexes. *Antimicrobial agents and chemotherapy* 55(10):4552-4559.

212. Eron JJ, Clotet B, Durant J, Katlama C, Kumar P, Lazzarin A, Poizot-Martin I, Richmond G, Soriano V, Ait-Khaled M, Fujiwara T, Huang J, Min S, Vavro C, Yeo J, & Group VS (2013) Safety and efficacy of dolutegravir in treatment-experienced subjects with raltegravir-resistant HIV type 1 infection: 24-week results of the VIKING Study. *The Journal of infectious diseases* 207(5):740-748.

213. Mesplede T & Wainberg MA (2014) Is resistance to dolutegravir possible when this drug is used in first-line therapy? *Viruses* 6(9):3377-3385.

214. Wells JA & McClendon CL (2007) Reaching for high-hanging fruit in drug discovery at protein-protein interfaces. *Nature* 450(7172):1001-1009.

215. Molteni V, Greenwald J, Rhodes D, Hwang Y, Kwiatkowski W, Bushman FD, Siegel JS, & Choe S (2001) Identification of a small-molecule binding site at the dimer interface of the HIV integrase catalytic domain. *Acta crystallographica. Section D, Biological crystallography* 57(Pt 4):536-544.

216. Lin Z, Neamati N, Zhao H, Kiryu Y, Turpin JA, Aberham C, Strebel K, Kohn K, Witvrouw M, Pannecouque C, Debyser Z, De Clercq E, Rice WG, Pommier Y, & Burke TR, Jr. (1999) Chicoric acid analogues as HIV-1 integrase inhibitors. *Journal of medicinal chemistry* 42(8):1401-1414.

217. Shkriabai N, Patil SS, Hess S, Budihas SR, Craigie R, Burke TR, Jr., Le Grice SF, & Kvaratskhelia M (2004) Identification of an inhibitor-binding site to HIV-1 integrase with affinity acetylation and mass spectrometry. *Proceedings of the National Academy of Sciences of the United States of America* 101(18):6894-6899.

218. Kessl JJ, Eidahl JO, Shkriabai N, Zhao Z, McKee CJ, Hess S, Burke TR, Jr., & Kvaratskhelia M (2009) An allosteric mechanism for inhibiting HIV-1 integrase with a small molecule. *Molecular pharmacology* 76(4):824-832.

219. Du L, Zhao YX, Yang LM, Zheng YT, Tang Y, Shen X, & Jiang HL (2008) Symmetrical 1-pyrrolidineacetamide showing anti-HIV activity through a new binding site on HIV-1 integrase. *Acta pharmacologica Sinica* 29(10):1261-1267.

220. Mazumder A, Wang S, Neamati N, Nicklaus M, Sunder S, Chen J, Milne GW, Rice WG, Burke TR, Jr., & Pommier Y (1996) Antiretroviral agents as inhibitors of both human immunodeficiency virus type 1 integrase and protease. *Journal of medicinal chemistry* 39(13):2472-2481.

221. Al-Mawsawi LQ, Fikkert V, Dayam R, Witvrouw M, Burke TR, Jr., Borchers CH, & Neamati N (2006) Discovery of a small-molecule HIV-1 integrase inhibitor-binding site. *Proceedings of the National Academy of Sciences of the United States of America* 103(26):10080-10085.

222. Hou Y, McGuinness DE, Prongay AJ, Feld B, Ingravallo P, Ogert RA, Lunn CA, & Howe JA (2008) Screening for antiviral inhibitors of the HIV integrase-LEDGF/p75 interaction using the AlphaScreen luminescent proximity assay. *Journal of biomolecular screening* 13(5):406-414.

223. Du L, Zhao Y, Chen J, Yang L, Zheng Y, Tang Y, Shen X, & Jiang H (2008) D77, one benzoic acid derivative, functions as a novel anti-HIV-1 inhibitor targeting the interaction between integrase and cellular LEDGF/p75. *Biochemical and biophysical research communications* 375(1):139-144.

224. De Luca L, Barreca ML, Ferro S, Christ F, Iraci N, Gitto R, Monforte AM, Debyser Z, & Chimirri A (2009) Pharmacophore-based discovery of small-molecule inhibitors of protein-protein interactions between HIV-1 integrase and cellular cofactor LEDGF/p75. *ChemMedChem* 4(8):1311-1316.

225. Christ F, Voet A, Marchand A, Nicolet S, Desimmie BA, Marchand D, Bardiot D, Van der Veken NJ, Van Remoortel B, Strelkov SV, De Maeyer M, Chaltin P, & Debyser Z (2010) Rational design of small-molecule inhibitors of the LEDGF/p75-integrase interaction and HIV replication. *Nature chemical biology* 6(6):442-448.

226. Fenwick CW, Tremblay S, Wardrop E, Bethell R, Coulomb R, Elston R, Faucher A-M, Mason S, Simoneau B, Tsantrizos Y, & Yoakim C (2011) Resistance studies with HIV-1 non-catalytic site integrase inhibitors. *Antiviral Ther.* 16 Suppl 1:A9.

227. Peat TS, Rhodes DI, Vandegraaff N, Le G, Smith JA, Clark LJ, Jones ED, Coates JA, Thienthong N, Newman J, Dolezal O, Mulder R, Ryan JH, Savage GP, Francis CL, & Deadman JJ (2012) Small molecule inhibitors of the LEDGF site of human immunodeficiency virus integrase identified by fragment screening and structure based design. *PloS one* 7(7):e40147.

228. Sharma A, Slaughter A, Jena N, Feng L, Kessl JJ, Fadel HJ, Malani N, Male F, Wu L, Poeschla E, Bushman FD, Fuchs JR, & Kvaratskhelia M (2014) A new class of multimerization selective inhibitors of HIV-1 integrase. *PLoS pathogens* 10(5):e1004171.

229. Tsantrizos YS, Boes, M., Brochu, C., Fenwick, C., Malenfant, E., Mason, S., and Pesant, M. (2007).

230. Tsiang M, Jones GS, Niedziela-Majka A, Kan E, Lansdon EB, Huang W, Hung M, Samuel D, Novikov N, Xu Y, Mitchell M, Guo H, Babaoglu K, Liu X, Geleziunas R, &

Sakowicz R (2012) New class of HIV-1 integrase (IN) inhibitors with a dual mode of action. *The Journal of biological chemistry* 287(25):21189-21203.

231. Christ F, Shaw S, Demeulemeester J, Desimmie BA, Marchand A, Butler S, Smets W, Chaltin P, Westby M, Debyser Z, & Pickford C (2012) Small-molecule inhibitors of the LEDGF/p75 binding site of integrase block HIV replication and modulate integrase multimerization. *Antimicrobial agents and chemotherapy* 56(8):4365-4374.

232. Kessl JJ, Jena N, Koh Y, Taskent-Sezgin H, Slaughter A, Feng L, de Silva S, Wu L, Le Grice SF, Engelman A, Fuchs JR, & Kvaratskhelia M (2012) Multimode, cooperative mechanism of action of allosteric HIV-1 integrase inhibitors. *The Journal of biological chemistry* 287(20):16801-16811.

233. Jurado KA, Wang H, Slaughter A, Feng L, Kessl JJ, Koh Y, Wang W, Ballandras-Colas A, Patel PA, Fuchs JR, Kvaratskhelia M, & Engelman A (2013) Allosteric integrase inhibitor potency is determined through the inhibition of HIV-1 particle maturation. *Proceedings of the National Academy of Sciences of the United States of America* 110(21):8690-8695.

234. Le Rouzic E, Bonnard D, Chasset S, Bruneau JM, Chevreuil F, Le Strat F, Nguyen J, Beauvoir R, Amadori C, Brias J, Vomscheid S, Eiler S, Levy N, Delelis O, Deprez E, Saib A, Zamborlini A, Emiliani S, Ruff M, Ledoussal B, Moreau F, & Benarous R (2013) Dual inhibition of HIV-1 replication by integrase-LEDGF allosteric inhibitors is predominant at the post-integration stage. *Retrovirology* 10:144.

235. Gupta K, Brady T, Dyer BM, Malani N, Hwang Y, Male F, Nolte RT, Wang L, Velthuisen E, Jeffrey J, Van Duyne GD, & Bushman FD (2014) Allosteric inhibition of human immunodeficiency virus integrase: late block during viral replication and

abnormal multimerization involving specific protein domains. *The Journal of biological chemistry* 289(30):20477-20488.

236. Wang H, Jurado KA, Wu X, Shun MC, Li X, Ferris AL, Smith SJ, Patel PA, Fuchs JR, Cherepanov P, Kvaratskhelia M, Hughes SH, & Engelman A (2012) HRP2 determines the efficiency and specificity of HIV-1 integration in LEDGF/p75 knockout cells but does not contribute to the antiviral activity of a potent LEDGF/p75-binding site integrase inhibitor. *Nucleic acids research* 40(22):11518-11530.

237. Feng L, Sharma A, Slaughter A, Jena N, Koh Y, Shkriabai N, Larue RC, Patel PA, Mitsuya H, Kessl JJ, Engelman A, Fuchs JR, & Kvaratskhelia M (2013) The A128T resistance mutation reveals aberrant protein multimerization as the primary mechanism of action of allosteric HIV-1 integrase inhibitors. *The Journal of biological chemistry* 288(22):15813-15820.

238. Summa V, Petrocchi A, Bonelli F, Crescenzi B, Donghi M, Ferrara M, Fiore F, Gardelli C, Gonzalez Paz O, Hazuda DJ, Jones P, Kinzel O, Laufer R, Monteagudo E, Muraglia E, Nizi E, Orvieto F, Pace P, Pescatore G, Scarpelli R, Stillmock K, Witmer MV, & Rowley M (2008) Discovery of raltegravir, a potent, selective orally bioavailable HIV-integrase inhibitor for the treatment of HIV-AIDS infection. *Journal of medicinal chemistry* 51(18):5843-5855.

239. Quashie PK, Mesplede T, & Wainberg MA (2013) Evolution of HIV integrase resistance mutations. *Current opinion in infectious diseases* 26(1):43-49.

240. Quashie PK, Sloan RD, & Wainberg MA (2012) Novel therapeutic strategies targeting HIV integrase. *BMC medicine* 10:34.

241. Engelman A & Cherepanov P (2008) The lentiviral integrase binding protein LEDGF/p75 and HIV-1 replication. *PLoS pathogens* 4(3):e1000046.

242. Poeschla EM (2008) Integrase, LEDGF/p75 and HIV replication. *Cellular and molecular life sciences : CMLS* 65(9):1403-1424.

243. Cherepanov P (2007) LEDGF/p75 interacts with divergent lentiviral integrases and modulates their enzymatic activity in vitro. *Nucleic acids research* 35(1):113-124.

244. Kessl JJ, Li M, Ignatov M, Shkriabai N, Eidahl JO, Feng L, Musier-Forsyth K, Craigie R, & Kvaratskhelia M (2011) FRET analysis reveals distinct conformations of IN tetramers in the presence of viral DNA or LEDGF/p75. *Nucleic acids research* 39(20):9009-9022.

245. Shen L, Peterson S, Sedaghat AR, McMahon MA, Callender M, Zhang H, Zhou Y, Pitt E, Anderson KS, Acosta EP, & Siliciano RF (2008) Dose-response curve slope sets class-specific limits on inhibitory potential of anti-HIV drugs. *Nature medicine* 14(7):762-766.

246. Limon A, Devroe E, Lu R, Ghory HZ, Silver PA, & Engelman A (2002) Nuclear localization of human immunodeficiency virus type 1 preintegration complexes (PICs): V165A and R166A are pleiotropic integrase mutants primarily defective for integration, not PIC nuclear import. *Journal of virology* 76(21):10598-10607.

247. Kutner RH, Zhang XY, & Reiser J (2009) Production, concentration and titration of pseudotyped HIV-1-based lentiviral vectors. *Nature protocols* 4(4):495-505.

248. Butler SL, Hansen MS, & Bushman FD (2001) A quantitative assay for HIV DNA integration in vivo. *Nature medicine* 7(5):631-634.

249. Li L, Olvera JM, Yoder KE, Mitchell RS, Butler SL, Lieber M, Martin SL, & Bushman FD (2001) Role of the non-homologous DNA end joining pathway in the early steps of retroviral infection. *The EMBO journal* 20(12):3272-3281.

250. Lu R, Limon A, Devroe E, Silver PA, Cherepanov P, & Engelman A (2004) Class II integrase mutants with changes in putative nuclear localization signals are primarily blocked at a postnuclear entry step of human immunodeficiency virus type 1 replication. *Journal of virology* 78(23):12735-12746.

251. Sundquist WI & Krausslich HG (2012) HIV-1 assembly, budding, and maturation. *Cold Spring Harbor perspectives in medicine* 2(7):a006924.

252. Yung E, Sorin M, Pal A, Craig E, Morozov A, Delattre O, Kappes J, Ott D, & Kalpana GV (2001) Inhibition of HIV-1 virion production by a transdominant mutant of integrase interactor 1. *Nature medicine* 7(8):920-926.

253. Motakis D & Parniak MA (2002) A tight-binding mode of inhibition is essential for anti-human immunodeficiency virus type 1 virucidal activity of nonnucleoside reverse transcriptase inhibitors. *Antimicrobial agents and chemotherapy* 46(6):1851-1856.

254. Esposito D & Craigie R (1999) HIV integrase structure and function. *Advances in virus research* 52:319-333.

255. Petit C, Schwartz O, & Mammano F (1999) Oligomerization within virions and subcellular localization of human immunodeficiency virus type 1 integrase. *Journal of virology* 73(6):5079-5088.

256. Figueiredo A, Moore KL, Mak J, Sluis-Cremer N, de Bethune MP, & Tachedjian G (2006) Potent nonnucleoside reverse transcriptase inhibitors target HIV-1 Gag-Pol. *PLoS pathogens* 2(11):e119.

257. Mousnier A, Leh H, Mouscadet JF, & Dargemont C (2004) Nuclear import of HIV-1 integrase is inhibited in vitro by styrylquinoline derivatives. *Molecular pharmacology* 66(4):783-788.

258. Bonnenfant S, Thomas CM, Vita C, Subra F, Deprez E, Zouhiri F, Desmaele D, D'Angelo J, Mouscadet JF, & Leh H (2004) Styrylquinolines, integrase inhibitors acting prior to integration: a new mechanism of action for anti-integrase agents. *Journal of virology* 78(11):5728-5736.

259. Mouscadet JF, Deprez E, Desmaele D, & D'Angelo J (2011) *HIV-1 Integrase: Mechanism and Inhibitor Design* (Wiley, Hoboken, NJ) pp 325–339.

260. Desimmie BA, Humbert M, Lescrinier E, Hendrix J, Vets S, Gijsbers R, Ruprecht RM, Dietrich U, Debyser Z, & Christ F (2012) Phage display-directed discovery of LEDGF/p75 binding cyclic peptide inhibitors of HIV replication. *Molecular therapy : the journal of the American Society of Gene Therapy* 20(11):2064-2075.

261. Taddeo B, Carlini F, Verani P, & Engelman A (1996) Reversion of a human immunodeficiency virus type 1 integrase mutant at a second site restores enzyme function and virus infectivity. *Journal of virology* 70(12):8277-8284.

262. Jenkins TM, Engelman A, Ghirlando R, & Craigie R (1996) A soluble active mutant of HIV-1 integrase: involvement of both the core and carboxyl-terminal domains in multimerization. *The Journal of biological chemistry* 271(13):7712-7718.

263. Kalpana GV, Reicin A, Cheng GS, Sorin M, Paik S, & Goff SP (1999) Isolation and characterization of an oligomerization-negative mutant of HIV-1 integrase. *Virology* 259(2):274-285.

264. Al-Mawsawi LQ, Hombrouck A, Dayam R, Debyser Z, & Neamati N (2008) Four-tiered pi interaction at the dimeric interface of HIV-1 integrase critical for DNA integration and viral infectivity. *Virology* 377(2):355-363.

265. Brown HE, Chen H, & Engelman A (1999) Structure-based mutagenesis of the human immunodeficiency virus type 1 DNA attachment site: effects on integration and cDNA synthesis. *Journal of virology* 73(11):9011-9020.

266. Hare S, Shun MC, Gupta SS, Valkov E, Engelman A, & Cherepanov P (2009) A novel co-crystal structure affords the design of gain-of-function lentiviral integrase mutants in the presence of modified PSIP1/LEDGF/p75. *PLoS pathogens* 5(1):e1000259.

267. Barnard RJ, Narayan S, Dornadula G, Miller MD, & Young JA (2004) Low pH is required for avian sarcoma and leukosis virus Env-dependent viral penetration into the cytosol and not for viral uncoating. *Journal of virology* 78(19):10433-10441.

268. Wu X, Liu H, Xiao H, Conway JA, Hunter E, & Kappes JC (1997) Functional RT and IN incorporated into HIV-1 particles independently of the Gag/Pol precursor protein. *The EMBO journal* 16(16):5113-5122.

269. Brandt SM, Mariani R, Holland AU, Hope TJ, & Landau NR (2002) Association of chemokine-mediated block to HIV entry with coreceptor internalization. *The Journal of biological chemistry* 277(19):17291-17299.

270. Cavrois M, De Noronha C, & Greene WC (2002) A sensitive and specific enzyme-based assay detecting HIV-1 virion fusion in primary T lymphocytes. *Nature biotechnology* 20(11):1151-1154.

271. Nilsen BM, Haugan IR, Berg K, Olsen L, Brown PO, & Helland DE (1996) Monoclonal antibodies against human immunodeficiency virus type 1 integrase: epitope mapping and differential effects on integrase activities in vitro. *Journal of virology* 70(3):1580-1587.

272. Maertens GN, Cherepanov P, & Engelman A (2006) Transcriptional co-activator p75 binds and tethers the Myc-interacting protein JPO2 to chromatin. *Journal of cell science* 119(Pt 12):2563-2571.

273. Pandey KK, Bera S, & Grandgenett DP (2011) The HIV-1 integrase monomer induces a specific interaction with LTR DNA for concerted integration. *Biochemistry* 50(45):9788-9796.

274. Otwinowski Z, Minor W, & W Jr CC (1997) Processing of X-ray diffraction data collected in oscillation mode.

275. McCoy AJ, Grosse-Kunstleve RW, Adams PD, Winn MD, Storoni LC, & Read RJ (2007) Phaser crystallographic software. *Journal of applied crystallography* 40(4):658-674.

276. Collaborative Computational Project N (1994) The CCP4 suite: programs for protein crystallography. *Acta crystallographica. Section D, Biological crystallography* 50(Pt 5):760-763.

277. Emsley P, Lohkamp B, Scott WG, & Cowtan K (2010) Features and development of Coot. *Acta crystallographica. Section D, Biological crystallography* 66(Pt 4):486-501.

278. Grunewald K, Desai P, Winkler DC, Heymann JB, Belnap DM, Baumeister W, & Steven AC (2003) Three-dimensional structure of herpes simplex virus from cryo-electron tomography. *Science* 302(5649):1396-1398.

279. Benjamin J, Ganser-Pornillos BK, Tivol WF, Sundquist WI, & Jensen GJ (2005) Three-dimensional structure of HIV-1 virus-like particles by electron cryotomography. *Journal of molecular biology* 346(2):577-588.

280. Frank GA, Narayan K, Bess JW, Jr., Del Prete GQ, Wu X, Moran A, Hartnell LM, Earl LA, Lifson JD, & Subramaniam S (2015) Maturation of the HIV-1 core by a non-diffusional phase transition. *Nature communications* 6:5854.

281. Wlodawer A & Vondrasek J (1998) Inhibitors of HIV-1 protease: a major success of structure-assisted drug design. *Annual review of biophysics and biomolecular structure* 27:249-284.

282. Li F, Goila-Gaur R, Salzwedel K, Kilgore NR, Reddick M, Matallana C, Castillo A, Zoumplis D, Martin DE, Orenstein JM, Allaway GP, Freed EO, & Wild CT (2003) PA-457: a potent HIV inhibitor that disrupts core condensation by targeting a late step in Gag processing. *Proceedings of the National Academy of Sciences of the United States of America* 100(23):13555-13560.

283. Zhou J, Yuan X, Dismuke D, Forshey BM, Lundquist C, Lee KH, Aiken C, & Chen CH (2004) Small-molecule inhibition of human immunodeficiency virus type 1 replication by specific targeting of the final step of virion maturation. *Journal of virology* 78(2):922-929.

284. Balakrishnan M, Yant SR, Tsai L, O'Sullivan C, Bam RA, Tsai A, Niedziela-Majka A, Stray KM, Sakowicz R, & Cihlar T (2013) Non-catalytic site HIV-1 integrase inhibitors disrupt core maturation and induce a reverse transcription block in target cells. *PloS one* 8(9):e74163.

285. Kvaratskhelia M, Sharma A, Larue RC, Serrao E, & Engelman A (2014) Molecular mechanisms of retroviral integration site selection. *Nucleic acids research* 42(16):10209-10225.

286. Desimmie BA, Schrijvers R, Demeulemeester J, Borrenberghs D, Weydert C, Thys W, Vets S, Van Remoortel B, Hofkens J, De Rijck J, Hendrix J, Bannert N, Gijsbers R,

Christ F, & Debyser Z (2013) LEDGINs inhibit late stage HIV-1 replication by modulating integrase multimerization in the virions. *Retrovirology* 10:57.

287. Keller PW, Adamson CS, Heymann JB, Freed EO, & Steven AC (2011) HIV-1 maturation inhibitor bevirimat stabilizes the immature Gag lattice. *Journal of virology* 85(4):1420-1428.

288. Keller PW, Huang RK, England MR, Waki K, Cheng N, Heymann JB, Craven RC, Freed EO, & Steven AC (2013) A two-pronged structural analysis of retroviral maturation indicates that core formation proceeds by a disassembly-reassembly pathway rather than a displacive transition. *Journal of virology* 87(24):13655-13664.

289. de Marco A, Heuser AM, Glass B, Krausslich HG, Muller B, & Briggs JA (2012) Role of the SP2 domain and its proteolytic cleavage in HIV-1 structural maturation and infectivity. *Journal of virology* 86(24):13708-13716.

290. de Marco A, Muller B, Glass B, Riches JD, Krausslich HG, & Briggs JA (2010) Structural analysis of HIV-1 maturation using cryo-electron tomography. *PLoS pathogens* 6(11):e1001215.

291. Johnson BC, Metifiot M, Ferris A, Pommier Y, & Hughes SH (2013) A homology model of HIV-1 integrase and analysis of mutations designed to test the model. *Journal of molecular biology* 425(12):2133-2146.

292. Briggs JA, Simon MN, Gross I, Krausslich HG, Fuller SD, Vogt VM, & Johnson MC (2004) The stoichiometry of Gag protein in HIV-1. *Nature structural & molecular biology* 11(7):672-675.

293. Lanman J, Lam TT, Emmett MR, Marshall AG, Sakalian M, & Prevelige PE, Jr. (2004) Key interactions in HIV-1 maturation identified by hydrogen-deuterium exchange. *Nature structural & molecular biology* 11(7):676-677.

294. Chertova E, Chertov O, Coren LV, Roser JD, Trubey CM, Bess JW, Jr., Sowder RC, 2nd, Barsov E, Hood BL, Fisher RJ, Nagashima K, Conrads TP, Veenstra TD, Lifson JD, & Ott DE (2006) Proteomic and biochemical analysis of purified human immunodeficiency virus type 1 produced from infected monocyte-derived macrophages. *Journal of virology* 80(18):9039-9052.

295. Yu Z, Dobro MJ, Woodward CL, Levandovsky A, Danielson CM, Sandrin V, Shi J, Aiken C, Zandi R, Hope TJ, & Jensen GJ (2013) Unclosed HIV-1 capsids suggest a curled sheet model of assembly. *Journal of molecular biology* 425(1):112-123.

296. Wu W, Thomas JA, Cheng N, Black LW, & Steven AC (2012) Bubblegrams reveal the inner body of bacteriophage phiKZ. *Science* 335(6065):182.

297. Cheng N, Wu W, Watts NR, & Steven AC (2014) Exploiting radiation damage to map proteins in nucleoprotein complexes: the internal structure of bacteriophage T7. *Journal of structural biology* 185(3):250-256.

298. Conway JF, Trus BL, Booy FP, Newcomb WW, Brown JC, & Steven AC (1993) The effects of radiation damage on the structure of frozen hydrated HSV-1 capsids. *Journal of structural biology* 111(3):222-233.

299. Leapman RD & Sun S (1995) Cryo-electron energy loss spectroscopy: observations on vitrified hydrated specimens and radiation damage. *Ultramicroscopy* 59(1-4):71-79.

300. Meents A, Gutmann S, Wagner A, & Schulze-Briese C (2010) Origin and temperature dependence of radiation damage in biological samples at cryogenic temperatures.

Proceedings of the National Academy of Sciences of the United States of America 107(3):1094-1099.

301. Schneider R, Campbell M, Nasioulas G, Felber BK, & Pavlakis GN (1997) Inactivation of the human immunodeficiency virus type 1 inhibitory elements allows Rev-independent expression of Gag and Gag/protease and particle formation. *Journal of virology* 71(7):4892-4903.

302. Stauffer S, Rahman SA, de Marco A, Carlson LA, Glass B, Oberwinkler H, Herold N, Briggs JA, Muller B, Grunewald K, & Krausslich HG (2014) The nucleocapsid domain of Gag is dispensable for actin incorporation into HIV-1 and for association of viral budding sites with cortical F-actin. *Journal of virology* 88(14):7893-7903.

303. Engelman A, Englund G, Orenstein JM, Martin MA, & Craigie R (1995) Multiple effects of mutations in human immunodeficiency virus type 1 integrase on viral replication. *J. Virol.* 69(5):2729-2736.

304. Rabi SA, Laird GM, Durand CM, Laskey S, Shan L, Bailey JR, Chioma S, Moore RD, & Siliciano RF (2013) Multi-step inhibition explains HIV-1 protease inhibitor pharmacodynamics and resistance. *The Journal of clinical investigation* 123(9):3848-3860.

305. Cochrane AW, McNally MT, & Mouland AJ (2006) The retrovirus RNA trafficking granule: from birth to maturity. *Retrovirology* 3:18.

306. Lyonnais S, Gorelick RJ, Heniche-Boukhalfa F, Bouaziz S, Parissi V, Mouscadet JF, Restle T, Gatell JM, Le Cam E, & Mirambeau G (2013) A protein ballet around the viral genome orchestrated by HIV-1 reverse transcriptase leads to an architectural switch: from nucleocapsid-condensed RNA to Vpr-bridged DNA. *Virus research* 171(2):287-303.

307. Accola MA, Ohagen A, & Gottlinger HG (2000) Isolation of human immunodeficiency virus type 1 cores: retention of Vpr in the absence of p6(gag). *Journal of virology* 74(13):6198-6202.

308. Welker R, Hohenberg H, Tessmer U, Huckhagel C, & Krausslich HG (2000) Biochemical and structural analysis of isolated mature cores of human immunodeficiency virus type 1. *Journal of virology* 74(3):1168-1177.

309. Forshey BM & Aiken C (2003) Disassembly of human immunodeficiency virus type 1 cores in vitro reveals association of Nef with the subviral ribonucleoprotein complex. *Journal of virology* 77(7):4409-4414.

310. Lee SK, Potempa M, & Swanstrom R (2012) The choreography of HIV-1 proteolytic processing and virion assembly. *The Journal of biological chemistry* 287(49):40867-40874.

311. Ganser BK, Li S, Klishko VY, Finch JT, & Sundquist WI (1999) Assembly and analysis of conical models for the HIV-1 core. *Science* 283(5398):80-83.

312. Butan C, Winkler DC, Heymann JB, Craven RC, & Steven AC (2008) RSV capsid polymorphism correlates with polymerization efficiency and envelope glycoprotein content: implications that nucleation controls morphogenesis. *Journal of molecular biology* 376(4):1168-1181.

313. Dimonte S, Babakir-Mina M, & Aquaro S (2014) HIV-1 B-subtype capsid protein: a characterization of amino acid's conservation and its significant association with integrase signatures. *Virus genes* 48(3):429-437.

314. Chang LJ, Urlacher V, Iwakuma T, Cui Y, & Zucali J (1999) Efficacy and safety analyses of a recombinant human immunodeficiency virus type 1 derived vector system. *Gene therapy* 6(5):715-728.

315. Nakajima N, Lu R, & Engelman A (2001) Human immunodeficiency virus type 1 replication in the absence of integrase-mediated dna recombination: definition of permissive and nonpermissive T-cell lines. *Journal of virology* 75(17):7944-7955.

316. Fontana J, Cardone G, Heymann JB, Winkler DC, & Steven AC (2012) Structural changes in Influenza virus at low pH characterized by cryo-electron tomography. *Journal of virology* 86(6):2919-2929.

317. Mastronarde DN (2005) Automated electron microscope tomography using robust prediction of specimen movements. *Journal of structural biology* 152(1):36-51.

318. Heymann JB, Cardone G, Winkler DC, & Steven AC (2008) Computational resources for cryo-electron tomography in Bsoft. *Journal of structural biology* 161(3):232-242.

319. Frangakis AS & Hegerl R (2001) Noise reduction in electron tomographic reconstructions using nonlinear anisotropic diffusion. *Journal of structural biology* 135(3):239-250.

320. Pettersen EF, Goddard TD, Huang CC, Couch GS, Greenblatt DM, Meng EC, & Ferrin TE (2004) UCSF Chimera--a visualization system for exploratory research and analysis. *Journal of computational chemistry* 25(13):1605-1612.

321. Carteau S, Gorelick RJ, & Bushman FD (1999) Coupled integration of human immunodeficiency virus type 1 cDNA ends by purified integrase in vitro: stimulation by the viral nucleocapsid protein. *Journal of virology* 73(8):6670-6679.

322. Bouvard V, Baan R, Straif K, Grosse Y, Secretan B, El Ghissassi F, Benbrahim-Tallaa L, Guha N, Freeman C, Galichet L, Cogliano V, & Group WHOIAfRoCMW (2009) A review of human carcinogens--Part B: biological agents. *The Lancet. Oncology* 10(4):321-322.

323. Craigie R & Bushman FD (2012) HIV DNA integration. *Cold Spring Harbor perspectives in medicine* 2(7):a006890.

324. Jurado KA & Engelman A (2013) Multimodal mechanism of action of allosteric HIV-1 integrase inhibitors. *Expert reviews in molecular medicine* 15:e14.

325. Fontana J, Jurado KA, Cheng N, Ly NL, Fuchs JR, Gorelick RJ, Engelman AN, & Steven AC (2015) Distribution and Redistribution of HIV-1 Nucleocapsid Protein in Immature, Mature, and Integrase-inhibited Virions: A Role for Integrase in Maturation. *Journal of virology*.

326. Desimmie BA, Weydert C, Schrijvers R, Vets S, Demeulemeester J, Proost P, Paron I, De Rijck J, Mast J, Bannert N, Gijsbers R, Christ F, & Debyser Z (2015) HIV-1 IN/Pol recruits LEDGF/p75 into viral particles. *Retrovirology* 12:16.

327. Matreyek KA, Wang W, Serrao E, Singh PK, Levin HL, & Engelman A (2014) Host and viral determinants for MxB restriction of HIV-1 infection. *Retrovirology* 11:90.

328. Kent WJ (2002) BLAT--the BLAST-like alignment tool. *Genome research* 12(4):656-664.

329. Quinlan AR & Hall IM (2010) BEDTools: a flexible suite of utilities for comparing genomic features. *Bioinformatics* 26(6):841-842.

330. van Bel N, van der Velden Y, Bonnard D, Le Rouzic E, Das AT, Benarous R, & Berkhout B (2014) The allosteric HIV-1 integrase inhibitor BI-D affects virion

maturation but does not influence packaging of a functional RNA genome. *PloS one* 9(7):e103552.

331. Shkriabai N, Dharmarajan V, Slaughter A, Kessl JJ, Larue RC, Feng L, Fuchs JR, Griffin PR, & Kvaratskhelia M (2014) A critical role of the C-terminal segment for allosteric inhibitor-induced aberrant multimerization of HIV-1 integrase. *The Journal of biological chemistry* 289(38):26430-26440.

332. Slaughter A, Feng L, Venkatasubramanian D, Sharma A, Kessl JJ, Fuchs JR, Bushman F, Griffin PR, & Kvaratskhelia M (2015) LEDGF/p75 competitively reverses allosteric integrase inhibitor induced abberrant multimerization of HIV-1 integrase. *Retroviruses*, (Cold Spring Harbor Labortory).

333. Hare S, Di Nunzio F, Labeja A, Wang J, Engelman A, & Cherepanov P (2009) Structural basis for functional tetramerization of lentiviral integrase. *PLoS pathogens* 5(7):e1000515.

334. Fader LD, Malenfant E, Parisien M, Carson R, Bilodeau F, Landry S, Pesant M, Brochu C, Morin S, Chabot C, Halmos T, Bousquet Y, Bailey MD, Kawai SH, Coulombe R, LaPlante S, Jakalian A, Bhardwaj PK, Wernic D, Schroeder P, Amad M, Edwards P, Garneau M, Duan J, Cordingley M, Bethell R, Mason SW, Bos M, Bonneau P, Poupart MA, Faucher AM, Simoneau B, Fenwick C, Yoakim C, & Tsantrizos Y (2014) Discovery of BI 224436, a Noncatalytic Site Integrase Inhibitor (NCINI) of HIV-1. *ACS medicinal chemistry letters* 5(4):422-427.

335. Fenwick C, Amad M, Bailey MD, Bethell R, Bos M, Bonneau P, Cordingley M, Coulombe R, Duan J, Edwards P, Fader LD, Faucher AM, Garneau M, Jakalian A, Kawai S, Lamorte L, LaPlante S, Luo L, Mason S, Poupart MA, Rioux N, Schroeder P, Simoneau B, Tremblay S, Tsantrizos Y, Witvrouw M, & Yoakim C (2014) Preclinical

profile of BI 224436, a novel HIV-1 non-catalytic-site integrase inhibitor. *Antimicrobial agents and chemotherapy* 58(6):3233-3244.

336. Ingelheim B (2009-2014) Safety and Pharmacokinetics of Single Rising Oral Doses of BI 224436 ZW in Healthy Male Volunteers. NCT02183662. URL: https://clinicaltrials.gov/ct2/show/NCT02183662

337. Ingelheim B (2011-2012) Safety and Pharmacokinetics of Multiple Rising Oral Doses of BI 224436 in Healthy Male Volunteers. NCT01276990. URL: https://clinicaltrials.gov/show/NCT01276990

338. Fader LD, Carson R, Morin S, Bilodeau F, Chabot C, Halmos T, Bailey MD, Kawai SH, Coulombe R, Laplante S, Mekhssian K, Jakalian A, Garneau M, Duan J, Mason SW, Simoneau B, Fenwick C, Tsantrizos Y, & Yoakim C (2014) Minimizing the Contribution of Enterohepatic Recirculation to Clearance in Rat for the NCINI Class of Inhibitors of HIV. *ACS medicinal chemistry letters* 5(6):711-716.

Appendix 1: Published Reviews

Jurado KA & Engelman A (2013) Multimodal mechanism of action of allosteric HIV-1 integrase inhibitors. *Expert reviews in molecular medicine* 15:e14.

Appendix 2: Contributions to additional authored publications

Wang H, **Jurado KA**, Wu X, Shun MC, Li X, Ferris AL, Smith SJ, Patel PA, Fuchs JR, Cherepanov P, Kvaratskhelia M, Hughes SH, & Engelman A (2012) HRP2 determines the efficiency and specificity of HIV-1 integration in LEDGF/p75 knockout cells but does not contribute to the antiviral activity of a potent LEDGF/p75-binding site integrase inhibitor. *Nucleic acids research* 40(22):11518-11530.

Slaughter A, **Jurado KA**, Deng N, Feng L, Kessl JJ, Larue RC, Fadel H, Patel PA, Jena N, Fuchs JR, Poeschla E, Levy RM, Engelman A, Kvaratskhelia. (2014) The mechanism of H171T resistance reveals the importance of N-protonated His171 for allosteric integrase inhibitor binding. *Retrovirology*, 11(1):100.

Li M, **Jurado KA,** Lin S, Engelman A, and Craigie R. (2014) Engineered hyperactive integrase for concerted HIV-1 DNA integration. *PLoS ONE*: 10.1371/journal.pone.0105078.